nature portfolio

Peer Review File

Combined targeting of glioblastoma stem cells of different cellular states disrupts malignant progression

Corresponding Author: Professor Xiuxing Wang

This file contains all reviewer reports in order by version, followed by all author rebuttals in order by version.

Attachments originally included by the reviewers as part of their assessment can be found at the end of this file.

Version 0:

Reviewer comments:

Reviewer #1

(Remarks to the Author)
Lu et al. focus on addressing the heterogeneity of glioblastoma stem cells (GSCs), particularly by targeting the classical (CL) and mesenchymal (MES) subpopulations. They identified MEOX2 and SRGN as specific targets for CL and MES GSCs, respectively. Moreover, their study highlights the critical roles of the MEOX2-NOTCH and SRGN-NFkB signaling pathways in maintaining the stemness characteristics of these GSC subtypes. By employing both genetic and pharmacological strategies, Lu et al. successfully pinpointed FDA-approved compounds that potentially target MEOX2 and SRGN and affect cell growth. These findings offer insights into potential therapeutic targets for glioblastoma and strategies to address intratumoral heterogeneity. However, the manuscript would benefit from further clarification on several points to enhance its clarity and potential for guiding future drug development.

Major Questions:

1. It is unclear whether the markers MEOX2 and SRGN are predominantly enriched in glioblastoma stem cells (GSCs), which are more enriched in neural progenitor cells (NPCs), or whether they are more prevalent in astrocyte-like (AC-like) or mesenchymal-like (MES-like) cells. In current manuscript, the researchers used a combination of markers including CD133, CD15, and OCT4 along with SOX2 to identify GSC-like tumor cells. These cells were then classified into four distinct cellular states based on signatures from Neftel et al. It is important to note that the cellular states described by Neftel encompass all tumor cells, indicating that these states represent heterogeneity across the entire tumor population, not just within GSCs in glioblastoma. So there is a difference between how this study and Neftel et al. define the cell states. For clarification, can authors plot the expression of these two genes across all the malignant cells and see which cell state is more enriched? Notably, the expression of SRGN is much higher in immune cells in the microenvironment, compared to malignant cells. So its function in malignant cells could be minor.

2. It is unclear which cell populations are most affected by the knocking down of MEOX2 and SRGN. Although the knockdown of these genes is effective specifically in the classical (CL) and mesenchymal (MES) glioblastoma (GBM) cell lines, the impacted genes—such as SOX2 and ID1—are part of the neural progenitor cell (NPC) gene signature. This raises the question of which of the four cell states (NPC-like, AC-like, OPC-like, and MES-like) are most significantly impacted by the knockdown of MEOX2 and SRGN. It would be great to explore whether these genes facilitate transitions/portion change between cell states in a more heterogeneous model, like GBM organoids.

3. The authors propose that Notch signaling is primarily affected by MEOX2 perturbation. However, other studies (PMID: 35468210 and PMID: 34885053) highlight that the ERK pathways are influenced by MEOX2. Whether the authors observe any effects on ERK pathways in their experiments? Additionally, it remains uncertain if Notch signaling is indeed the most affected pathway when MEOX2 is perturbed. To address these points, the authors should investigate the impact on ERK pathways within their study and discuss possible reasons for the discrepancy between their results and those of other studies, which offer deeper insights into its mechanistic pathways.

4. The specificity of the drug targeting is unclear in the study. When the authors utilized compounds to target classical (CL) and mesenchymal (MES) glioblastoma stem cells (GSCs), they showed changes in the expression of NFkB1, NOTCH, and

stemness markers (SOX2 and ID1). However, to provide robust evidence of the drug's on-target effects, it would be beneficial if the authors could demonstrate whether mutations at the targeted sites of MEOX2 and SRGN affect the activity or expression of these genes. Such evidence could significantly clarify the drug's specificity and its direct interaction with these targets.

Other questions:
1. The authors utilized CIBERSORTx to analyze the bulk TCGA GBM dataset and found that macrophages were more prevalent in GBM samples with high classical (CL)-mesenchymal (MES) signatures. To strengthen their conclusion, additional datasets and experiments could be useful, such as spatial analysis or co-staining with macrophage markers and CL-MES markers.
2. The validation of the predictive results in this paper is conducted using four cell lines (CL: 3028 and RKI, MES: 2907 and 839). However, additional information (e.g. genetic background) regarding these cell lines and any existing literature references detailing their derivation or prior use in research should be provided. Furthermore, an assessment of the basal expression levels of cellular state signatures in these four cell lines would be beneficial.
3. The authors' ATAC-seq data presented in Supplementary Figure 4b shows an absence of signal across all genes in the genome, which is unusual and raises concerns about the quality of the data obtained.
4. In all mouse experiments, the sample size should be labeled for each group.

Reviewer #2

(Remarks to the Author)
I co-reviewed this manuscript with one of the reviewers who provided the listed reports. This is part of the Nature Communications initiative to facilitate training in peer review and to provide appropriate recognition for Early Career Researchers who co-review manuscripts.

Reviewer #3

(Remarks to the Author)
The manuscript by Lu and co-workers demonstrate that classical (CL) and mesenchymal (MES) glioma stem cells (GSCs) are prevalent in immune-active regions of GBM. By analyzing GSC RNA they identified the targets MEOX2 for CL GSCs and SRGN for MES GSCs. They show that these genes are important in promoting proliferation, maintaining stemness, and conferring resistance to macrophage phagocytosis via MEOX2-NOTCH and SRGN-NFkB pathways. They show that the targeting of these genes with FDA-approved drugs, especially in combination, shows improved effectiveness against GBM in both lab and animal models.

The manuscript is well written and straightforward, however, there are some questions about how these data and the authors conclusions fit within the context of the known plasticity of GBM cellular states, the detailed mechanistic basis for the relationship between the MES cellular states and the myeloid cells with the tumor microenvironment and the novelty of the Notch and NFkB pathways as potential therapeutic targets. Below are several specific questions/comments for the authors to consider:

• Based on growing transcriptomic and other data, it is not clear that it is biologically valid to “define GSC-like tumor cells as any cell expressing CD133, CD15 or OCT4, in conjunction with SOX2”, for the glioma stem cell-like state is a dynamic one, as are all of the GBM cellular states and thus by selecting any one population, one may be skewing the data in these studies to a certain subset of genomic/epigenomic clones from the entire heterogenous population of clones that constitute any given GBM.

• The authors fail to acknowledge in a meaningful way the already rich body of published literature regarding the well documented single cell relationships between the MES-L cell states and the immune microenvironment.

• The survival curves in Fig 1D derived from patients from the investigators own institutions are not interpretable given the large number of biological and clinician factors that are known to be major prognostic factors in GBM patient survival. A multifactorial analysis of such factors, generally involving hundreds of patients, would be necessary to attribute any one molecular/genetic characteristic as an independent prognostic factor.

• It has been known for years that the PN subgroup of GBM has a slightly better survival than do other transcriptomic subtypes of GBM so the significance of Fig 1D is unclear.

• The differential expression gene list between the different transcriptomic/cellular states (e.g. Neftel) runs into the hundreds between each state. It is entirely unclear the rationale for how and why the investigators chose their comparator groups (Fig. 1f, manuscript pages 7/8) to come up with MEOX2 and SRGN as typical CL and MES GSCs targets.

• As above, KM survival curves for GBM based on solely the arbitrary assignment of “high” versus “low” expression of a gene, totally disregarding all of the other critically important survival prognostic factors in GBM is not statistically valid. Also, the designation of “high” vs. “low” is an arbitrary chosen nominal data point in data that are actually continuous.

• I do not understand the point being made by showing that MEOX2/SRGN in GBM, a glial tumor, but not in systemic tumor types in Fig 1l)?

• The knockdown experiments of MEOX2/SRGN in 2D are difficult to interpret because it has been clearly shown that the distribution of cellular states in almost all GSCs are contextually-based and when grown in vitro is heavily (and for some GSC lines, exclusively) skewed toward AC/MES-L states. Thus, it would not be surprising that knockdown of a MES-L dependence factor cause decreased proliferation and clonogenicity in vitro as shown in Fig. 2. To that point, however, it is curious that it did not cause such an effect on PN GSCs for even these lines should have a significant percentage of AC/MES-L cells in vitro as assessed by scRNA-seq and should therefore show some effects on proliferation albeit maybe not as much as the predominant AC/MES-L cells..

• Despite a modest increase in survival of the MEOX2/SRGN knockdown in Fig 2v, all the animals still died in a relatively quick amount of time. How can this be explained when the in vitro data show almost complete inhibition of proliferation and clonogenicity following MEOX2/SRGN knockdown?

• What were the cellular state distributions of the MEOX2/SRGN knockdown versus the control GSCs in vitro and in the growing intracranial tumors? It would be important to perform comparative scRNA-seq in both of these scenarios.

• It would be important to look at the effect of Notch pathway activity in the different cellular states by scRNA-seq and to assess whether the effects of MEOX2/SRGN knockdown on chromatic accessibility at the single cell level to see if this is indeed an AC/MES-L specific effect.

•. Did overexpression of Notch restore the transcriptomic profile of the the CL state in the MEOX2 knockdown cell lines?

• Did re-introducing Notch 1 into CL GSCs with MEOX2 knockdown restore in vivo growth to levels of non-knockdown lines?

• Although re-introducing NFKB1 into MES GSCs with SRGN knockdown restored the defect in cell proliferation and stem cell frequency, did it restore the MES-L transcriptomic profile?

• Did re-introducing NFKB1 into MES GSCs with SRGN knockdown restore in vivo growth to the levels non-knockdown lines?

• Although the presence of myeloid cells (including macrophages) in the GBM microenvironment is clearly important as has been demonstrated by numerous other investigators, is there any real data to think that macrophage-mediate glioma cell phagocytosis is a potent anti-tumor mechanism operative in human gliomas? This raises the question of the physiological relevance of the GSC-macrophage phagocytosis mixing experiments.

• It would be important to demonstrate that the Notch and NFkB inhibitor drugs identified in your screen (Fig. 7) where specific both against GSCs compared to, 1. other, non-glioma tumor types, and 2: CL/MES GSCs compared to PN GSCs and the MEOX2 knockdown GSCs.

Reviewer #4

(Remarks to the Author)
In this manuscript, the authors present a detailed investigation into the heterogeneity of GSCs. Through a series of integrated analyses, the authors identify MEOX2 and SRGN as specific targets for CL and MES GSCs, which function through MEOX2-NOTCH and SRGN-NFκB pathways essential for GSC proliferation, stemness, and resistance to macrophage-mediated phagocytosis. Further, they used genetic and pharmacological strategies to identify FDA-approved drugs targeting these pathways, suggesting simultaneously targeting CL and MES GSCs could improve therapeutic outcomes.

Overall, this is a very dense manuscript with an overwhelming amount of data. I would suggest the authors thoroughly reorganize their figures, keeping only the essential data in the main figures while putting all the supporting data in the supplemental figures (refrain from presenting more than 10 panels per figure) to improve clarity and the logic flow. I also have some specific comments regarding the experimental results, data presentation and analysis.

Major concerns:
1. One major shortcoming of this study is that the authors are confusing interpatient/intertumoral heterogeneity with intratumoral heterogeneity. The single-cell analyses are based on pooled patient samples, and the functional validation is based on different patient-derived cell lines that are genetically and epigenetically distinct, yet in reality the intrinsic GSC heterogeneity the authors propose to target should be within the same patient/tumor. Therefore, it is questionable whether MEOX2 and SRGN are still specific targets for CL and MES GSCs from the same patient (adding paired single-cell analysis by patient throughout the manuscript could help). Along this line, at least for the combinatorial drug treatment experiments (Figure 5 and 7), the authors should use GSC cell lines that exhibit both CL and MES features after xenograft (refer to Ref. 8 regarding the plasticity of glioma cell states), instead of artificially mixing up cell lines from different patients, to assess the treatment effects. These experiments are essential to substantiate the major claims of this manuscript.
2. Figure 1a, typically this analysis should yield a p-value yet the authors presented scaled scores instead. They need to clarify how these scaled scores were calculated and justify their use here. Also, two methods for calculating ssGSEA are mentioned in the methods section. The author should specify which method was used for each plot presented.

3. Figure 1b, the authors identified GSCs from public scRNAseq data by the expression of specific genes. It would be helpful to provide expression profiles of individual markers confirming the accuracy of GSC isolation.
4. Figure 1j, it is more important to directly compare the protein levels of MEOX2 and SRGN between CL vs MES GSCs to demonstrate specificity.
5. Figure 1h, the authors should present normalized gene expression including a p-value. Scaled values may exaggerate the variation, potentially skewing the interpretation of the results.
6. Figure S1k, where 28 SRT datasets are available, why only two were selected for presentation ?
7. Figure 1k, it is necessary to conduct a statistical analysis to confirm the association between SOX2 and MEOX2/SRGN. Furthermore, the claim that CL and MES GSCs are enriched in the reactive immune region needs validation using classic CL or MES markers such as VIM, CD44 or GFAP.
8. Figure 2u and other Biolum results need quantification.
9. Figure 5a, the author should provide evidence that the designated cell clusters are reliable for subsequent deconvolution analysis.
10. The author has identified specific inhibitors by predicting interactions and BLI. To confirm drug specificity, the authors should consider using negative controls such as truncated proteins lacking the binding domain.

Minor issues:
1. Throughout the figures, the number of samples/cells in each group should be clearly labeled or specified in the legends.
2. The term 'estimate immune' in Figure S1a requires clarification regarding its definition and calculation. Also, the term ‘relative expression’ throughout needs clarification on how these values are calculated.
3. There are some inaccuracies in Methods. a) The author mentioned using the NormalizeData function to regress out sequencing depth and the percentage of mitochondrial genes. However, the correct function for these adjustments is typically ScaleData. b) When using Harmony, it is important to note that the dimension reduction should occur within the Harmony-adjusted space rather than a PCA space.
4. Figure 3f, the author should clarify what the dashed line represents in the legend.

Reviewer #5

(Remarks to the Author)
I co-reviewed this manuscript with one of the reviewers who provided the listed reports. This is part of the Nature Communications initiative to facilitate training in peer review and to provide appropriate recognition for Early Career Researchers who co-review manuscripts.

Version 1:

Reviewer comments:

Reviewer #1

(Remarks to the Author)
I appreciate the authors' efforts to address all my comments. In the revised manuscript, the authors added additional data and analyses to verify that the FDA-approved compounds specifically and effectively target MEOX2 and SRGN in the CL and MES GSC subpopulations. However, I still have some remaining concerns:

Major comments:

1. Related to my comment 1, how the authors define GSCs remains unclear. Glioblastoma stem cells (GSCs) are generally considered stem cell-like tumor cells, represented by NPC-like and OPC-like states in GBM, as reported by Neftel et al. However, the authors use SOX2, CD133, CD5, and OCT4 markers to identify GSCs in GBM datasets and then classify them into NPC-like, OPC-like, AC-like, and MES-like states. The authors need to clarify the overall proportion of GSCs in GBM, as well as the GSC proportion among the four GBM cell states.

2. Related to my comment 2, similar to point 1, the authors used GSC models (2907 and 3028) to identify that MEOX2 and SRGN knockouts would reduce the AC-like and MES-like signatures, respectively. However, in response to Figures R2 and R3, there is an increase in PN and NPC-like signals, while the western blot shows that both SOX2 and ID1 are decreased in Fig. 2.

3. Related to comment 8, the authors need to provide an overview of the quality of the ATAC-seq data, including TSS enrichment scores for these samples, the total number of peaks, and the number of differential peaks across all conditions, rather than just detailing the experimental procedures.

Reviewer #2

(Remarks to the Author)
I co-reviewed this manuscript with one of the reviewers who provided the listed reports. This is part of the Nature Communications initiative to facilitate training in peer review and to provide appropriate recognition for Early Career Researchers who co-review manuscripts.

Reviewer #4

(Remarks to the Author)
1) Although many of my concerns have been addressed, I share similar concerns with Reviewer 1 that low expression of SRGN in GBM cells in general raises doubt about its functional significance, after I examined its expression in the Neftel dataset myself(see attachment 1). The authors' data also suggest it is expressed only in a small fraction (around 10%) of MES GSCs in scRNA-seq.

2) Since we happen to have the Ravi et al. spatial dataset, we analyzed the expression of MEOX2 and SRGN, but couldn't replicate the authors' results in quite a few samples(see attachment 2, the obvious ones are highlighted by red boxes). Again, SRGN is barely expressed in some samples unlike what the authors are trying to show.

3) Moreover,the authors did not properly address my previous concern whether MEOX2 and SRGN are specific for CL and MES GSCs from the same patient.

Reviewer #5

(Remarks to the Author)
I co-reviewed this manuscript with one of the reviewers who provided the listed reports. This is part of the Nature Communications initiative to facilitate training in peer review and to provide appropriate recognition for Early Career Researchers who co-review manuscripts.

Reviewer #6

(Remarks to the Author)
This is a provocative yet often confounding paper constituted by a tremendous amount of work and analysis, purporting to show that MEOX2 and SRGN are targets of different glioma cell states. There are several layers of obfuscation between the Neftel cell states, TCGA signatures, and then GSC terminology--the later of which seems artificial or at least not essential to the findings. Further, a number of issues remain to be addressed based on previous reviews.

Specific points:

"medicate" in abstract is likely meant to be "mediate"

Methods: It's unclear if cells are always grown as spheres or if they are in monolayers in some experiments?

"Specificity" is often not really specific in terms of expression (e.g. Response Fig R4 and much single cell data in the paper.) Perhaps this should be softened to "enriched"

Reviewer 1, Comment 6: "The validation of the predictive results in this paper is conducted using four cell lines (CL: 3028 and RKI, MES: 2907 and 839)." This is critical point and sends the reader/reviewer down a "rabbit hole" looking for information. A comprehensive table of descriptive features should be included in the form of a supplementary table with many more pertinenet details than are presented.

Reviewer 3, Comment 1: (defining GSC) - I'm not convinced the authors address the point. Featureplots of CD133, SOX2, OCT4, and CD15 would be more informative than the somewhat misleading plots in Supp. Fig. 1b--where the scales change wildly. If I'm reading this correctly, OCT4 is expressed in only 3% of cells. However, adding a definition of GSC just adds another layer of abstraction that doesn't seem meaningful in the context of these experiments. Already the manuscript mixes TCGA and Neftel states. Futher, it is becoming increasingly apparent that most tumors express all states and signatures across a spectrum--with plasticity in response to standard-of-care and tumor progression.

Reviewer 3, Comment 2: (referencing meaningful literature on MES-CL immune microenvironment) - This was and continues to be an oversight of key references regarding the immune microenvironment in MES-CI states. Further, it is notable that MEOX2 and SRGN have been identified in glioma progression by a number of publications that are largely not referenced:
https://pmc.ncbi.nlm.nih.gov/articles/PMC5421891/
https://pubmed.ncbi.nlm.nih.gov/38672477/
https://pubmed.ncbi.nlm.nih.gov/28445977/
https://www.mdpi.com/2218-273X/14/4/461
https://pmc.ncbi.nlm.nih.gov/articles/PMC8672280/
https://www.nature.com/articles/s41419-022-04845-2

Reviewer 3, Comment 3: - addressed appropriately

Reviewer 3, Comment 4: - addressed appropriately

Reviewer 3, Comment 5: - "Single cell transcriptome differential analysis cannot guarantee that the isolated GSC like tumor cells function as true GSCs." This is a highly questionable statement. One can argue that scRNA-seq from a primary tumor is much more reflective of that natural state of glioma tumor propagating cells than cells cultured ex vivo--which are subject to cell culture artifacts, lack of stroma, drift, etc.

Reviewer 3, Comment 6: A valid point but unfortunately, the authors are right that KM data is presented as such--as misleading as it can be. It is the unfortunate convention.

Reviewer 3, Comment 7: "These results suggest that MEOX2 and SRGN are characteristically up regulated in GBM and could serve as unique therapeutic targets for GBM." I think this again ignores a number of papers that I could find showing that MEOX2 and SRGN are upregulated in a number of cancers. e.g. https://bmccancer.biomedcentral.com/articles/10.1186/s12885-020-06849-7 & https://journals.plos.org/plosone/article?id=10.1371/journal.pone.0114104

Reviewer 3, Comment 8: More detail is needed on how these cells compare to the parental tumors. The authors should present an integration of their "GSCs" with primary glioma datasets and compared DEGs.

Reviewer 3, Comment 9: Again, this suggests changing states between in vitro and in vivo data.

Reviewer 3, Comment 10: This doesn't directly address the point. There should be a direct comparison in low dimensional UMAP space to show if these cells align completely or if there are cellular states (likely in vitro due to culture artifacts) that don't appear in vivo. Scoring by modules by artificially normalized scales (e.g. Response Fig. R5) does not give the full picture as one gets aligning all of the data in a low dimensional space with batch correction/integration.

Reviewer 3, Comment 11: addressed appropriately

Reviewer 3, Comment 12: addressed appropriately

Reviewer 3, Comment 13: addressed appropriately. However, I can't find the details on how this was accomplished in the methods. Adding an 8KB receptor to a lentivirus is near the limits of a virus--especially with a promoter and other elements.

Reviewer 3, Comment 14: addressed appropriately

Reviewer 3, Comment 15: addressed appropriately

Reviewer 3, Comment 16: Again, the authors show expression in a normalized scale so it's not clear if there is any physiological relevance in terms of CD47-SIRPa.

Version 2:

Reviewer comments:

Reviewer #1

(Remarks to the Author)
The authors addressed my concern about GSC. Comment 2 is not addressed but it is OK to leave the inconsistency in the paper as it is not the major population. Comment 3 proved our concern about the quality of ATAC-seq data. I suggested removing those analyses and interpretations in the paper.

Reviewer #2

(Remarks to the Author)
I co-reviewed this manuscript with one of the reviewers who provided the listed reports. This is part of the Nature Communications initiative to facilitate training in peer review and to provide appropriate recognition for Early Career Researchers who co-review manuscripts.

Reviewer #4

(Remarks to the Author)
The authors have properly addressed my concerns.

Reviewer #5

(Remarks to the Author)
I co-reviewed this manuscript with one of the reviewers who provided the listed reports. This is part of the Nature Communications initiative to facilitate training in peer review and to provide appropriate recognition for Early Career Researchers who co-review manuscripts.

Reviewer #6

(Remarks to the Author)
Reviewer 6, Comment 5: Reviewer 3, Comment 1: (defining GSC) – I appreciate the authors providing featureplots which greatly clarify the expression.

However, the reasoning behind the definition of GSCs seems arbitrary and tautological. In the response they state:

“Our method for isolating GSC-like tumor cells was based on a protocol described in an article in Cell Stem Cell (2020, PMID: 31901251). The following method was employed in this study: “In order to identify the potential GSC cell types for each tumor, we defined GSCs within our scRNA-seq dataset as any cell (independent of the previous clustering) expressing PROM1, FUT4, or L1CAM, in conjunction with SOX2, and not expressing TLR4 (which has been shown to be downregulated by GSCs in order to avoid immune surveillance).”

But then they switch to saying:

“After isolating tumor cells in scRNA-seq datasets, we defined GSC-like tumor cells as any cell expressing CD133, CD15 or OCT4, in conjunction with SOX2 (Supplementary Fig.1b).”

And in the response:

“Therefore, we each selected two of the most reviewed transcription factors (SOX2 and OCT4) and surface markers (CD133 and CD15) to isolate GSC-like tumor cells from malignant cells in GBM scRNA-seq datasets (PMID: 26109046).” This reference is from 2015 and largely pre-dates what we’ve learned from scRNA-seq.

This "or" in "...any cell expressing CD133, CD15, or.." is quite arbitrary. Why not require a union of the markers or 2 of 3? Sox2 is basically expressed by a majority of cells in a tumor. But Sox2 is expressed by most proliferating neural progenitors--even more differentiated types. So requiring just one other marker seems capricious. I do not agree with the logic in the previous Cell Stem Cell paper (where they split so-called GSCs into 7 types), nor the current paper without functional justification.

Bottom two responses can be addressed by the same general approach:

Reviewer 6, Comment 9: Reviewer 3, Comment 8: More detail is needed on how these cells compare to the parental tumors. The authors should present an integration of their "GSCs" with primary glioma datasets and compared DEGs.
“We appreciate the reviewer’s comment. Unfortunately, we do not have sequencing data from the parental tumors corresponding to our GSCs.”

Reviewer 6, Comment 10: Reviewer 3, Comment 10: This doesn't directly address the point. There should be a direct comparison in low dimensional UMAP space to show if these cells align completely or if there are cellular states (likely in vitro due to culture artifacts) that don't appear in vivo. Scoring by modules by artificially normalized scales (e.g. Response Fig. R5) does not give the full picture as one gets aligning all of the data in a low dimensional space with batch correction/integration.
“The integrated analysis revealed that all cellular populations corresponded to states present in patient tumors.”

Specifically, scRNA-seq allows for facile integration across patients and datasets (e.g. Harmony, SCVI, or other atlas scale approaches). Large datasets of primary glioma are available (e.g. https://www.nature.com/articles/s41467-022-28372-y#data-availability) to easily integrate with the cell culture data. (The same parental data is not necessary as the tumors will generally fall into the same low dimensional space if enough samples are included. The authors should show whether their GSCs can be integrated with the primary datasets and fall within a similar low dimensional space. Simply scoring by the MES, CL, PN, etc. is too superficial to demonstrate the fidelity of these findings.

Version 3:

Reviewer comments:

Reviewer #1

(Remarks to the Author)
The authors addressed all my questions.

Reviewer #2

(Remarks to the Author)
I co-reviewed this manuscript with one of the reviewers who provided the listed reports. This is part of the Nature Communications initiative to facilitate training in peer review and to provide appropriate recognition for Early Career Researchers who co-review manuscripts.

Reviewer #6

(Remarks to the Author)
I will "agree to disagree" about the import and ability to define putative glioma stem cells using "OR" logic with 4 markers. And agree that the discovered targets would precipitate through DEG analysis.

I would just suggest that very strong language be tempered in the discussion. Examples:
1) "GSCs are a driving force of intertumoral and intratumoral heterogeneity." In the next sentence, they cite two papers: "Single-cell sequencing and lineage tracking methods confirmed the existence of stem-like cancer cells in GBM, supported their importance in maintaining cell hierarchy, and further strengthened the concept of cell plasticity49, 50." In fact, one of these papers (Nat. Gen.) demonstrates that WT glioma shows a preponderance of dedifferentiation and lineage plasticity that doesn't fit with a hierarchical stem cell model like IDH1-mut tumors. I would submit that we should not take the existence and function of GSCs as such an element of faith but much remains to be determine empirically.
2) "Using genetic and pharmacologic techniques, we found that combination therapy with FDA approved agents against both CL and MES GSCs achieved the most effective tumor control." -I don't see any evidence of "control."

NCOMMS-24-18139-T

Reviewer #1:

Major Questions:

Reviewer 1, Comment 1: It is unclear whether the markers MEOX2 and SRGN are predominantly enriched in glioblastoma stem cells (GSCs), which are more enriched in neural progenitor cells (NPCs), or whether they are more prevalent in astrocyte-like (AC-like) or mesenchymal-like (MES-like) cells. In current manuscript, the researchers used a combination of markers including CD133, CD15, and OCT4 along with SOX2 to identify GSC-like tumor cells. These cells were then classified into four distinct cellular states based on signatures from Neftel et al. It is important to note that the cellular states described by Neftel encompass all tumor cells, indicating that these states represent heterogeneity across the entire tumor population, not just within GSCs in glioblastoma. So there is a difference between how this study and Neftel et al. define the cell states. For clarification, can authors plot the expression of these two genes across all the malignant cells and see which cell state is more enriched? Notably, the expression of SRGN is much higher in immune cells in the microenvironment, compared to malignant cells. So its function in malignant cells could be minor.

Response:

We appreciate the constructive comment from the reviewer, which raised an important question regarding the expression of MEOX2 and SRGN in GBM. In the revised version, we re-analyzed the expression of MEOX2 and SRGN across all the malignant cells in our in-house scRNA-seq datasets (dataset 1 and dataset 2) and six public scRNA-seq datasets (GSE103224, GSE117891, GSE131928, GSE141383, GSE173278 and GSE182109). The malignant cells were classified into four cellular states using the method reported by Neftel et al. We also analyzed the expression of MEOX2 and SRGN in different subtypes of GBM in three other bulk RNA-seq datasets (CGGA, Rembrandt, and Ivy GAP). Our current data support that MEOX2 and SRGN were characteristically enriched in CL/AC-like and MES/MES-like malignant cells, respectively (Response Fig. R1). The above results, combined with our previous RNA-seq datasets analysis results (GSCs vs. DGCs and GSCs vs. NSCs) and experimental results (Fig. 1e-h and Supplementary Fig. 3a-c), we

demonstrated that the expression of MEOX2 and SRGN are higher in CL and MES GSCs than other malignant cells in GBM.

Regarding the concern that the expression of SRGN is also high in immune cells in the microenvironment, we noticed that many MES/MES-like markers are highly expressed in immune cells that mediate malignant progression of GSCs and GBM. These markers include CD44 (*PMID:* 21156287 and 20197461), NAMPT (*PMID:* 34260721 and 31119097) and ANXA1 (*PMID:* 38049523). It has been reported that MES-like state present both in malignant cells and macrophages in GBM (*PMID:* 34087162). This suggests that MES-like marker genes, which are also highly expressed in immune cells, could play important roles in malignant cells. Our experimental results in Fig. 2 and Supplementary Fig.4 showed that SRGN promotes cell proliferation, self-renewal, and stemness in MES GSCs suggesting its important function in MES GSCs.

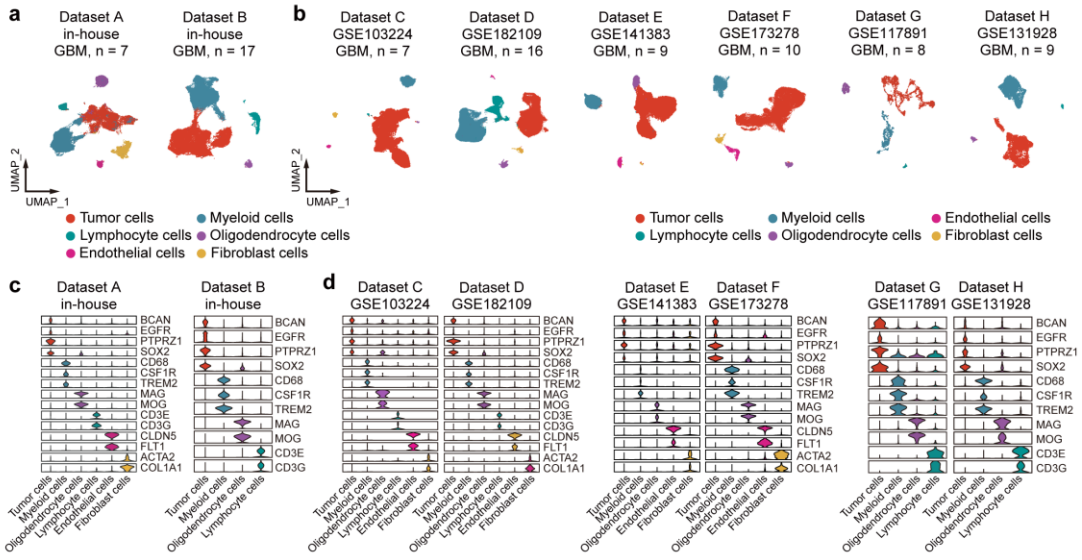

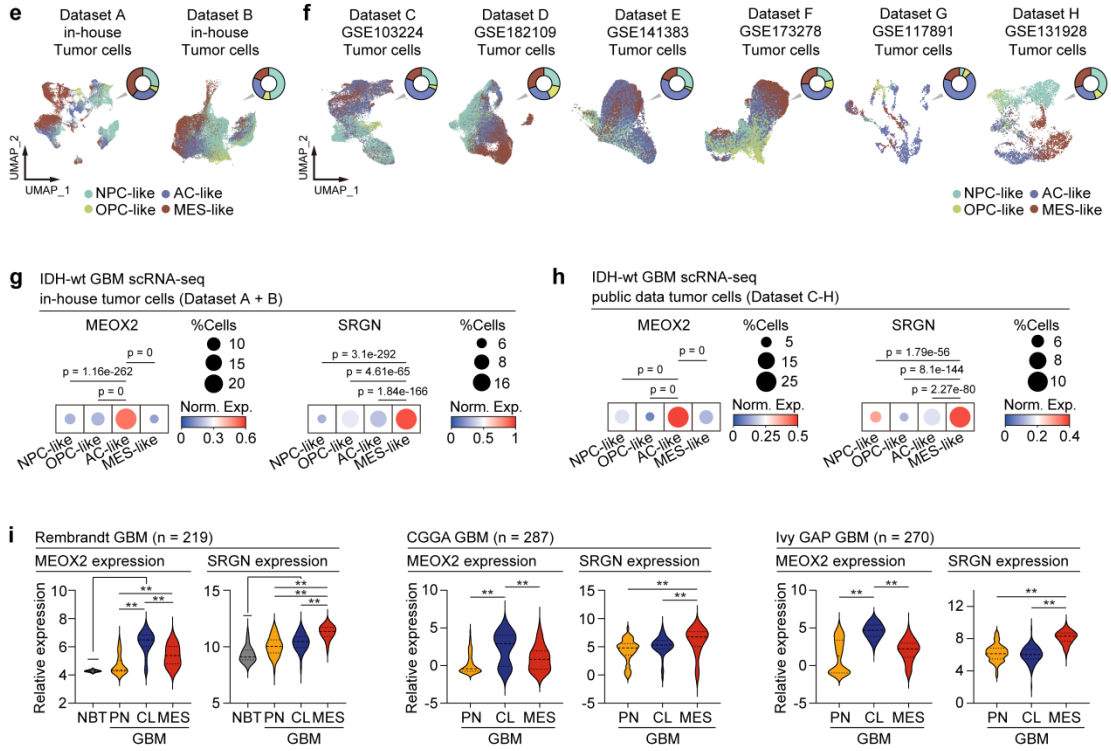

Response Fig R1. MEOX2 and SRGN are specific targets in CL and MES GBM, respectively

a, The UMAP plot of GBM samples annotated by major cell types in dataset A (in-house) and dataset B (in-house). **b,** The UMAP plot of GBM samples annotated by major cell types in dataset C (GSE103224), dataset D (GSE182109), dataset E (GSE141383), dataset F (GSE173278), dataset G (GSE117891), and dataset H (GSE131928). **c,** Violin plot of mean expression of marker genes for primary cell types in dataset A (in-house), dataset B (n-house). **d,** Violin plot of mean expression of marker genes for primary cell types in dataset C (GSE103224), dataset D (GSE182109), dataset E (GSE141383), dataset F (GSE173278), dataset G (GSE117891), and dataset H (GSE131928). **e,** Four tumor cellular states mapped in UMAP coordinates from dataset A (in-house) and dataset B (in-house). **f,** Four tumor cellular states mapped in UMAP coordinates from dataset C (GSE103224), dataset D (GSE182109), dataset E (GSE141383), dataset F (GSE173278), dataset G (GSE117891), and dataset H (GSE131928). **g,** Bubble plot showing proportions and normalized expression levels of MEOX2 and SRGN in different cellular state tumor cells from dataset A (in-house) and dataset B (in-house). **h,** Bubble plot showing proportions and normalized expression levels of MEOX2 and SRGN in different cellular state tumor cells from dataset C (GSE103224), dataset D (GSE182109), dataset E (GSE141383), dataset F (GSE173278), dataset G (GSE117891), and dataset H (GSE131928). **i,** MEOX2 (left) and SRGN (right) gene expression in the Rembrandt, CGGA, and Ivy GAP GBM dataset.

Reviewer 1, Comment 2: It is unclear which cell populations are most affected by the

knocking down of MEOX2 and SRGN. Although the knockdown of these genes is effective specifically in the classical (CL) and mesenchymal (MES) glioblastoma (GBM) cell lines, the impacted genes—such as SOX2 and ID1—are part of the neural progenitor cell (NPC) gene signature. This raises the question of which of the four cell states (NPC-like, AC-like, OPC-like, and MES-like) are most significantly impacted by the knockdown of MEOX2 and SRGN. It would be great to explore whether these genes facilitate transitions/portion change between cell states in a more heterogeneous model, like GBM organoids.

Response:

We appreciate the constructive comments regarding the roles of MEOX2 and SRGN in transitions/proportion change between cell states in GBM. By analyzing RNA-seq data from our 3028 (CL) and 2907 (MES) GSCs, we found a subtype transition in GSCs upon MEOX2 and SRGN knockout (Response Fig. R2). 3028 (CL) and 2907 (MES) were both patient-derived xenograft models and were not sorted by subtype-specific surface markers. Although RNA-seq data showed that 3028 and 2907 revealed a preference for CL and MES subtype, we considered them to be heterogeneous cell models containing different cellular states of GSCs. To validate this, we performed single-cell RNA sequencing on 3028 and 2907 GSCs. The analysis results showed that 3028 and 2907 models contained all four cellular states GSCs. Consistent with the bulk RNA-seq results, 3028 had a higher proportion of AC-like GSCs and 2907 had a higher proportion of MES-like GSCs. After knocking down MEOX2 in 3028, the proportion of AC-like GSCs decreased. After knocking down SRGN in 2907, the proportion of MES-like GSCs decreased (Response Fig. R3). The above results demonstrated that knocking down MEOX2 mainly affected AC-like GSCs and knocking down SRGN primarily affected MES-like GSCs.

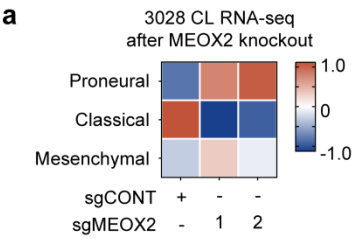

b

Group	gsva score			p value		
	PN	CL	MES	PN	CL	MES
sgCONT	-0.0202	0.4154	0.0965	0.9041	0.0009	0.8761
sgMEOX2-1	0.0363	-0.4899	-0.0882	0.3556	0.9910	0.4985
sgMEOX2-2	0.3746	-0.2124	0.0337	0.3187	0.9800	0.9800

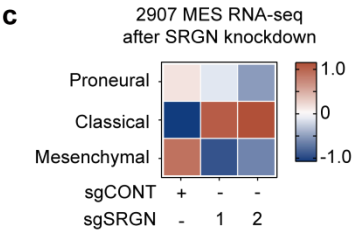

d

Group	gsva score			p value		
	PN	CL	MES	PN	CL	MES
sgCONT	0.2261	-0.0415	0.3863	0.0389	0.7602	0.0010
sgSRGN-1	0.0077	0.0649	-0.0311	0.7822	0.2468	0.9660
sgSRGN-2	-0.2876	-0.1140	-0.2998	0.8262	0.4765	0.9910

Response Fig R2. MEOX2 and SRGN maintained a CL and MES signature, respectively

a, Heatmap depicting the changes in subtype signature after MEOX2 knockout in 3028 CL GSCs. **b,** Summary of gsva score and p value of 3028 CL GSCs transduced with sgCONT, sgMEOX2-1, and sgMEOX2-2. **c,** Heatmap depicting the changes in subtype signature after SRGN knockout in 2907 MES GSCs. **d,** Summary of gsva score and p value of 2907 MES GSCs transduced with sgCONT, sgSRGN-1, and sgSRGN-2.

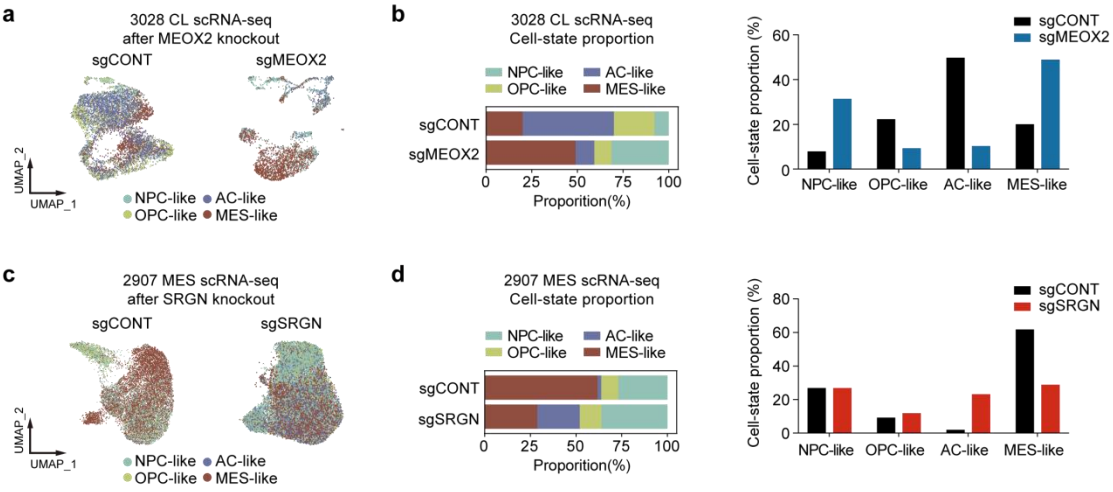

Response Fig R3. Knocking down MEOX2 mainly affected AC-like GSCs and knocking down SRGN primarily affected MES-like GSCs

a, The UMAP plot of 3028 CL GSCs annotated by four cellular states. **b,** Proportion changes of four cellular states cells in 3028 CL GSCs transduced with MEOX2 sgRNA or control sgRNA. **c,** The UMAP plot of 2907 MES GSCs annotated by four cellular states. **d,** Proportion changes of four cellular states cells in 2907 MES GSCs transduced with SRGN sgRNA or control sgRNA.

Reviewer 1, Comment 3: The autinhors propose that Notch signaling is primarily affected by MEOX2 perturbation. However, other studies (PMID: 35468210 and PMID: 34885053) highlight that the ERK pathways are influenced by MEOX2. Whether the authors observe any effects on ERK pathways in their experiments? Additionally, it remains uncertain if Notch signaling is indeed the most affected pathway when MEOX2 is perturbed. To address these points, the authors should investigate the impact on ERK pathways within their study and discuss possible reasons for the discrepancy between their results and those of other studies, which offer deeper insights into its mechanistic pathways.

Response:

We thank the reviewer for raising this interesting question. To interrogate the mechanism of MEOX2 in CL GSCs, we performed multi-omics sequencing including RNA-seq, ATAC-seq and ChIP-seq. In our MEOX2 ChIP-seq data as shown in Fig. 3e, KEGG pathway enrichment analysis also identified enrichment of the MAPK signaling pathway. We focused on the regulatory effects of MEOX2 on Notch signaling mainly for the following reasons: (1) Pathway enrichment analysis of GSCs RNA-seq and scRNA-seq datasets highlighted that Notch signaling was enriched in CL/AC-like GSCs. ERK signaling did not show characteristic enrichment in CL/AC-like GSCs. These results suggested a key role of Notch signaling pathway in CL/AC-like GSCs; (2) Based on the comprehensive analysis results of RNA-seq, ChIP-seq, and ATAC-seq, the Notch signaling pathway was most significantly affected by MEOX2 expression in CL GSCs. Our newly added scRNA-seq data further validated the above conclusions. After knockdown of MEOX2, the proportion of AC-like GSCs decreased, and the enrichment of the Notch signaling pathway in the entire GSCs population also decreased (Response Fig. R4).

We believe that MEOX2 does have a regulatory effect on MAPK signaling pathway. In fact, the indirect regulation effect of Notch signaling on MAPK signaling was also labeled in KEGG pathway database (https://www.kegg.jp/pathway/hsa04330). We think that one of the reasons for this difference is that different GBM models were used. We and other studies (*PMID:* 35468210 and *PMID:* 34885053) all performed RNA-seq after MEOX2 knockdown. However, we used CL GSCs which were more enriched with Notch signaling. Among all these RNA-seq data, our results showed the highest knockdown efficiency of MEOX2, with more significant transcriptome changes. Combining the results of our

multi-omic analysis with the newly added data, we think these are sufficient to prove that Notch signaling is indeed the most affected pathway when MEOX2 is perturbed.

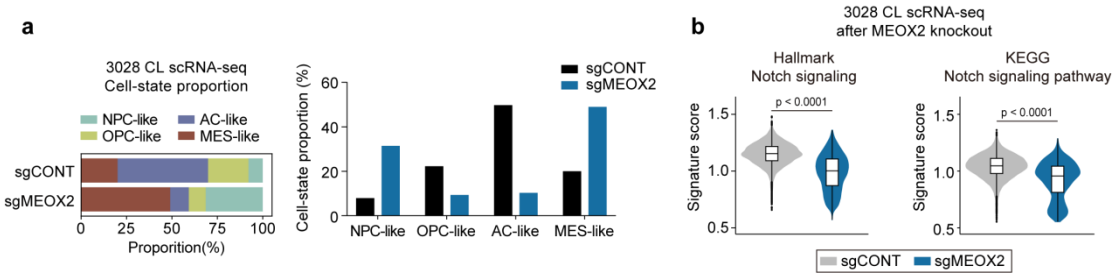

Response Fig R4. Knocking down MEOX2 mainly affected AC-like GSCs and knocking down SRGN primarily affected MES-like GSCs

a, Proportion changes of four cellular states cells in 3028 CL GSCs transduced with MEOX2 sgRNA or control sgRNA. **b,** Violin-box plots showing the notch signaling score (Hallmark and KEGG) of the GSCs scRNA-seq data (sgCONT vs. sgMEOX2). Two-tailed unpaired Wilcoxon rank-sum test.

Reviewer 1, Comment 4: The specificity of the drug targeting is unclear in the study. When the authors utilized compounds to target classical (CL) and mesenchymal (MES) glioblastoma stem cells (GSCs), they showed changes in the expression of NFkB1, NOTCH, and stemness markers (SOX2 and ID1). However, to provide robust evidence of the drug's on-target effects, it would be beneficial if the authors could demonstrate whether mutations at the targeted sites of MEOX2 and SRGN affect the activity or expression of these genes. Such evidence could significantly clarify the drug's specificity and its direct interaction with these targets.

Response:

We thank the reviewer for this critical suggestion. The Alphafold 2 database model was applied to predict the potential binding region of the MEOX2 and SRGN proteins (DNA binding region of MEOX2: 187-246 amino acids; binding pocket of SRGN: 28-60 amino acids). To confirm drug specificity, we used truncated MEOX2 and SRGN proteins lacking the binding domain as negative control and performed BLI experiment. The results showed that the truncated MEOX2 and SRGN proteins could not bind to drugs (nilotinib and DHEC for MEOX2, paliperidone and risperidone for SRGN) (Response Fig. R5).

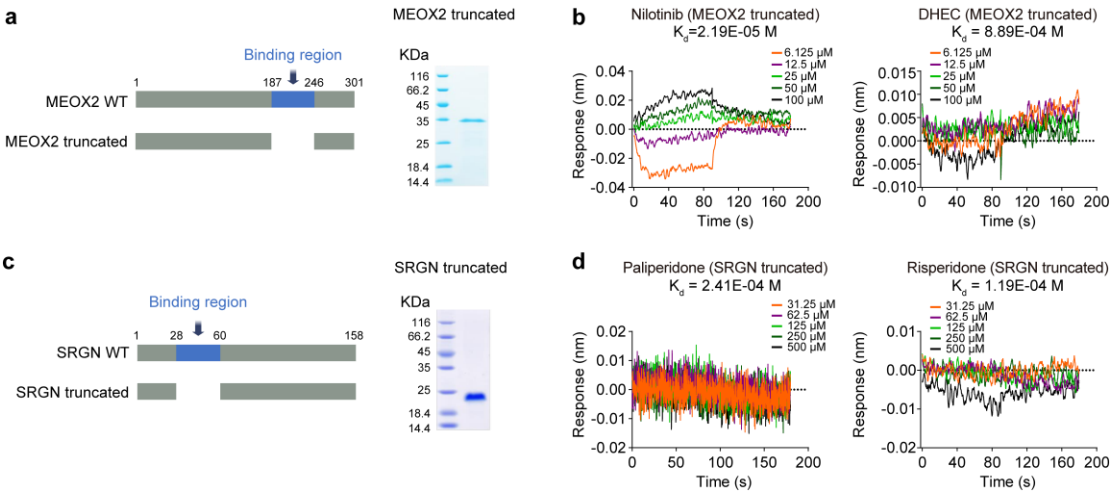

Response Fig R5. Truncated MEOX2 protein could not bind to Nilotinib and DHEC, and truncated SRGN protein could not bind to Paliperidone and Risperidone

a, (Left) Schematic representation of MEOX2 truncated protein. (Right) Coomassie blue-stained SDS-PAGE gel of truncated MEOX2 protein. **b,** Bio-layer interferometry (BLI) was used to detect the equilibrium dissociation constant (K_d) between nilotinib and DHEC with truncated MEOX2 protein. **c,** (Left) Schematic representation of SRGN truncated protein. (Right) Coomassie blue-stained SDS-PAGE gel of truncated SRGN protein. **d,** Bio-layer interferometry (BLI) was used to detect the equilibrium dissociation constant (K_d) between paliperidone and risperidone with truncated MEOX2 protein.

Other Questions:

Reviewer 1, Comment 5: The authors utilized CIBERSORTx to analyze the bulk TCGA GBM dataset and found that macrophages were more prevalent in GBM samples with high classical (CL)-mesenchymal (MES) signatures. To strengthen their conclusion, additional datasets and experiments could be useful, such as spatial analysis or co-staining with macrophage markers and CL-MES markers.

Response:

We appreciate the constructive comments. We utilized CIBERSORTx to analyze another three GBM datasets (CGGA, Rembrandt, and Ivy GAP). The proportion of myeloid cells in GBM with high CL-MES signatures was significantly higher than that in GBM with low CL-MES signatures. Moreover, CL-MES signature was positively correlated with enrichment of macrophages in CGGA, Rembrandt, and Ivy GAP GBM datasets (Response Fig. R6). We also performed immunofluorescence using co-staining of CD45 (macrophage marker) with SOX2 (stemness marker) and EGFR

(CL marker) / CD44 (MES marker). These results further confirmed that macrophages were more prevalent in GBM samples with high CL-MES signatures (Response Fig. R7).

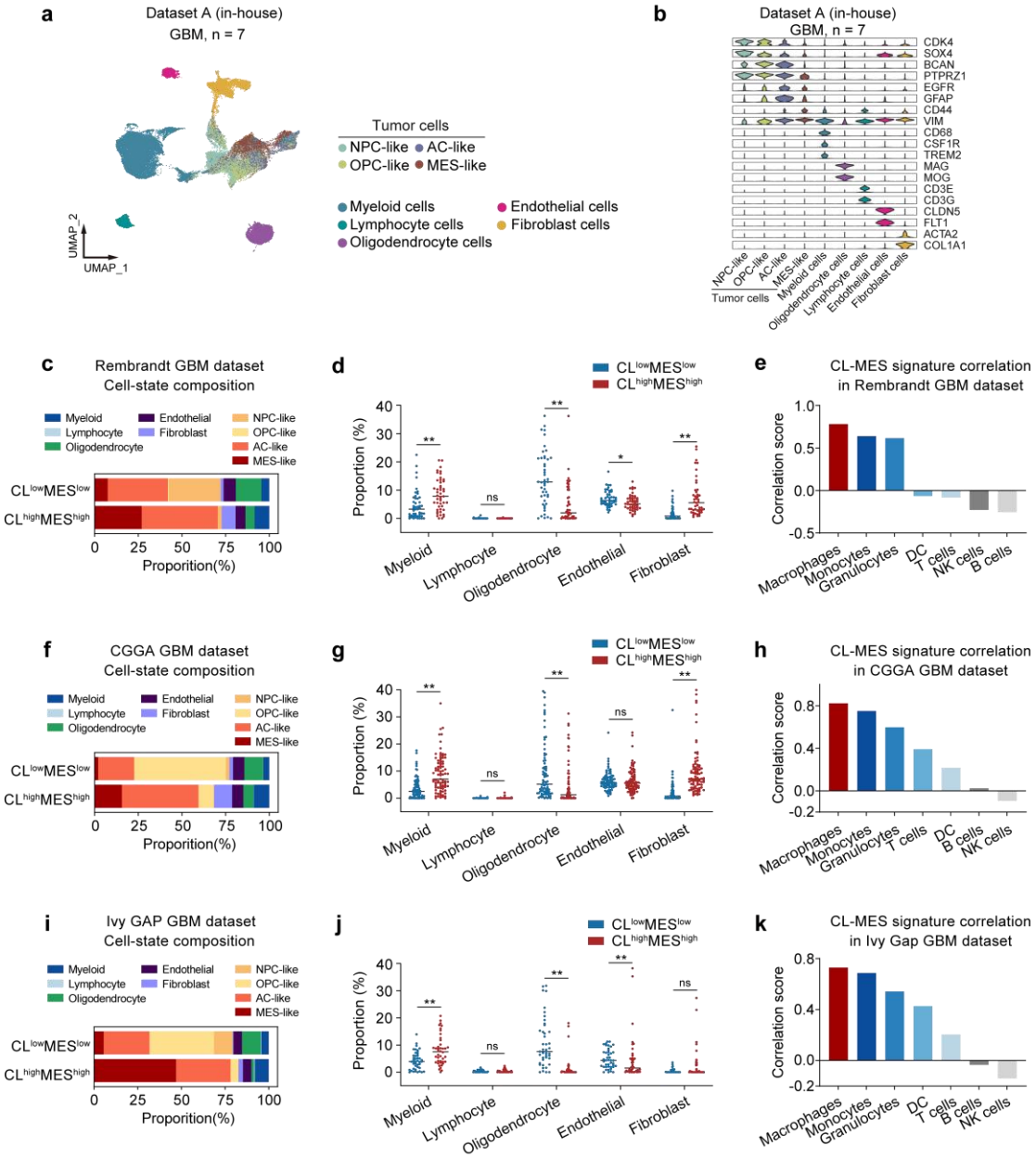

Response Fig R6. CL-MES signature was positively correlated with macrophages enrichment in GBM

a, The UMAP plot of GBM samples annotated by major cell types in dataset A (in-house). **b,** Violin plot of mean expression of marker genes for primary cell types in dataset A (in-house). **c,** Stacked bar plots indicate the cell composition of $CL^{low}MES^{low}$ and $CL^{high}MES^{high}$ GBM in the Rembrandt GBM dataset based on the single-cell-based deconvolution method, CIBERSORTx. **d,** Comparison of the proportion of cell composition between $CL^{low}MES^{low}$ and $CL^{high}MES^{high}$ GBM in the Rembrandt GBM dataset. **p < 0.01, p values from the t-test. **e,** Correlation coefficient

between CL-MES signatures and various types of immune cell signatures in Rembrandt GBM dataset. **f,** Stacked bar plots indicate the cell composition of $CL^{low}MES^{low}$ and $CL^{high}MES^{high}$ GBM in the CGGA GBM dataset based on the single-cell-based deconvolution method, CIBERSORTx. **g,** Comparison of the proportion of cell composition between $CL^{low}MES^{low}$ and $CL^{high}MES^{high}$ GBM in the CGGA GBM dataset. **p < 0.01, p values from the t-test. **h,** Correlation coefficient between CL-MES signatures and various types of immune cell signatures in the CGGA GBM dataset. **i,** Stacked bar plots indicate the cell composition of $CL^{low}MES^{low}$ and $CL^{high}MES^{high}$ GBM in the Ivy GAP GBM dataset based on the single-cell-based deconvolution method, CIBERSORTx. **j,** Comparison of the proportion of cell composition between $CL^{low}MES^{low}$ and $CL^{high}MES^{high}$ GBM in the Ivy GAP GBM dataset. **p < 0.01, p values from the t-test. **k,** Correlation coefficient between CL-MES signatures and various types of immune cell signatures in the Ivy GAP GBM dataset.

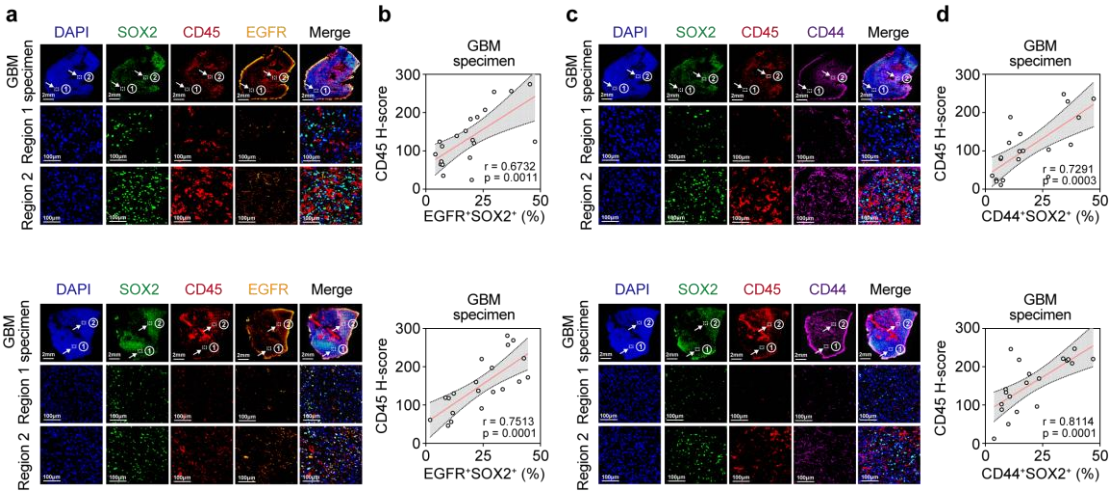

Response Fig R7. CL and MES GSCs were enriched in reactive immune region in GBM

a, Immunofluorescence images of DAPI (blue), SOX2 (green), CD45 (red), EGFR (yellow) expression in glioblastoma samples. Scale bar, 2 mm (top), 100 μm (middle), 100 μm (down). **b,** The correlations between EGFR, SOX2, and CD45 expressions are shown. **c,** Immunofluorescence images of DAPI (blue), SOX2 (green), CD45 (red), CD44 (purple) expression in glioblastoma samples. Scale bar, 2 mm (top), 100 μm (middle), 100 μm (down). **d,** The correlations between CD44, SOX2, and CD45 expressions are shown.

Reviewer 1, Comment 6: The validation of the predictive results in this paper is conducted using four cell lines (CL: 3028 and RKI, MES: 2907 and 839). However, additional information (e.g. genetic background) regarding these cell lines and any existing literature references detailing their derivation or prior use in research should be provided. Furthermore, an assessment of the basal expression levels of cellular state signatures in these four cell lines would be beneficial.

Response:

We thank the reviewer for the constructive suggestion. Four GSCs cell lines used in this paper (CL: 3028 and RKI, MES: 2907 and 839) have been widely used in previous studies. The PMIDs of studies that have used them are as follows: 37198486, 32619406, 30948495, and 36795488. The basal expression levels of subtype signatures in these four cell lines are shown as follows.

GSCs	gsva score			p value		
	PN	CL	MES	PN	CL	MES
3028	-0.0202	0.4154	0.0965	0.9041	0.0009	0.8761
RKI	0.3277	0.4056	-0.5830	0.0133	0.0002	0.9988
2907	-0.2492	-0.1116	0.4025	0.8414	0.9202	0.0004
839	0.0229	-0.4848	0.4292	0.2695	0.9998	0.0002

Reviewer 1, Comment 7: The authors' ATAC-seq data presented in Supplementary Figure 4b shows an absence of signal across all genes in the genome, which is unusual and raises concerns about the quality of the data obtained.

Response:

We thank the reviewer for pointing out this critical concern. ATAC-seq was conducted according to standardized procedures. Cell counting was performed using trypan blue staining. A desired number of cells was taken for transposition reaction. The PCR reaction system was configured to initiate PCR amplification of the transposition products. Single-stranded PCR products were produced via denaturation. The reaction system and program for circularization were subsequently configured and set up. Single-stranded cyclized products were produced, while uncyclized linear DNA molecules were digested. Single-stranded circle DNA molecules were replicated via rolling cycle amplification, and a DNA nanoball (DNB) which contain multiple copies of DNA was generated. Sufficient quality DNBs were then loaded into patterned nanoarrays using high-intensity DNA nanochip technique and sequenced through combinatorial Probe-Anchor Synthesis (cPAS). The poor cell viability after MEOX2 knockdown might be the reason for these results.

Reviewer 1, Comment 8: In all mouse experiments, the sample size should be labeled for each group.

Response:

We appreciate the constructive comments. We have labeled the sample size of all mouse experiments in our revised manuscript and figures.

Reviewer #3:

Reviewer 3, Comment 1: Based on growing transcriptomic and other data, it is not clear that it is biologically valid to "define GSC-like tumor cells as any cell expressing CD133, CD15 or OCT4, in conjunction with SOX2", for the glioma stem cell-like state is a dynamic one, as are all of the GBM cellular states and thus by selecting any one population, one may be skewing the data in these studies to a certain subset of genomic/epigenomic clones from the entire heterogenous population of clones that constitute any given GBM.

Response:

We thank the reviewer for this outstanding and constructive suggestion. In the eight scRNA-seq datasets we analyzed, the proportions of four cellular states malignant cells were as follows: NPC-like (22.19%), OPC-like (12.63%), AC-like (39.17%), MES-like (26.01%). The proportion of four cellular states of GSC-like tumor cells were similar to the proportion of all malignant cells, with NPC-like (21.23%), OPC-like (21.34%), AC-like (35.69%), MES-like (21.74%) (Response Fig. R1). These results suggest that our previous analysis didn't skew the data from the entire heterogeneous population of clones in GBM. For clarification, in order to interrogate the expression of MEOX2 and SRGN across all the malignant cells, we re-analyzed our in-house generated scRNA-seq datasets (dataset 1 and dataset 2) and six public scRNA-seq datasets (GSE103224, GSE117891, GSE131928, GSE141383, GSE173278 and GSE182109). The malignant cells were classified into four cellular states using the method reported by Neftel et al (*PMID:* 31327527). We also analyzed the expression of MEOX2 and SRGN in different subtypes GBM in three other bulk rna-seq datasets (CGGA, Rembrandt, and Gravendeel). Our current data support that MEOX2 and SRGN were characteristically enriched in CL/AC-like and MES/MES-like malignant cells, respectively (Response Fig. R2).

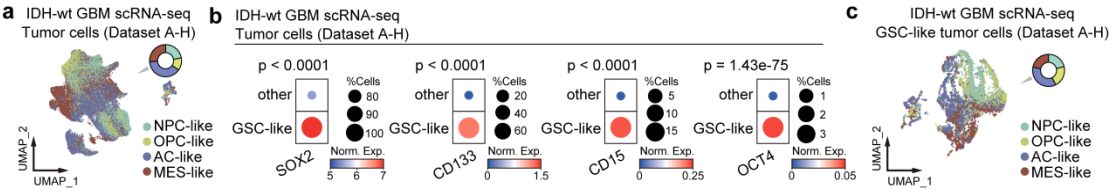

Response Fig R1. The expression profiles of GSCs markers confirming the accuracy of GSCs isolation

a, Four tumor cellular states mapped in UMAP coordinates of all tumor cells from dataset A-H. **b,** Bubble plot showing proportions and normalized expression levels of SOX2, CD133, CD15, and OCT4 in GSC-like tumor cells and other tumor cells from

dataset A-H. **c,** Four tumor cellular states mapped in UMAP coordinates of GSC-like tumor cells from dataset A-H.

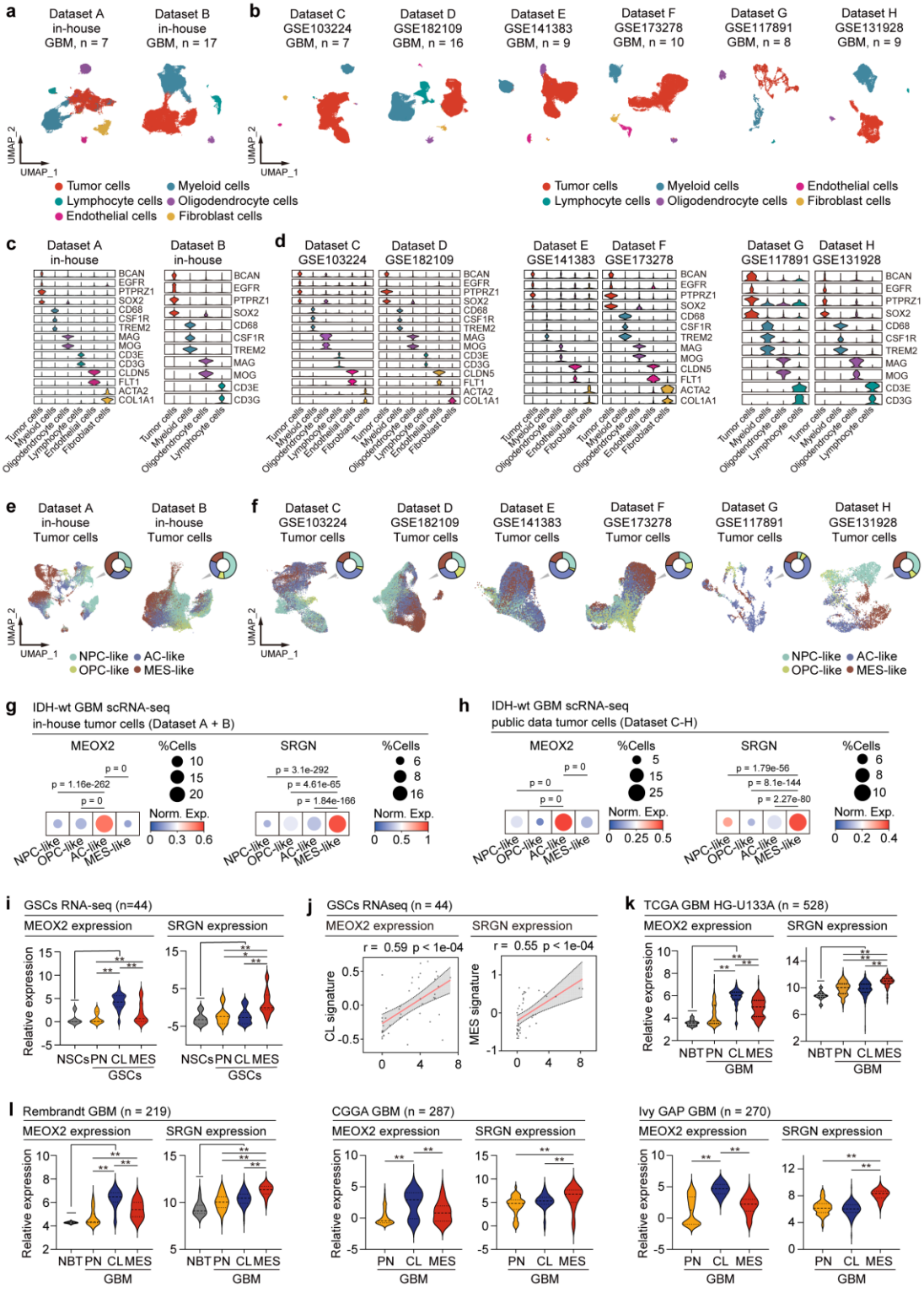

Response Fig R2. MEOX2 and SRGN are specific targets in CL and MES GBM, respectively

a, The UMAP plot of GBM samples annotated by major cell types in dataset A (in-house) and dataset B (in-house). **b,** The UMAP plot of GBM samples annotated by

major cell types in dataset C (GSE103224), dataset D (GSE182109), dataset E (GSE141383), dataset F (GSE173278), dataset G (GSE117891), and dataset H (GSE131928). **c,** Violin plot of mean expression of marker genes for primary cell types in dataset A (in-house), dataset B (n-house). **d,** Violin plot of mean expression of marker genes for primary cell types in dataset C (GSE103224), dataset D (GSE182109), dataset E (GSE141383), dataset F (GSE173278), dataset G (GSE117891), and dataset H (GSE131928). **e,** Four tumor cellular states mapped in UMAP coordinates from dataset A (in-house) and dataset B (in-house). **f,** Four tumor cellular states mapped in UMAP coordinates from dataset C (GSE103224), dataset D (GSE182109), dataset E (GSE141383), dataset F (GSE173278), dataset G (GSE117891), and dataset H (GSE131928). **g,** Bubble plot showing proportions and normalized expression levels of MEOX2 and SRGN in different cellular state tumor cells from dataset A (in-house) and dataset B (in-house). **h,** Bubble plot showing proportions and normalized expression levels of MEOX2 and SRGN in different cellular state tumor cells from dataset C (GSE103224), dataset D (GSE182109), dataset E (GSE141383), dataset F (GSE173278), dataset G (GSE117891), and dataset H (GSE131928). **i,** MEOX2 (left) and SRGN (right) gene expression in the Rembrandt, CGGA, and Ivy GAP GBM dataset.

Reviewer 3, Comment 2: The authors fail to acknowledge in a meaningful way the already rich body of published literature regarding the well documented single cell relationships between the MES-CL cell states and the immune microenvironment.

Response:

We thank the reviewer for pointing out this critical concern. Published literature suggested that MES cellular state was closely related with the immune microenvironment (PMID: 34087162, 33361384, 34562087, and 33857425). However, there are few reports on the relationship between CL cellular state and immune microenvironment. We also performed co-staining immunofluorescence using CD45 and EGFR (CL marker) to validate the enrichment of CL and MES GSCs in the reactive immune region. Immunofluorescence results showed that $SOX2^{+}EGFR^{+}$ cells were enriched in $CD45^{+}$ regions (Response Fig. R3). These results confirmed that CL GSCs were enriched in the reactive immune region. In our subsequent experiments, we observed high expression of anti-phagocytosis signals in CL GSCs, and MEOX2 regulated the resistance of macrophage phagocytosis in CL GSCs. Our analysis and experimental results are complementary to the existing findings. Given the limited significance of this finding, we have moved Fig. 1c to the supplemental figure.

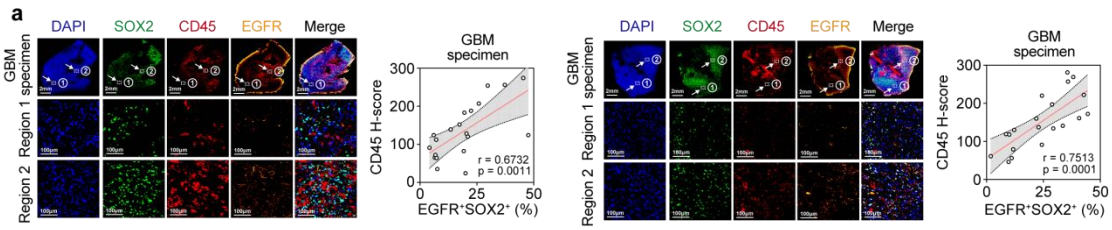

Response Fig R3. CL GSCs were enriched in reactive immune region in GBM

a, Immunofluorescence images of DAPI (blue), SOX2 (green), CD45 (red), EGFR (yellow) expression in glioblastoma samples. Scale bar, 2 mm (top), 100 μm (middle), 100 μm (down).

Reviewer 3, Comment 3: The survival curves in Fig 1D derived from patients from the investigators own institutions are not interpretable given the large number of biological and clinician factors that are known to be major prognostic factors in GBM patient survival. A multifactorial analysis of such factors, generally involving hundreds of patients, would be necessary to attribute any one molecular/genetic characteristic as an independent prognostic factor.

Response:

We thank the reviewer for pointing out this critical concern. Currently, there are few publicly available GBM single-cell transcriptome sequencing datasets that also disclose the survival time and clinical information of patients. Our results showed an association between the high proportion of malignant cells in CL and MES cellular states and poor survival in GBM patients at the single-cell scale. However, the statistical power for multifactorial analysis will be limited given the small number of patients involved. We acknowledged the importance of sample size in determining independent prognostic factors by using multifactorial analysis (*PMID:* 32289278, 36808285). We will increase the sample size in the future and use multifactorial analysis to observe whether this signature can serve as an independent prognostic factor.

Reviewer 3, Comment 4: It has been known for years that the PN subgroup of GBM has a slightly better survival than do other transcriptomic subtypes of GBM so the significance of Fig 1D is unclear.

Response:

We thank the reviewer for pointing out this critical concern. Given the limited significance of this finding, we have rearranged Figure 1. In the current Figure 1, we are focusing on screening targets with targeted therapeutic value in CL and MES GSCs.

Reviewer 3, Comment 5: The differential expression gene list between the different transcriptomic/cellular states (e.g. Neftel) runs into the hundreds between each state. It is entirely unclear the rationale for how and why the investigators chose their comparator groups (Fig. 1f, manuscript pages 7/8) to come up with MEOX2 and SRGN as typical CL and MES GSCs targets.

Response:

We thank the reviewer for pointing out this critical concern. Single-cell transcriptome differential analysis cannot guarantee that the isolated GSC-like tumor cells function as true GSCs. To screen for typical CL and MES GSCs targets, we combined the GSCs bulk RNA-seq data for joint analysis and screening. The GSCs used for bulk RNA-seq have undergone *in vitro* and *in vivo* functional validation. We selected NSCs and DGCs as controls to screen for targets that are typically overexpressed in GSCs. TCGA GBM datasets were used to verify the expression characteristics of the screened targets. Detailed screening procedures and reasons are as follows:

Step01. Differential gene expression analysis.

Identifying genes that were highly expressed in AC-like/CL and MES-like/MES GSCs.

For scRNA-seq data：AC-like/MES-like GSC-like tumor cells vs. other cellular state GSC-like tumor cells (scRNA-seq datasets, n = 80). MEOX2 expression was 2.2-fold higher in AC-like GSC-like tumor cells, SRGN expression was 1.78-fold higher in MES-like GSC-like tumor cells.

For bulk RNA-seq data:

GSCs bulk RNA-seq data: (1) CL/MES GSCs vs. CL/MES differentiated glioblastoma cells (DGCs) (in-house generated). MEOX2 expression was 3.02-fold higher in CL GSCs, SRGN expression was 4.73-fold higher in MES GSCs; (2) CL/MES GSCs vs. non-neoplastic neural stem cells (NSCs) (GSE119834). MEOX2 expression was 103.16-fold higher in CL GSCs, SRGN expression was 15.31-fold higher in MES GSCs; (3) CL/MES GSCs vs. other subtype GSCs (GSE119834). MEOX2 expression was 20.22-fold higher in CL GSCs, SRGN expression was 10.77-fold higher in MES

GSCs;

TCGA GBM bulk RNA-seq data: (1) GBM vs. non-neoplastic brain tissue (TCGA GBM HG-U133A), MEOX2 expression was 4.95-fold higher in CL GBM, SRGN expression was 4.24-fold higher in MES GBM; (2) CL/MES GBM vs. other subtype GBM (TCGA GBM HG-U133A), MEOX2 expression was 2.43-fold higher in CL GBM, SRGN expression was 2.03-fold higher in MES GBM.

Step02. CL/MES signature correlation analysis.

Identifying genes which expression were positively correlated with CL/MES subtype signature score.

Step03. Survival prognosis analysis.

Screening out genes which higher expression was associated with poorer patient survival in TCGA GBM datasets.

After the above screening steps, MEOX2 and SRGN were selected as typical CL and MES GSCs targets for subsequent studies.

Reviewer 3, Comment 6: As above, KM survival curves for GBM based on solely the arbitrary assignment of "high" versus "low" expression of a gene, totally disregarding all of the other critically important survival prognostic factors in GBM is not statistically valid. Also, the designation of "high" vs. "low" is an arbitrary chosen nominal data point in data that are actually continuous.

Response:

We thank the reviewer for pointing out this critical concern. We distinguish "high" or "low" based on the median value of gene or signature expression. Indeed, this approach does not adequately account for other critically important survival prognostic factors that are critical in GBM. However, most articles (like *PMID:* 27225120, 37737247, 28697342, and 32541784) use this method to analyze the correlation between target genes and patient survival prognosis currently.

Reviewer 3, Comment 7: I do not understand the point being made by showing that MEOX2/SRGN in GBM, a glial tumor, but not in systemic tumor types in Fig 1I?

Response:

We thank the reviewer for pointing out this critical concern. Through the analysis of the pan-cancer datasets in TCGA, we found that MEOX2 and SRGN expression were not elevated in most tumor types. These results suggest that MEOX2 and SRGN are characteristically up-regulated in GBM and could serve as unique therapeutic targets for GBM.

Reviewer 3, Comment 8: The knockdown experiments of MEOX2/SRGN in 2D are difficult to interpret because it has been clearly shown that the distribution of cellular states in almost all GSCs are contextually-based and when grown in vitro is heavily (and for some GSC lines, exclusively) skewed toward AC/MES-L states. Thus, it would not be surprising that knockdown of a MES-L dependence factor cause decreased proliferation and clonogenicity in vitro as shown in Fig. 2. To that point, however, it is curious that it did not cause such an effect on PN GSCs for even these lines should have a significant percentage of AC/MES-L cells in vitro as assessed by scRNA-seq and should therefore show some effects on proliferation albeit maybe not as much as the predominant AC/MES-L cells.

Response:

We thank the reviewer for pointing out this critical concern. This phenomenon is indeed interesting, but from our repeated experimental results, it was observed that the knockdown of MEOX2/SRGN has very little effect on the two PN GSCs that we tested. This may be due to the very low expression of MEOX2/SRGN in these two PN GSCs (Response Fig. R4).

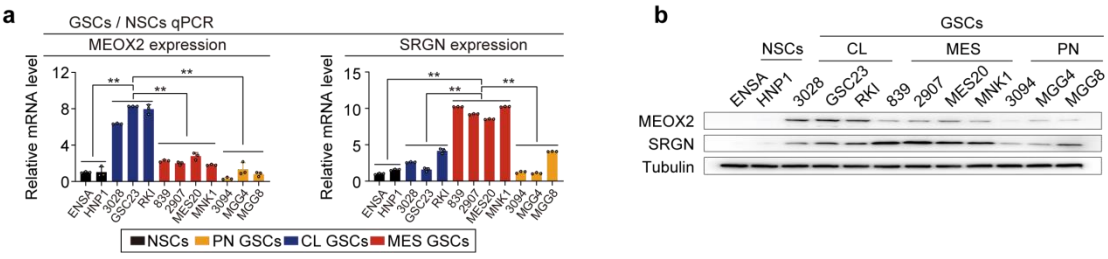

Response Fig R4. MEOX2 and SRGN expression were low in PN GSCs.

a, Relative mRNA expression of MEOX2 or SRGN normalized to 18S mRNA level in NSCs (n = 2) and different subtype GSCs (n = 10). **b,** MEOX2 and SRGN protein levels were measured by western blotting in NSCs (n = 2) and GSCs (n = 10). Tubulin was used as the loading control.

Reviewer 3, Comment 9: Despite a modest increase in survival of the

MEOX2/SRGN knockdown in Fig 2v, all the animals still died in a relatively quick amount of time. How can this be explained when the in vitro data show almost complete inhibition of proliferation and clonogenicity following MEOX2/SRGN knockdown?

Response:

We thank the reviewer for pointing out this critical concern. We found that this is common phenomenon for GSCs-derived GBM mouse models (*PMID:* 34615656, 30392959, 33023892, and 38563585). We believe that the reason for this result may be due to the difference in the number of cells used *in vitro* (2,000 cells) and i*n vivo* (50,000 cells). At the same time, the 96-well plate used in the cell viability experiment had a limited volume of medium. In fact, if fresh medium is added to the 96-well plate midway, the test results will be affected. There is a difference between this and the nutritionally adequate state after tumor formation in mice.

Reviewer 3, Comment 10: What were the cellular state distributions of the MEOX2/SRGN knockdown versus the control GSCs in vitro and in the growing intracranial tumors? It would be important to perform comparative scRNA-seq in both of these scenarios.

Response:

We thank the reviewer for this outstanding question and constructive suggestion. By analyzing our 3028 (CL) and 2907 (MES) GSCs RNA-seq data, we found a subtype transition in GSCs upon MEOX2 and SRGN knockout (Response Fig. R5). 3028 (CL) and 2907 (MES) were both patient-derived cell models and were not sorted by subtype-specific surface markers. Although RNA-seq data showed that 3028 and 2907 revealed a preference for CL and MES subtype, we considered them to be heterogeneous cell models containing GSCs of different cellular states. To validate this, we performed single-cell RNA sequencing on 3028 and 2907 GSCs. The analysis results showed that 3028 and 2907 models contained all four cellular states GSCs. Corresponding to the bulk RNA-seq results, 3028 had a higher proportion of AC-like GSCs and 2907 had a higher proportion of MES-like GSCs. After knocking down MEOX2 in 3028, the proportion of AC-like GSCs decreased. After knocking down SRGN in 2907, the proportion of MES-like GSCs decreased (Response Fig. R6). The above results proved that knocking out of MEOX2 mainly affected AC-like GSCs

and knocking out of SRGN mainly affected MES-like GSCs.

a

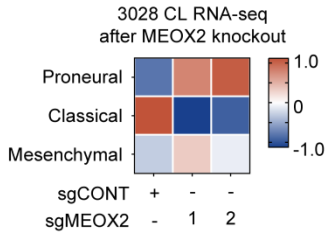

b

Group	gsva score			p value		
	PN	CL	MES	PN	CL	MES
sgCONT	-0.0202	0.4154	0.0965	0.9041	0.0009	0.8761
sgMEOX2-1	0.0363	-0.4899	-0.0882	0.3556	0.9910	0.4985
sgMEOX2-2	0.3746	-0.2124	0.0337	0.3187	0.9800	0.9800

c

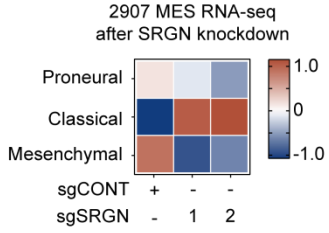

d

Group	gsva score			p value		
	PN	CL	MES	PN	CL	MES
sgCONT	0.2261	-0.0415	0.3863	0.0389	0.7602	0.0010
sgSRGN-1	0.0077	0.0649	-0.0311	0.7822	0.2468	0.9660
sgSRGN-2	-0.2876	-0.1140	-0.2998	0.8262	0.4765	0.9910

Response Fig R5. MEOX2 and SRGN maintained a CL and MES signature, respectively

a, Heatmap depicting the changes in subtype signature after MEOX2 knockout in 3028 CL GSCs. **b,** Summary of gsva score and p value of 3028 CL GSCs transduced with sgCONT, sgMEOX2-1, and sgMEOX2-2. **c,** Heatmap depicting the changes in subtype signature after SRGN knockout in 2907 MES GSCs. **d,** Summary of gsva score and p value of 2907 MES GSCs transduced with sgCONT, sgSRGN-1, and sgSRGN-2.

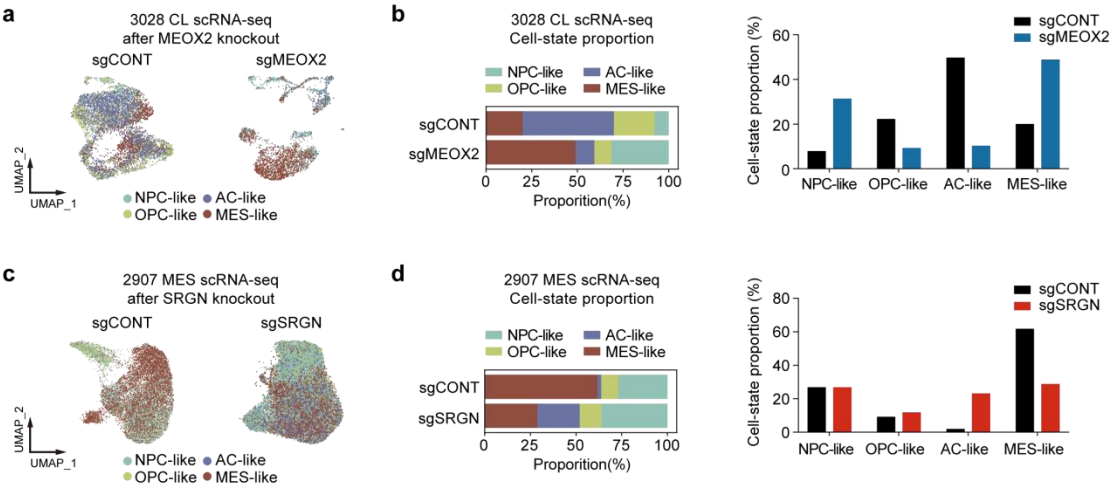

Response Fig R6. Knocking down MEOX2 mainly affected AC-like GSCs and knocking down SRGN primarily affected MES-like GSCs

a, The UMAP plot of 3028 CL GSCs annotated by four cellular states. **b,** Proportion changes of four cellular states cells in 3028 CL GSCs transduced with MEOX2 sgRNA or control sgRNA. **c,** The UMAP plot of 2907 MES GSCs annotated by four cellular states. **d,** Proportion changes of four cellular states cells in 2907 MES GSCs transduced with SRGN sgRNA or control sgRNA.

Reviewer 3, Comment 11: It would be important to look at the effect of Notch pathway activity in the different cellular states by scRNA-seq and to assess whether the effects of MEOX2/SRGN knockdown on chromatic accessibility at the single cell level to see if this is indeed an AC/MES-L specific effect.

Response:

We thank the reviewer for this outstanding question and constructive suggestion. Analysis of hallmark and KEGG pathway gene sets in four GBM scRNA-seq datasets highlighted that Notch signaling was enriched in AC-like subtype tumor cells. In contrast, NF-κB signaling was enriched in MES-like subtype tumor cells. By analyzing our newly added scRNA-seq data, we found that the enrichment level of Notch/NFκB signaling in all GSCs decreased after MEOX2/SRGN knockout (Response Fig. R7). These results proved that MEOX2-NOTCH and SRGN-NFκB axis were CL and MES specific effect, respectively.

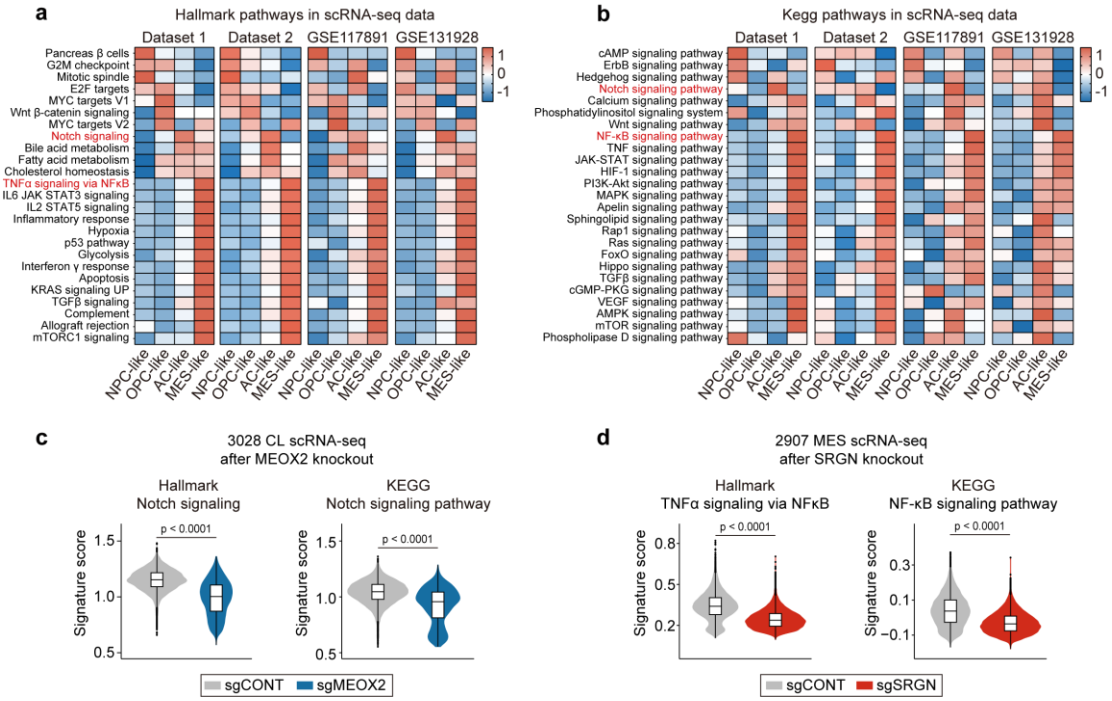

Response Fig R7. MEOX2-NOTCH and SRGN-NFκB axis maintain classical or mesenchymal status in GSCs, respectively

a and b, Heatmap of the pathway activities scored per cell by GSVA between four cellular states (NPC-like, OPC-like, AC-like, and MES-like) tumor cells in scRNA-seq datasets, using Hallmark (left) and KEGG (right) genesets. **c,** Violin-box plots showing the notch signaling score (Hallmark and KEGG) of the GSCs scRNA-seq data (sgCONT vs. sgMEOX2). Two-tailed unpaired Wilcoxon rank-sum test. **d,** Violin-box plots showing the NF-κB signaling score (Hallmark and KEGG) of the GSCs

scRNA-seq data (sgCONT vs. sgSRGN). Two-tailed unpaired Wilcoxon rank-sum test.

Reviewer 3, Comment 12: Did overexpression of Notch restore the transcriptomic profile of the the CL state in the MEOX2 knockdown cell lines?

Response:

We thank the reviewer for this excellent question. We overexpressed NOTCH1 in the MEOX2 knockdown 3028 and RKI CL GSCs. qRT-PCR validated the effects of NOTCH1 overexpression on the expression of CL state markers (Response Fig. R8). Our experimental results indicated that overexpression of NOTCH1 in CL GSCs restored the transcriptomic profile of the CL state (*PMID*: 28697342) in the MEOX2 knockdown GSCs.

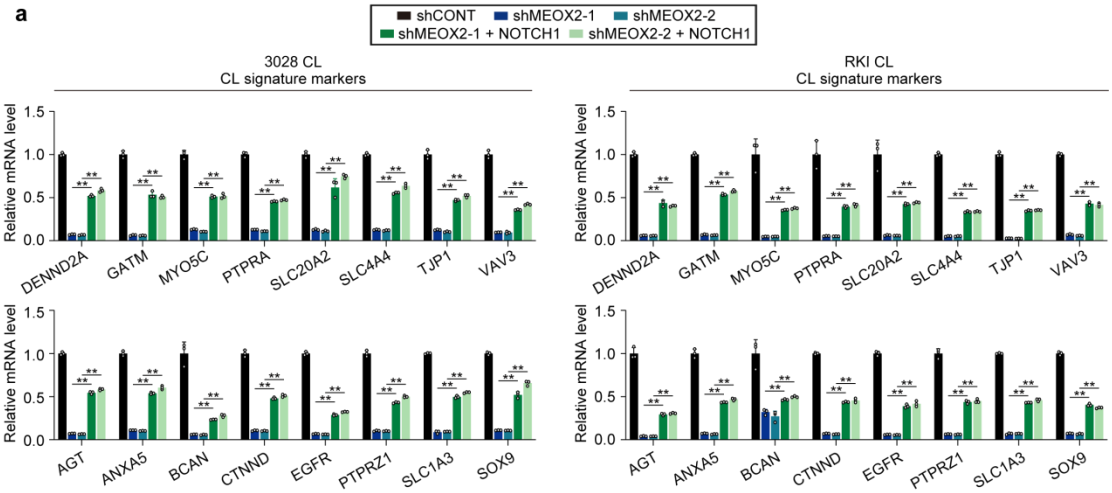

Response Fig R8. Overexpression of NOTCH1 restored the transcriptomic profile of the CL state in the MEOX2 knockdown CL GSCs

a, Classical signature markers expressions assessed by quantitative RT-PCR after CL GSCs transduced with shCONT, shMEOX2-1, shMEOX2-2, shMEOX2-1 + NOTCH1, or shMEOX2-2 + NOTCH1. Data are presented as mean ± SD from three independent experiments. **p < 0.01.

Reviewer 3, Comment 13: Did re-introducing Notch 1 into CL GSCs with MEOX2 knockdown restore in vivo growth to levels of non-knockdown lines?

Response:

We thank the reviewer for this excellent question. We overexpressed NOTCH1 in MEOX2 knockdown 3028 CL GSCs and performed *in vivo* experiments. Re-introducing NOTCH1 into CL GSCs with MEOX2 knockdown restored the *in vivo*

growth of tumor (Response Fig. R9).

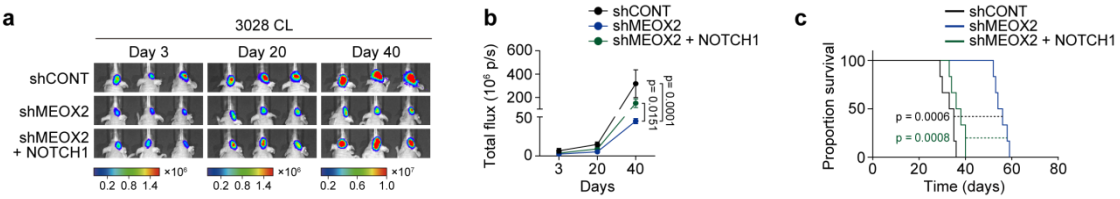

Response Fig R9. Re-introducing NOTCH1 into CL GSCs with MEOX2 knockdown restored the *in vivo* growth of tumor

a, Bioluminescence images of mice bearing orthotopic xenografts derived from luciferase-expressing 3028 (CL) cells, show the effect of shMEOX2 or shMEOX2 + NOTCH1 on tumor growth. **b,** Intensities of luciferase signal in mice in (a) are shown. **c,** Kaplan-Meier survival curves of mice bearing intracranial tumors derived from 3028 CL GSCs (n = 6) from the three groups in (a).

Reviewer 3, Comment 14: Although re-introducing NFKB1 into MES GSCs with SRGN knockdown restored the defect in cell proliferation and stem cell frequency, did it restore the MES-L transcriptomic profile?

Response:

We thank the reviewer for this excellent question. We overexpressed NFKB1 in the SRGN knockdown 2907 and 839 MES GSCs. qRT-PCR validated the effects of NFKB1 overexpression on the expression of SRGN state markers. Our experimental results indicated that overexpression of NFKB1 in MES GSCs restored the transcriptomic profile of the MES state (*PMID*: 28697342) in the SRGN knockdown GSCs (Response Fig. R10).

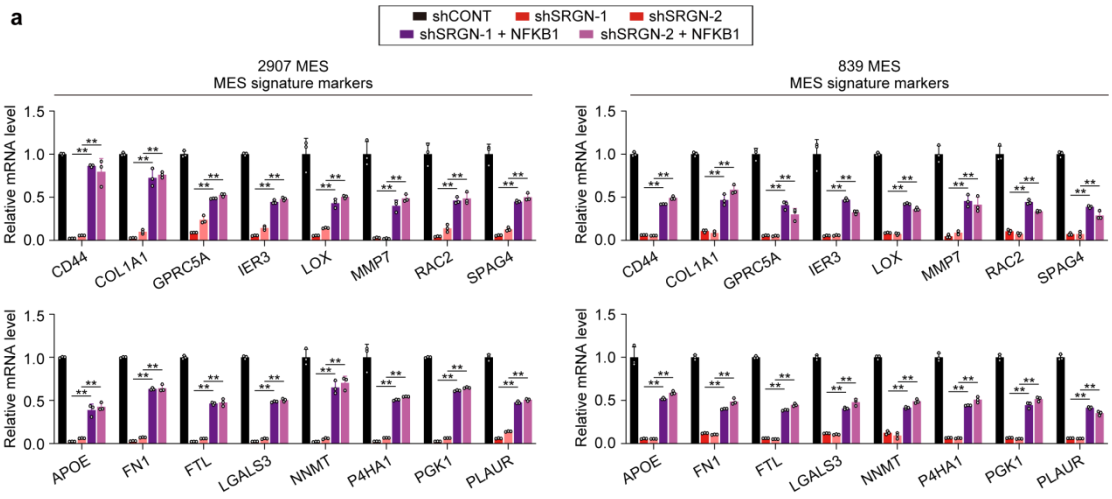

Response Fig R10. Overexpression of NFKB1 restored the transcriptomic profile of the MES state in the SRGN knockdown MES GSCs

a, Mesenchymal signature markers expressions assessed by quantitative RT-PCR after MES GSCs transduced with shCONT, shSRGN-1, shSRGN-2, shSRGN + NFKB1, or shSRGN + NFKB1. Data are presented as mean ± SD from three independent experiments. **p < 0.01.

Reviewer 3, Comment 15: Did re-introducing NFKB1 into MES GSCs with SRGN knockdown restore in vivo growth to the levels non-knockdown lines?

Response:

We thank the reviewer for this excellent question. We overexpressed NFKB1 in SRGN knockdown 2907 MES GSCs and performed *in vivo* experiments. Re-introducing NFKB1 into MES GSCs with SRGN knockdown restored in vivo growth of tumor (Response Fig. R11).

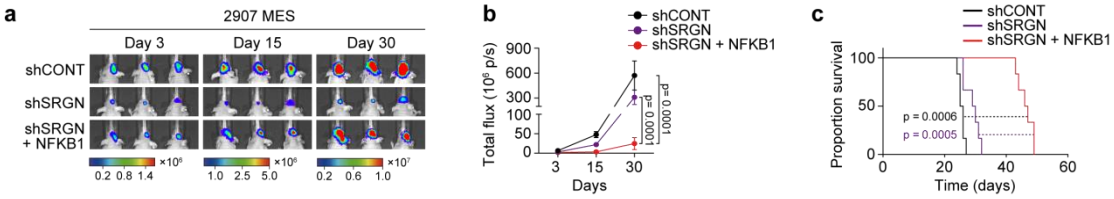

Response Fig R11. Re-introducing NFKB1 into MES GSCs with SRGN knockdown restored the *in vivo* growth of tumor

a, Bioluminescence images of mice bearing orthotopic xenografts derived from luciferase-expressing 2907 (MES) cells, show the effect of shSRGN or shSRGN + NFKB1 on tumor growth. **b,** Intensities of luciferase signal in mice in (a) are shown. **c,** Kaplan-Meier survival curves of mice bearing intracranial tumors derived from 2907 MES GSCs (n = 6) from the three groups in (a).

Reviewer 3, Comment 16: Although the presence of myeloid cells (including macrophages) in the GBM microenvironment is clearly important as has been demonstrated by numerous other investigators, is there any real data to think that macrophage-mediate glioma cell phagocytosis is a potent anti-tumor mechanism operative in human gliomas? This raises the question of the physiological relevance of the GSC-macrophage phagocytosis mixing experiments.

Response:

We thank the reviewer for this excellent question. The existing literature shows that reprogramming tumor-promoting macrophages into tumor-suppressive macrophages can effectively inhibit GBM growth (PMID: 35122055). It was shown that inhibition of the CD47-SIRPα (signal regulatory protein α) axis in TAMs inhibited brain tumor

growth in animal models (PMID: 30602457 and 28298418). Therefore, the methods related to enhancing the phagocytic effect of macrophages on GSCs also have high research significance. We revised the discussion section and added discussion about potential anti-tumor mechanisms of macrophage-mediated tumor cell phagocytosis in human GBM to highlight this point. The revised discussion sections are as follows:

Macrophage phagocytosis of tumor cells is governed by a balance of pro- and anti-phagocytic inputs, so-called 'Eat me' and 'Don't eat me' signals. When inhibitory receptors are predominantly triggered, macrophage activation is suppressed. The best-studied inhibitory receptor on macrophages is SIRPα, which recognizes as ligand the cell surface molecule CD47, often overexpressed on tumor cells. Reprogramming tumor-promoting macrophages into tumor-suppressive macrophages can effectively inhibit GBM growth. It was shown that inhibition of the CD47-SIRPα (signal regulatory protein α) axis in TAMs inhibited brain tumor growth in animal models. Therefore, the methods related to enhancing the phagocytic effect of macrophages on GSCs also have high research significance. We found high expression of anti-phagocytosis checkpoint in CL and MES GSCs. MEOX2 and SRGN are involved in regulating anti-phagocytosis checkpoint expression in CL and MES GSCs, respectively. Targeting MEOX2 and SRGN enhanced macrophage phagocytosis of CL and MES GSCs.

Reviewer 3, Comment 17: It would be important to demonstrate that the Notch and NFkB inhibitor drugs identified in your screen (Fig. 7) where specific both against GSCs compared to, 1. other, non-glioma tumor types, and 2: CL/MES GSCs compared to PN GSCs and the MEOX2 knockdown GSCs.

Response:

We thank the reviewer for this excellent question and constructive suggestion. We added experiments grouped as follows: 1. CL/MES GSCs vs. MUM-2B (Uveal melanoma tumor cells) / HEC-1-A (Uterine Corpus Endometrial Carcinoma tumor cells). These two tumor cells were chosen because MEOX2 and SRGN expression were low in these two tumor cells in pan-cancer analysis; 2. CL/MES GSCs vs. PN GSCs; 3. CL/MES GSCs vs. MEOX2/SRGN knockdown GSCs (Response Fig. R12). Compared with non-glioma tumor types and PN GSCs, nilotinib and DHEC were more effective against CL GSCs and paliperidone and risperidone were more effective against MES GSCs. MEOX2 knockdown decreased the sensitivity of CL GSCs to

nilotinib and DHEC. SRGN knockdown decreased the sensitivity of MES GSCs to paliperidone and risperidone. The above results further demonstrated the specificity of the drugs.

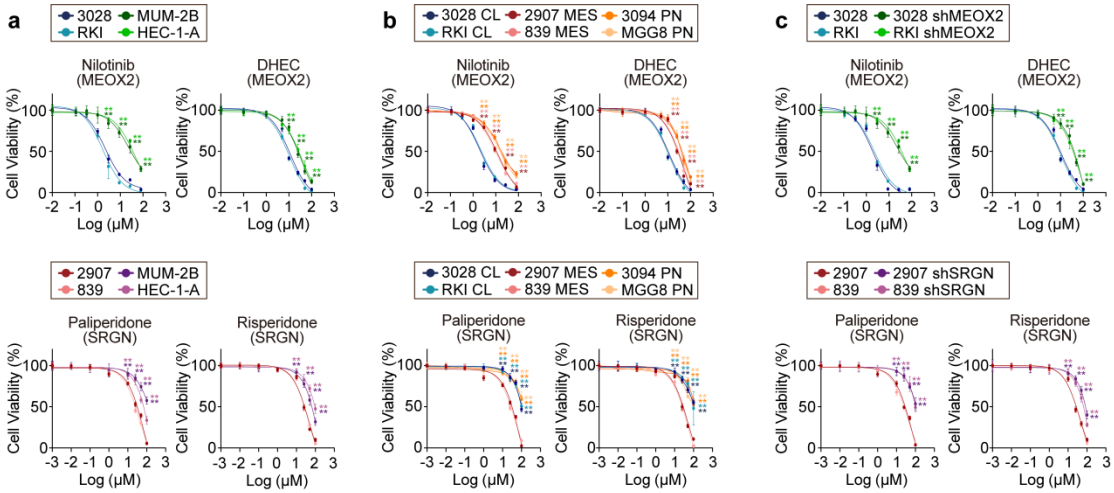

Response Fig R12. Nilotinib and DHEC have inhibitory effects on MEOX2, while paliperidone and risperidone have inhibitory effects on SRGN

a, Dose-response curves for potentially bound drugs with MEOX2/SRGN selected by virtual molecular screening in CL GSCs (3028, RKI)/MES GSCs (2907, 839), MUM-2B, and HEC-1-A . n = 6 per group. **p < 0.01, using one-way ANOVA. **b,** Dose-response curves for potentially bound drugs with MEOX2/SRGN selected by virtual molecular screening in PN GSCs (3094, MGG8), CL GSCs (3028, RKI), and MES GSCs (2907, 839). n = 6 per group. **p < 0.01, using one-way ANOVA. **c,** Dose-response curves for potentially bound drugs with MEOX2/SRGN selected by virtual molecular screening CL GSCs (3028, RKI)/MES GSCs (2907, 839) after MEOX2/SRGN knockdown . n = 6 per group. **p < 0.01, using one-way ANOVA.

Reviewer #4:

Major concerns:

Reviewer 4, Comment 1: One major shortcoming of this study is that the authors are confusing interpatient/intertumoral heterogeneity with intratumoral heterogeneity. The single-cell analyses are based on pooled patient samples, and the functional validation is based on different patient-derived cell lines that are genetically and epigenetically distinct, yet in reality the intrinsic GSC heterogeneity the authors propose to target should be within the same patient/tumor. Therefore, it is questionable whether MEOX2 and SRGN are still specific targets for CL and MES GSCs from the same patient (adding paired single-cell analysis by patient throughout the manuscript could help). Along this line, at least for the combinatorial drug treatment experiments (Figure 5 and 7), the authors should use GSC cell lines that exhibit both CL and MES features after xenograft (refer to Ref. 8 regarding the plasticity of glioma cell states), instead of artificially mixing up cell lines from different patients, to assess the treatment effects. These experiments are essential to substantiate the major claims of this manuscript.

Response:

We thank the reviewer for this excellent question and constructive suggestion. We completely agree that xenograft model from one GSC cell line should be used to demonstrate the combinatorial drug treatment efficacy. GSCs WL1 were derived in our laboratory from a 55-year-old male patient with recurrent GBM. We performed scRNA-seq on WL1 to determine its cellular states distribution. The results showed that WL1 contained cells of all four cellular states. The proportions of four cellular states cells in WL1 were as follows: NPC-like (33.44%), OPC-like (13.17%), AC-like (14.83%), MES-like (38.56%). GSCs WL1 were functionally validated by *in vivo* serial transplantation assays (Response Fig. R1). To obtain cells of CL/AC-like and MES/MES-like features, we isolated EGFR-high (CL/AC-like cell-surface marker) and CD44-high (MES/MES-like cell-surface marker) cells from WL1. We then implanted these GSCs (1:1) orthotopically into immunocompromised mice to establish the model. Next, we examined the therapeutic effects of drugs on this model. Bioluminescence imaging confirmed that combined therapy was more effective than monotherapy or vehicle control (Response Fig. R2). These results indicated that combined targeting of CL and MES GSCs with FDA-approved agents is an effective treatment strategy for heterogeneous GBM.

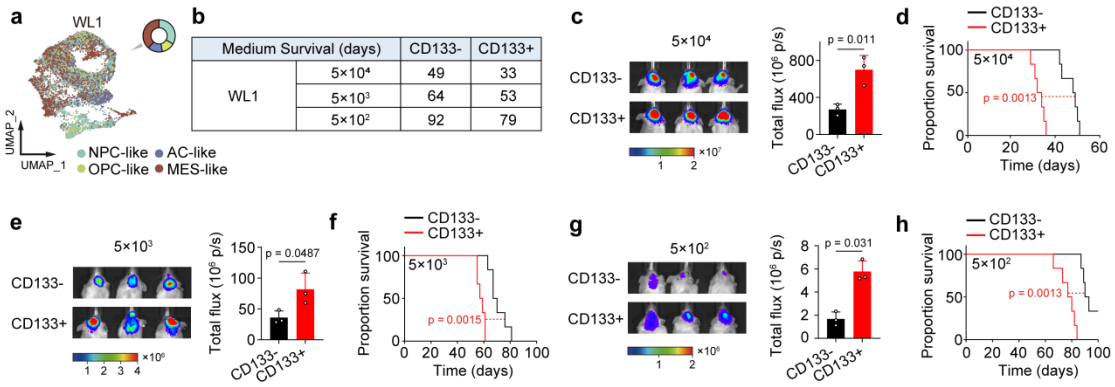

Medium Survival (days)		CD133-	CD133+
WL1	5×10⁴	49	33
	5×10³	64	53
	5×10²	92	79

Response Fig R1. WL1 GSCs is a heterogeneous model contains both CL and MES features

a, Four tumor cellular states mapped in UMAP coordinates from WL1 scRNA-seq data. **b,** Summary of mice medium survival in the in vivo limiting dilution assay. **c,** Bioluminescence images of mice bearing xenografts derived from 5 × 10^4 luciferase-expressing WL1 GSCs. *In vivo* bioluminescence imaging and intensities of luciferase signal in mice are shown. **d,** Kaplan–Meier survival curves of mice implanted with 5 × 10^4 WL1 GSCs (n = 6) are shown. **e,** Bioluminescence images of mice bearing xenografts derived from 5 × 10^3 luciferase-expressing WL1 GSCs. *In vivo* bioluminescence imaging and intensities of luciferase signal in mice are shown. **f,** Kaplan–Meier survival curves of mice implanted with 5 × 10^3 WL1 GSCs (n = 6) are shown. **g,** Bioluminescence images of mice bearing xenografts derived from 5 × 10^2 luciferase-expressing WL1 GSCs. *In vivo* bioluminescence imaging and intensities of luciferase signal in mice are shown. **h,** Kaplan–Meier survival curves of mice implanted with 5 × 10^2 WL1 GSCs (n = 6) are shown.

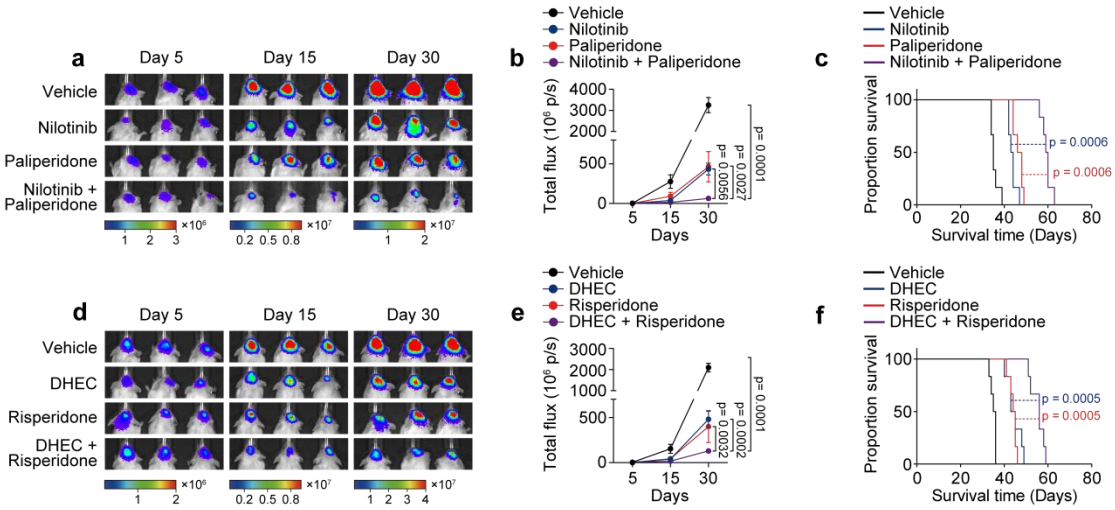

Response Fig R2. Combined therapy is more effective than monotherapy or vehicle control

a, Bioluminescence images of mice bearing mixed CL and MES xenografts derived from luciferase-expressing WL1 GSCs, showing the effect of combined treatment of

nilotinib and paliperidone on tumor growth. Time points indicate days after intracranial injection of mixed GSC populations. **b,** Intensities of luciferase signal in mice in (a) are shown. **c,** Kaplan-Meier survival curves for mice bearing subtype-mixed orthotopic tumors (WL1) (n = 6) after combined treatment of nilotinib (25 mg/kg) and paliperidone (10 mg/kg). P values were determined by the log-rank test. **d,** Bioluminescence images of mice bearing mixed CL and MES xenografts derived from luciferase-expressing WL1 GSCs, showing the effect of combined treatment of DHEC and risperidone on tumor growth. Time points indicate days after intracranial injection of mixed GSC populations. **e,** Intensities of luciferase signal in mice in (d) are shown. **f,** Kaplan-Meier survival curves for mice bearing subtype-mixed orthotopic tumors (WL1) (n = 6) after combined treatment of DHEC (15 mg/kg) and risperidone (10 mg/kg). P values were determined by the log-rank test.

Reviewer 4, Comment 2: Figure 1a, typically this analysis should yield a p-value yet the authors presented scaled scores instead. They need to clarify how these scaled scores were calculated and justify their use here. Also, two methods for calculating ssGSEA are mentioned in the methods section. The author should specify which method was used for each plot presented.

Response:

We appreciate the constructive comments from the reviewer. We re-analyzed the exact molecular signatures by GSVA package and using the permutation analysis to get the p-value. The signature score and p-value for each sample has been added in the Supplementary Table 1. This method was used for all analyses of cellular states definitions in this paper. We have revised the description in the method.

ID	NPClike	OPClike	AClike	MESlike	NPClike_pval	OPClike_pval	AClike_pval	MESlike_pval
GSC1	0.0244368	0.2790678	0.3698649	-0.105902	0.527363184	0.184079602	0.004975124	1
GSC10	0.184267	0.4707915	-0.362015	-0.474299	0.129353234	0.004975124	0.76119403	1
GSC11	0.3302665	0.5780171	0.5816078	-0.484313	0.004975124	0.004975124	0.004975124	1
GSC12	0.3119744	0.0990964	0.2891254	-0.050964	0.004975124	0.059701493	0.019900498	0.014925373
GSC13	0.4441103	0.3909692	0.5170721	-0.132236	0.004975124	0.07960199	0.004975124	0.60199005
GSC14	-0.188122	-0.340647	-0.363348	-0.346362	0.895522388	1	0.980099502	1
GSC15	-0.075012	-0.394108	-0.260665	0.2230592	0.955223881	1	0.950248756	0.567164179
GSC16	-0.337783	-0.27832	-0.122669	0.2796836	1	1	0.965174129	0.004975124
GSC17	-0.253087	-0.363001	-0.300496	0.420849	1	1	1	0.004975124
GSC18	-0.575674	-0.504183	-0.627165	0.3347846	1	1	1	0.004975124
GSC19	-0.402389	-0.450829	-0.351189	0.3740757	1	1	0.915422886	0.004975124
GSC2	0.5196773	0.696417	0.8178036	-0.240587	0.004975124	0.004975124	0.004975124	0.965174129
GSC20	0.1931838	0.0413395	0.2796193	0.267971	0.15920398	0.55721393	0.154228856	0.004975124
GSC21	-0.045429	0.1789179	0.1962195	0.5071799	0.328358209	0.044776119	0.004975124	0.004975124
GSC22	-0.307408	-0.421006	-0.397021	0.4183624	1	1	1	0.004975124
GSC23	-0.311436	-0.318515	0.2011069	0.6421887	1	1	0.721393035	0.004975124
GSC24	-0.395175	-0.476658	-0.434828	0.1769122	1	1	1	0.447761194
GSC25	0.0305903	-0.169433	-0.192956	0.2711849	0.552238806	0.825870647	0.691542289	0.014925373
GSC26	-0.367805	-0.414156	-0.12305	-0.255368	0.945273632	0.995024876	0.293532338	0.417910448
GSC27	-0.184139	0.3389289	0.3909868	-0.249087	0.378109453	0.004975124	0.004975124	0.218905473
GSC28	0.3839681	0.4520825	0.5502083	-0.192818	0.004975124	0.004975124	0.004975124	0.517412935
GSC29	-0.277191	-0.281228	-0.171487	-0.349398	0.109452736	0.169154229	0.004975124	0.014925373
GSC3	0.4738351	0.5262307	0.0484223	-0.519846	0.004975124	0.004975124	0.084577114	0.980099502
GSC30	-0.110944	-0.111906	0.1510979	0.2180024	0.412935323	0.268656716	0.039800995	0.004975124
GSC31	0.3659683	0.2505291	0.4007718	0.4456745	0.378109453	0.925373134	0.422885572	0.004975124
GSC32	0.3728359	0.6403839	-0.179604	-0.336906	0.004975124	0.004975124	0.810945274	1
GSC33	-0.111203	-0.339485	-0.307543	0.0978107	0.437810945	1	0.985074627	0.004975124
GSC34	0.2376393	-0.278864	0.4584436	0.3576274	0.109452736	0.965174129	0.004975124	0.004975124
GSC35	-0.344189	-0.252662	-0.255238	0.6065201	1	1	1	0.004975124
GSC36	0.4843208	-0.471222	-0.606727	-0.546057	0.004975124	1	1	1
GSC37	-0.23483	-0.385348	-0.515203	0.1586142	1	1	1	0.213930348
GSC38	-0.441027	-0.57536	-0.416832	-0.107013	1	1	0.870646766	0.004975124
GSC39	0.1510674	-0.213974	0.3178698	0.0244862	0.014925373	0.537313433	0.004975124	0.184079602
GSC4	0.6513792	0.7452317	0.391394	-0.473586	0.004975124	0.004975124	0.004975124	0.980099502
GSC40	-0.51357	-0.418614	-0.477146	0.2311127	1	1	1	0.293532338
GSC41	-0.392424	-0.316438	-0.397479	0.4789792	1	1	1	0.004975124
GSC42	0.1887366	-0.419221	-0.628624	-0.527943	0.039800995	1	1	1
GSC43	0.3553374	0.1651395	0.2042264	-0.490572	0.004975124	0.059701493	0.004975124	1
GSC44	-0.384402	0.3491952	-0.378856	-0.220175	1	0.004975124	0.995024876	1
GSC5	0.3113424	0.349546	0.5237004	0.2423976	0.104477612	0.044776119	0.004975124	0.407960199
GSC6	0.2535601	0.4870177	0.4614936	-0.081379	0.084577114	0.004975124	0.004975124	0.830845771
GSC7	0.4718289	0.4514355	0.3536351	-0.616603	0.004975124	0.004975124	0.004975124	1
GSC8	-0.083356	0.3902522	0.695589	-0.397937	0.572139303	0.024875622	0.004975124	0.721393035
GSC9	-0.099985	-0.256942	-0.255562	-0.48763	0.278606965	0.55721393	0.144278607	1

Reviewer 4, Comment 3: Figure 1b, the authors identified GSCs from public scRNAseq data by the expression of specific genes. It would be helpful to provide expression profiles of individual markers confirming the accuracy of GSC isolation.

Response:

We appreciate the constructive comments. We have added the expression profiles of CD133, CD15, OCT4, and SOX2 in isolated GSCs and other malignant cells. The expression of CD133, CD15, OCT4, and SOX2 were higher in GSC-like tumor cells than other malignant cells (Response Fig. R3).

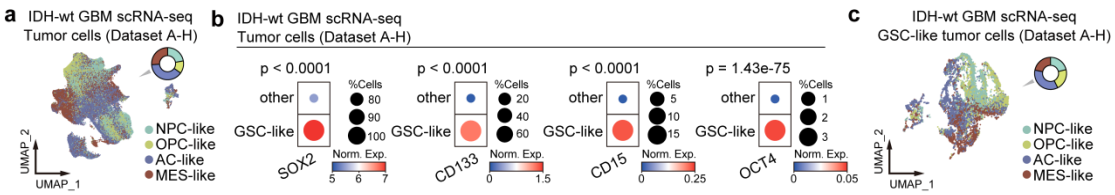

Response Fig R3. The expression profiles of GSCs markers confirming the accuracy of GSCs isolation

a, Four tumor cellular states mapped in UMAP coordinates of all tumor cells from dataset A-H. **b,** Bubble plot showing proportions and normalized expression levels of SOX2, CD133, CD15, and OCT4 in GSC-like tumor cells and other tumor cells from dataset A-H. **c,** Four tumor cellular states mapped in UMAP coordinates of GSC-like tumor cells from dataset A-H.

Reviewer 4, Comment 4: Figure 1j, it is more important to directly compare the protein levels of MEOX2 and SRGN between CL vs MES GSCs to demonstrate specificity.

Response:

We appreciate the reviewer's constructive comments. We have directly compared the protein levels of MEOX2 and SRGN in PN, CL, MES GSCs and NSCs in Supplemental Fig. 1g in the initial submission. Given the importance of these data, we have rearranged its position and updated it in Fig. 1h in revised manuscript (Response Fig. R4).

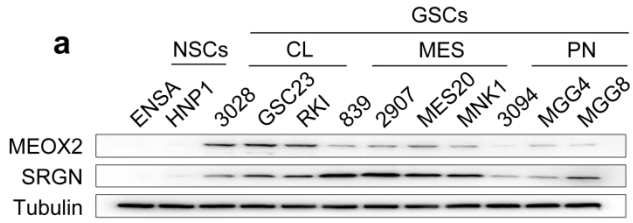

Response Fig R4. MEOX2 and SRGN are specific targets of CL and MES GSCs, respectively

a, MEOX2 and SRGN protein levels were measured by western blotting in NSCs (n = 2) and GSCs (n = 10). Tubulin was used as the loading control.

Reviewer 4, Comment 5: Figure 1h, the authors should present normalized gene expression including a p-value. Scaled values may exaggerate the variation, potentially skewing the interpretation of the results.

Response:

We thank the reviewer for the constructive suggestion. We have used dot plots to present normalized MEOX2 and SRGN expression including a p-value in our revised manuscript (Response Fig. R5).

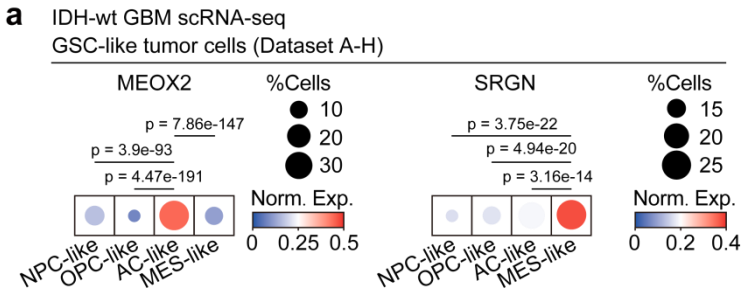

Response Fig R5. Normalized expression of MEOX2 and SRGN in GSC-like tumor cells

a, Bubble plot showing proportions and normalized expression levels of MEOX2 and SRGN in GSC-like tumor cells from dataset A-H.

Reviewer 4, Comment 6: Figure S1k, where 28 SRT datasets are available, why only two were selected for presentation?

Response:

We appreciate the constructive comments from the reviewer. In Supplemental Fig. 1k, we selected the representative images for presentation. To present the MEOX2 expression, SRGN expression, AC-like signature, MES-like signature, and Reactive immune signature from all 28 samples (16 of 28 are IDH-WT GBM), we quantified the putative distance between MEOX2/SRGN expressed spots and GBM subtypes/reactive immune region. MEOX2 enriched spots were in proximity to AC-like and reactive immune region. SRGN enriched spots were in proximity to MES-like and reactive region. We also presented scatter plots of another four samples (Response Fig. R6).

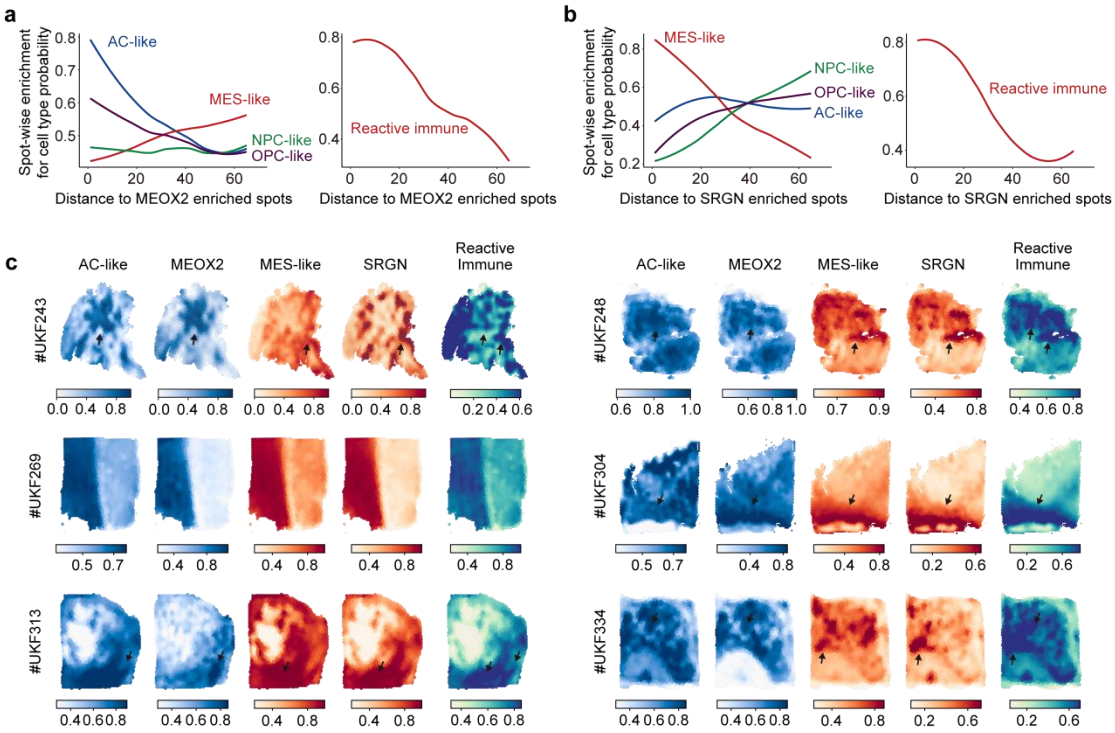

Response Fig R6. MEOX2 and SRGN enriched regions overlapped with reactive immune regions

a and b, Line diagrams show the spatial relationship between MEOX2/SRGN, AC-like/MES-like, and reactive immune region. The x-axis represents the relative distance to MEOX2/SRGN. The y-axis shows the probability of a particular gene set probability. If high cell probability values are displayed at a short distance from MEOX2/SRGN, the likelihood of a spatial relationship is high, n = 16. **c,** Scatter plot of the 2D representation of AC-like/MES-like cellular stat, MEOX2/SRGN expression and reactive immune signature in GBM spatical transriptomics.

Reviewer 4, Comment 7: Figure 1k, it is necessary to conduct a statistical analysis to confirm the association between SOX2 and MEOX2/SRGN. Furthermore, the claim that CL and MES GSCs are enriched in the reactive immune region needs validation using classic CL or MES markers such as VIM, CD44 or GFAP.

Response:

We thank the reviewer for the constructive suggestion. We have added the statistical analysis to confirm the association between SOX2 and MEOX2/SRGN (Response Fig. R7). We also performed co-staining immunofluorescence using CD45 and EGFR (CL marker)/ CD44 (MES marker) to validate the enrichment of CL and MES GSCs in the reactive immune region. Immunofluorescence results showed that $SOX2^{+}EGFR^{+}$ and $SOX2^{+}CD44^{+}$ cells were enriched in $CD45^{+}$ regions (Response Fig. R8). These results confirmed that CL and MES GSCs were enriched in the reactive immune region.

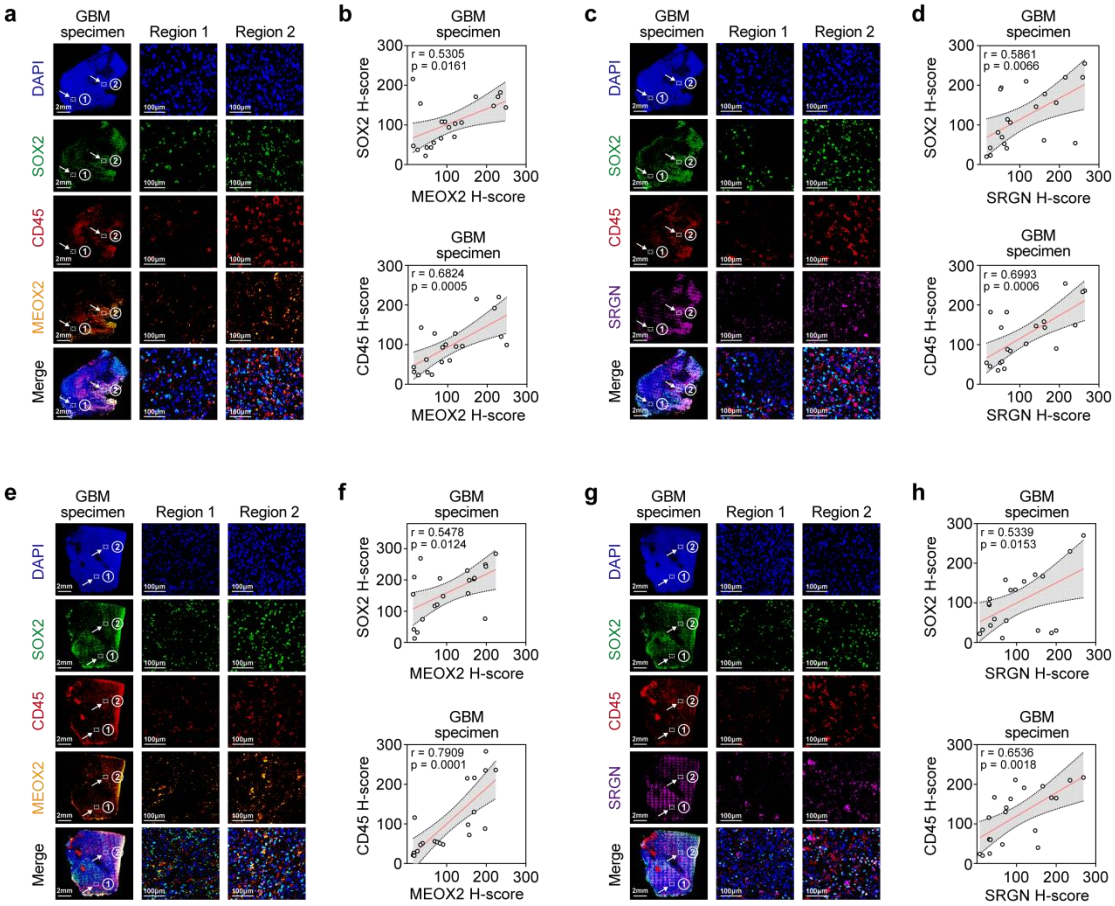

Response Fig R7. CL and MES GSCs were enriched in reactive immune region in GBM

a and c, Immunofluorescence images of DAPI (blue), SOX2 (green), CD45 (red), MEOX2 (yellow) expression in glioblastoma samples. Scale bar, 2 mm (left), 100 μm (middle), 100 μm (right). **b and d,** The correlations between MEOX2 and SOX2/CD45 expressions are shown. **e and g,** Immunofluorescence images of DAPI (blue), SOX2 (green), CD45 (red), SRGN (purple) expression in glioblastoma samples. Scale bar, 2 mm (left), 100 μm (middle), 100 μm (right). **f and h,** The correlations between SRGN and SOX2/CD45 expressions are shown.

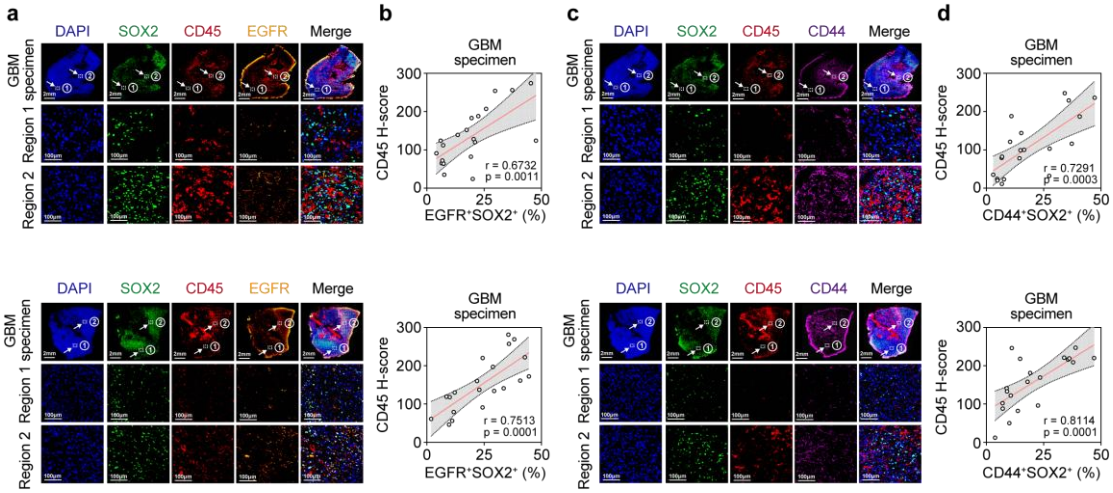

Response Fig R8. CL and MES GSCs were enriched in reactive immune region in GBM

a, Immunofluorescence images of DAPI (blue), SOX2 (green), CD45 (red), EGFR (yellow) expression in glioblastoma samples. Scale bar, 2 mm (top), 100 μm (middle), 100 μm (down). **b,** The correlations between EGFR, SOX2, and CD45 expressions are shown. **c,** Immunofluorescence images of DAPI (blue), SOX2 (green), CD45 (red), CD44 (purple) expression in glioblastoma samples. Scale bar, 2 mm (top), 100 μm (middle), 100 μm (down). **d,** The correlations between CD44, SOX2, and CD45 expressions are shown.

Reviewer 4, Comment 8: Figure 2u and other Biolum results need quantification.

Response:

We thank the reviewer for the constructive suggestion. We have added the quantitative values of luciferase signal in mice for all Biolum results. The revised Figure. 2u is shown as follows (Response Fig. R9).

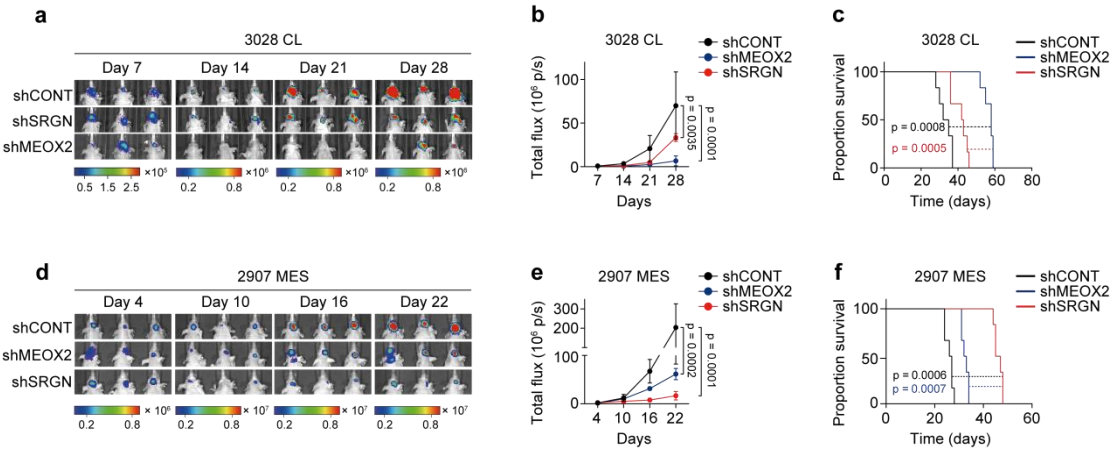

Response Fig R9. The anti-tumor effects of MEOX2 and SRGN knockdown were more effective in CL and MES GSCs, respectively

a, Bioluminescence images of mice bearing orthotopic xenografts derived from

luciferase-expressing 3028 (CL) cells, show the effect of shCONT, shSRGN, or shMEOX2 on tumor growth. **b,** Intensities of luciferase signal in mice in (a) are shown. **c,** Kaplan-Meier survival curves of mice bearing intracranial tumors derived from 3028 CL GSCs (n = 6) from the three groups in (a). **d,** Bioluminescence images of mice bearing orthotopic xenografts derived from luciferase-expressing 2907 (MES) cells, show the effect of shCONT, shMEOX2, or shSRGN on tumor growth. **e,** Intensities of luciferase signal in mice in (d) are shown. **f,** Kaplan-Meier survival curves of mice bearing intracranial tumors derived from 2907 MES GSCs (n = 6) from the three groups in (d).

Reviewer 4, Comment 9: Figure 5a, the author should provide evidence that the designated cell clusters are reliable for subsequent deconvolution analysis.

Response:

We thank the reviewer for the constructive suggestion. We have added violin plots to show the reliability of the designated cell clusters. The results showed that our annotation effectively distinguished different cell types and four cellular states of tumor cells in GBM scRNA-seq data. We also utilized CIBERSORTx to analyze another three GBM datasets (CGGA, Rembrandt, and Ivy GAP). The proportion of myeloid cells in GBM with high CL-MES signatures was significantly higher than that in GBM with low CL-MES signatures. Moreover, CL-MES signature was positively correlated with enrichment of macrophages in CGGA, Rembrandt, and Ivy GAP GBM datasets (Response Fig. R10).

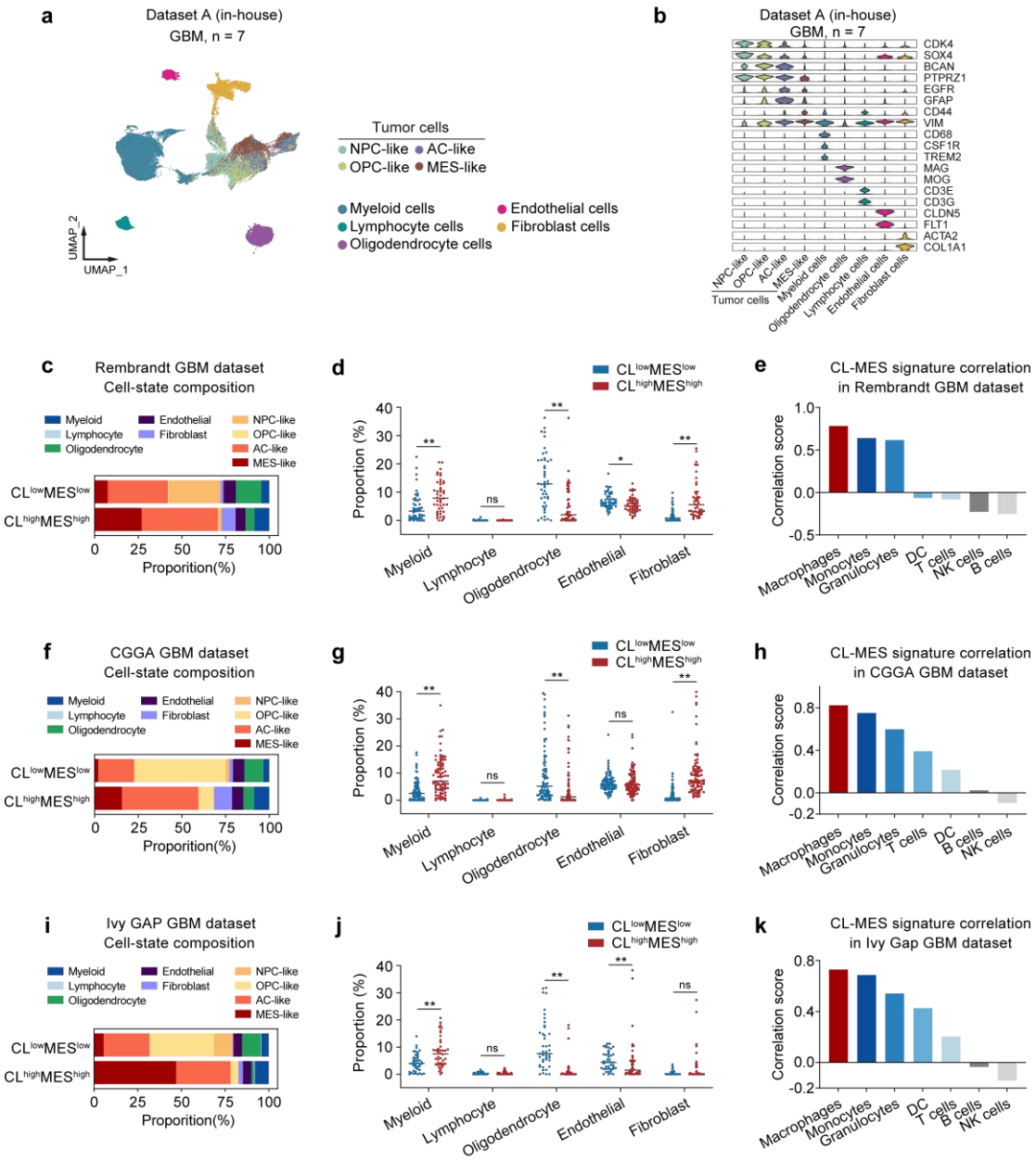

Response Fig R10. CL-MES signature was positively correlated with macrophages enrichment in GBM

a, The UMAP plot of GBM samples annotated by major cell types in dataset A (in-house). **b,** Violin plot of mean expression of marker genes for primary cell types in dataset A (in-house). **c,** Stacked bar plots indicate the cell composition of $CL^{low}MES^{low}$ and $CL^{high}MES^{high}$ GBM in the Rembrandt GBM dataset based on the single-cell-based deconvolution method, CIBERSORTx. **d,** Comparison of the proportion of cell composition between $CL^{low}MES^{low}$ and $CL^{high}MES^{high}$ GBM in the Rembrandt GBM dataset. **p < 0.01, p values from the t-test. **e,** Correlation coefficient between CL-MES signatures and various types of immune cell signatures in Rembrandt GBM dataset. **f,** Stacked bar plots indicate the cell composition of $CL^{low}MES^{low}$ and $CL^{high}MES^{high}$ GBM in the CGGA GBM dataset based on the single-cell-based deconvolution method, CIBERSORTx. **g,** Comparison of the proportion of cell

composition between $CL^{low}MES^{low}$ and $CL^{high}MES^{high}$ GBM in the CGGA GBM dataset. **p < 0.01, p values from the t-test. **h,** Correlation coefficient between CL-MES signatures and various types of immune cell signatures in the CGGA GBM dataset. **i,** Stacked bar plots indicate the cell composition of $CL^{low}MES^{low}$ and $CL^{high}MES^{high}$ GBM in the Ivy GAP GBM dataset based on the single-cell-based deconvolution method, CIBERSORTx. **g,** Comparison of the proportion of cell composition between $CL^{low}MES^{low}$ and $CL^{high}MES^{high}$ GBM in the Ivy GAP GBM dataset. **p < 0.01, p values from the t-test. **h,** Correlation coefficient between CL-MES signatures and various types of immune cell signatures in the Ivy GAP GBM dataset.

Reviewer 4, Comment 10: The author has identified specific inhibitors by predicting interactions and BLI. To confirm drug specificity, the authors should consider using negative controls such as truncated proteins lacking the binding domain.

Response:

We thank the reviewer for this critical suggestion. The Alphafold 2 database model was applied to predict the potential binding region of the MEOX2 and SRGN protein (DNA binding region of MEOX2: 187-246 amino acids; Binding pocket of SRGN: 28-60 amino acids). To confirm drug specificity, we used truncated MEOX2 and SRGN proteins lacking the binding domain as negative control and performed BLI experiment. The results showed that the truncated MEOX2 and SRGN proteins could not bind to their pertinent drugs (nilotinib and DHEC for MEOX2, paliperidone and risperidone for SRGN) (Response Fig. R11).

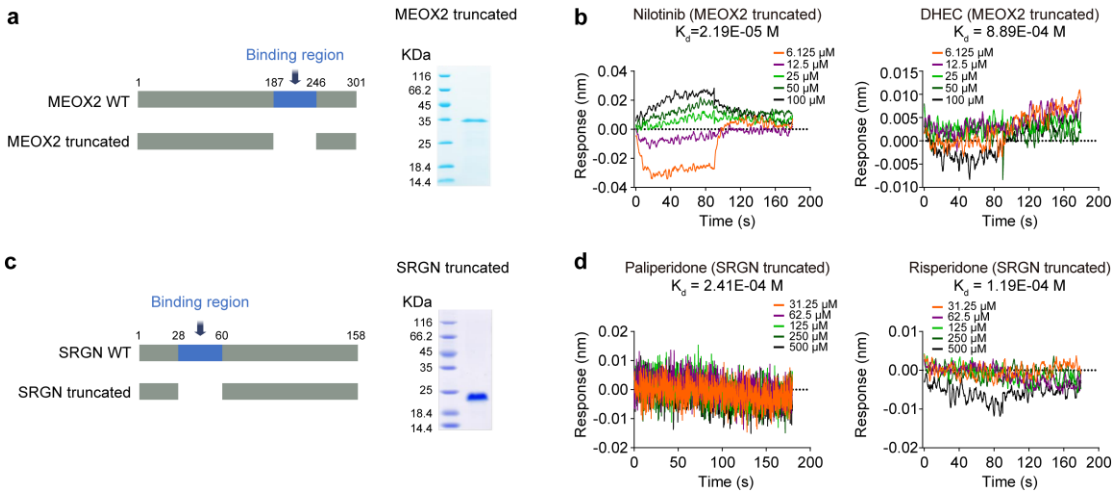

Response Fig R11. Truncated MEOX2 protein could not bind to Nilotinib and DHEC, and truncated SRGN protein could not bind to Paliperidone and Risperidone

a, (Left) Schematic representation of MEOX2 truncated protein. (Right) Coomassie

blue-stained SDS-PAGE gel of truncated MEOX2 protein. **b,** Bio-layer interferometry (BLI) was used to detect the equilibrium dissociation constant (K_d) between nilotinib and DHEC with truncated MEOX2 protein. **c,** (Left) Schematic representation of SRGN truncated protein. (Right) Coomassie blue-stained SDS-PAGE gel of truncated SRGN protein. **d,** Bio-layer interferometry (BLI) was used to detect the equilibrium dissociation constant (K_d) between paliperidone and risperidone with truncated MEOX2 protein.

Minor issues:

Reviewer 4, Comment 11: Throughout the figures, the number of samples/cells in each group should be clearly labeled or specified in the legends.

Response:

We thank the reviewer for the constructive suggestion. The number of samples/cells have been added in the labels and legends in all main and supplementary figures.

Reviewer 4, Comment 12: The term 'estimate immune' in Figure S1a requires clarification regarding its definition and calculation. Also, the term 'relative expression' throughout needs clarification on how these values are calculated.

Response:

We thank the reviewer for the constructive suggestion. The geneset of 'estimate immune' was from the following paper (*PMID:* 24113773). This reference has now been cited in the revised manuscript. The signature score genes (containing 141 genes) was calculated using GSVA package. We have added the definition of 'relative expression' in the legends of each figure.

Reviewer 4, Comment 13: There are some inaccuracies in Methods. a) The author mentioned using the NormalizeData function to regress out sequencing depth and the percentage of mitochondrial genes. However, the correct function for these adjustments is typically ScaleData. b) When using Harmony, it is important to note that the dimension reduction should occur within the Harmony-adjusted space rather than a PCA space.

Response:

We thank the reviewer for pointing out this concern and apologize for the confusion. We have re-examined our code and found that the analysis methods we adopted were consistent with what you described. We have corrected the corresponding

description in the Method section. The revised descriptions are as follows:

After quality control, we normalized data by NormalizeData function in Seurat. The most variable 2000 genes were determined using the FindVariableGenes function with default parameters. We used the ScaleData function in Seurat to regress out UMI count and percentage of mitochondrial genes. PCA was performed using the RunPCA with these 2000 genes in Seurat.

We performed the 'RunHarmony' Harmony function to remove the effect of confounding factors in different samples. Dimensionality reduction was then performed using Harmony-adjusted space and UMAP plots were generated by the RunUMAP Seurat function. To identify cell clusters, we performed the FindNeighbors and FindClusters function in Seurat with the FindClusters parameter "resolution = 1".

Reviewer 4, Comment 14: Figure 3f, the author should clarify what the dashed line represents in the legend.

Response:

We thank the reviewer for the constructive suggestion. We have added the description of the dashed line that represents FDR = 0.05 in the legend.

Reviewer #1:

Major Questions:

Reviewer 1, Comment 1: Related to my comment 1, how the authors define GSCs remains unclear. Glioblastoma stem cells (GSCs) are generally considered stem cell-like tumor cells, represented by NPC-like and OPC-like states in GBM, as reported by Neftel et al. However, the authors use SOX2, CD133, CD5, and OCT4 markers to identify GSCs in GBM datasets and then classify them into NPC-like, OPC-like, AC-like, and MES-like states. The authors need to clarify the overall proportion of GSCs in GBM, as well as the GSC proportion among the four GBM cell states.

Response:

We appreciate the constructive comments. The definition of GSCs has been a subject of controversy. A review published in ***Nature Reviews Cancer*** (2022, *PMID*: 35710946) offered refreshed perspective on the definition of GSCs: "*GSCs occupy a functionally defined cellular state characterized by self-renewal and tumour-initiating capacity with inherent plasticity that is agnostic to the cell of origin, frequency, proliferation rate or specific molecular markers."* The GSCs used in this study have undergone *in vitro* and *in vivo* functional validation as reported in several prior publications (*PMIDs*: 37198486, 32619406, 30948495, and 36795488). In fact, the corresponding author of the article, Neftel et al., discussed the relationship between GSCs and GBM cellular states in a review article published in ***Cancer Cell*** (2020, *PMID*: 32396858). The review described this: "*As described here for GBM, multiple cellular states may function as GSCs, these states might interconvert, and functionally established GSC markers might isolate distinct cellular states rather than a unique subpopulation."* Furthermore, the review reported the following: *"Strikingly, most of these GSC markers showed a significant bias toward one of the four GBM cellular states, and each of the four states was enriched by some of the markers."* (Response Fig. R1). We also analyzed the expression of GSC markers in our in-house scRNA-seq datasets (dataset 1 and dataset 2), including GSC surface markers (CD133, CD15, CD24, CD44, L1CAM, EGFR, and PDGFRA) as well as transcription factors (TFs) and lineage markers (SOX2, OCT4, BRN2, OLIG2, ID1, NANOG, and NES) . Most markers showed expression in two of the four states or no discernable pattern, while CD24 is the highest in NPC-like cells, CD133 and PDGFRA in OPC-like cells, EGFR in AC-like cells, and CD44 in MES-like cells (Response Fig. R2).

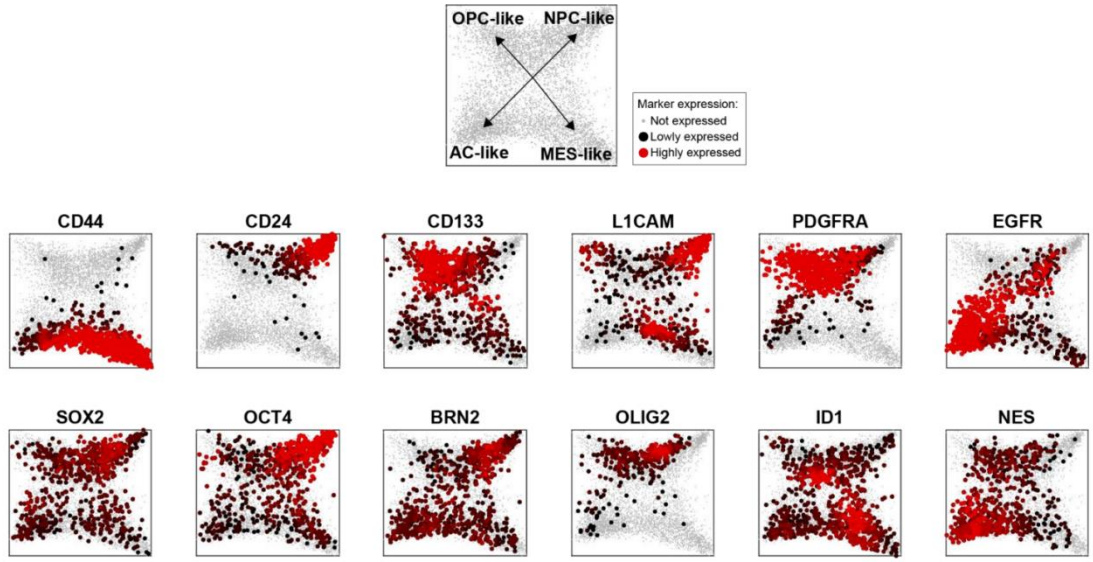

Response Fig R1 (reported in *PMID*: 32396858). Expression of established GSCs markers across GBM cellular states reported by Mario et al.

Each panel represents the diversity of glioblastoma malignant cells, with each cell colored based on the expression of a specific GSC marker, including cell-surface markers (middle row), transcription factors (bottom row), and Nestin (bottom right). The top panel is a legend, showing the position of each cellular state in the 2D representation and the color code for cells based on expression of the marker gene. The data for this figure is taken from Neftel et al. 2019.

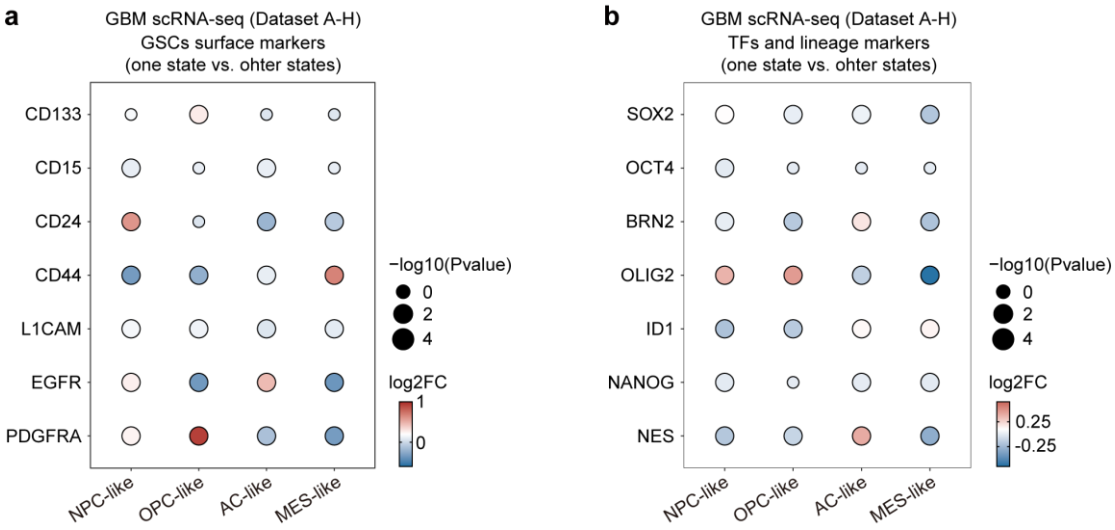

Response Fig R2. Expression of established GSCs markers in different cellular states malignant cells in GBM scRNA-seq datasets.

a, GSCs surface markers expression across different cellular states malignant cells.
b, TFs and lineage markers expression across different cellular states malignant cells.

Our method for isolating GSC-like tumor cells was based on a protocol described

in an article in ***Cell Stem Cell*** (2020, PMID: 31901251). The following method was employed in this study: *"In order to identify the potential GSC cell types for each tumor, we defined GSCs within our scRNA-seq dataset as any cell (independent of the previous clustering) expressing PROM1, FUT4, or L1CAM, in conjunction with SOX2, and not expressing TLR4 (which has been shown to be downregulated by GSCs in order to avoid immune surveillance)."* Additionally, this study also found: *"Our data suggest that stemness programs are heterogeneous and that multiple cell types may recruit stemness programs, even within a single tumor."* GSCs are driven by a series of core transcriptional regulators and cell surface markers. Therefore, we each selected two of the most reviewed transcription factors (SOX2 and OCT4) and surface markers (CD133 and CD15) to isolate GSC-like tumor cells from malignant cells in GBM scRNA-seq datasets (*PMID*: 26109046). GSC-like tumor cells isolated by this approach comprised 7.80% of the total malignant cell population. The proportion of GSCs among malignant cells in four cellular states were as follows: 6.93% in NPC-like, 11.81% in OPC-like, 7.62% in AC-like, and 7.47% in MES-like. These results indicated that GSC-like tumor cells isolated using this approach did not exhibit preferential distribution towards a paticular cellular state. The distribution of GSC-like tumor cells across four cellular states for individual GBM samples was previously illustrated in Fig.1a. Here, we further show the composition of the four cellular states among the malignant cells in each GBM sample (Response Fig. R3). The numbers of tumor cells and GSC-like tumor cells across four cellular states for each sample are detailed in the following table (Response Table R4).

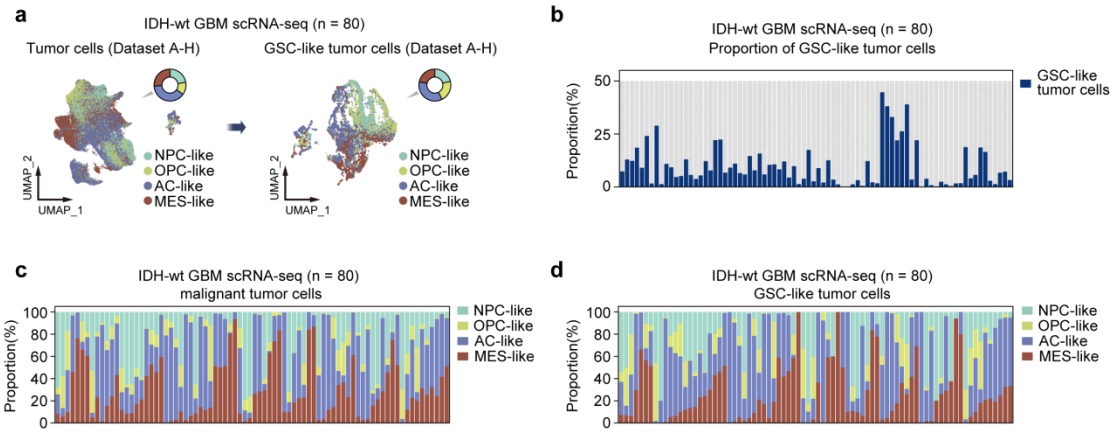

Response Fig R3. The proportion of GSCs and their distribution among the four cellular states in GBM scRNA-seq datasets.

a, Four tumor cellular states mapped in UMAP coordinates of all tumor cells from dataset A-H (left). Four tumor cellular states mapped in UMAP coordinates of GSC-like tumor cells from dataset A-H (right). **b,** Proportion of GSC-like tumor cells in

each GBM sample from scRNA-seq dataset (in-house, GSE103224, GSE117891, GSE131928, GSE141383, GSE173278, and GSE182109). **c,** Composition of four cellular states malignant cells in each GBM sample from scRNA-seq dataset (in-house, GSE103224, GSE117891, GSE131928, GSE141383, GSE173278, and GSE182109). **d,** Composition of four cellular states GSC-like tumor cells in each GBM sample from scRNA-seq dataset (in-house, GSE103224, GSE117891, GSE131928, GSE141383, GSE173278, and GSE182109).

Dataset	Tumor cells				GSC-like tumor cells			
	NPC-like	OPC-like	AC-like	MES-like	NPC-like	OPC-like	AC-like	MES-like
Dataset 1	3053	261	785	367	177	29	97	24
	3143	1587	420	304	355	243	60	49
	468	970	1046	260	68	123	127	20
	8	2	168	151	0	1	42	18
	8	5	612	2011	0	1	80	158
	187	423	161	1501	58	121	59	309
	1451	369	1344	4859	15	7	40	65
Dataset 2	763	549	64	68	191	220	7	0
	68	16	207	87	4	0	1	0
	314	70	2873	50	17	4	335	3
	106	35	206	63	8	4	24	2
	216	192	855	393	14	15	44	5
	7	13	90	84	1	3	5	1
	1917	848	616	443	221	117	102	59
	4707	181	1739	570	174	4	174	54
	11218	1582	2892	1512	350	23	180	92
	728	108	354	239	27	2	31	18
	6761	166	1987	2385	745	12	287	335
	125	5	368	363	13	0	34	20
	493	392	548	1587	133	120	128	287
	969	538	1082	2168	156	86	332	489
	26	10	566	884	1	0	48	52

Dataset	Tumor cells				GSC-like tumor cells			
	NPC-like	OPC-like	AC-like	MES-like	NPC-like	OPC-like	AC-like	MES-like
GSE182109	2	5	26	0	0	0	3	0
	265	151	2465	52	18	13	287	4
	3168	1132	8730	422	193	74	568	43
	441	186	205	95	30	13	11	1
	71	0	3323	84	9	0	475	23
	34	61	851	65	5	12	55	7
	788	153	163	102	64	40	46	40
	140	41	3570	626	2	2	210	44
	334	293	3665	554	9	0	475	23
	2234	9463	4473	2583	167	1025	421	377
	59	1	1986	2135	5	0	138	205
	11	6	461	476	1	0	66	48
	567	30	4087	4925	13	0	212	197
	224	178	28	1757	44	39	6	126
	0	0	14	210	0	0	0	3
GSE131928	33	43	138	19	3	4	2	0
	538	62	67	10	97	9	12	0
	924	176	59	54	13	12	6	1
	28	1	1269	462	1	0	98	57
	12	5	439	181	0	1	12	0
	777	56	75	376	30	10	26	95
	40	11	2	92	2	0	0	3
	0	3	19	61	0	0	0	1
	18	63	391	2385	0	0	1	1
GSE103224	20	0	4624	494	0	0	9	1
	2119	268	264	281	24	5	3	4
	1104	4	1319	549	74	0	12	9
	416	82	1850	672	2	0	13	1
	928	398	233	455	117	37	19	73
	0	0	87	460	0	0	2	10
	16	0	52	450	1	0	1	7
GSE117891	140	21	114	7	50	10	62	4
	2	2	235	8	0	0	90	4
	12	6	608	83	1	2	206	25
	11	45	143	33	1	13	28	9
	257	141	96	256	46	51	29	71
	44	47	10	58	18	25	3	16
	324	239	857	430	2	1	35	27
	0	1	78	125	0	0	14	31
GSE141383	288	44	1137	86	0	0	3	0
	801	117	742	39	44	2	18	1
	791	240	5295	235	7	2	43	1
	1378	62	212	304	4	0	0	1
	2423	141	373	790	55	5	9	24
	248	1	2931	1262	2	0	37	16
	758	108	124	821	5	0	0	3
	174	11	74	756	1	0	0	16
	11	3	257	293	0	0	2	8
GSE173278	2090	822	93	11	394	153	16	3
	873	443	755	277	31	32	27	5
	333	364	1453	635	25	41	77	16
	526	672	129	330	82	133	38	55
	247	93	1180	686	50	18	221	75
	490	104	900	502	15	2	29	13
	858	17	3562	2106	12	0	56	16
	169	9	1925	668	12	0	128	46
	29	14	1361	999	3	6	108	56
	52	14	519	614	2	0	24	13

Response Table R4. The numbers of tumor cells and GSC-like tumor cells across four cellular states for each sample

Reviewer 1, Comment 2: Related to my comment 2, similar to point 1, the authors used GSC models (2907 and 3028) to identify that MEOX2 and SRGN knockouts would reduce the AC-like and MES-like signatures, respectively. However, in response to Figures R2 and R3, there is an increase in PN and NPC-like signals, while the western blot shows that both SOX2 and ID1 are decreased in Fig. 2.

Response:

We appreciate the constructive comments. As shown in our response to comment 1 and consistent with previous findings (*PMID*: 32396858), SOX2 and ID1 did not exhibit elevated expression patterns in NPC-like or OPC-like cellular states. EGFR and CD44 are GSC surface markers characteristic of AC-like and MES-like states, respectively. As shown in Supplementary Fig. 7e and Supplementary Fig. 9g, EGFR expression decreased following MEOX2 knockdown in CL GSCs, while CD44 expression was reduced after SRGN knockdown in MES GSCs (Response Fig. R5). Based on the above evidence, we concluded that these experimental results are not contradictory.

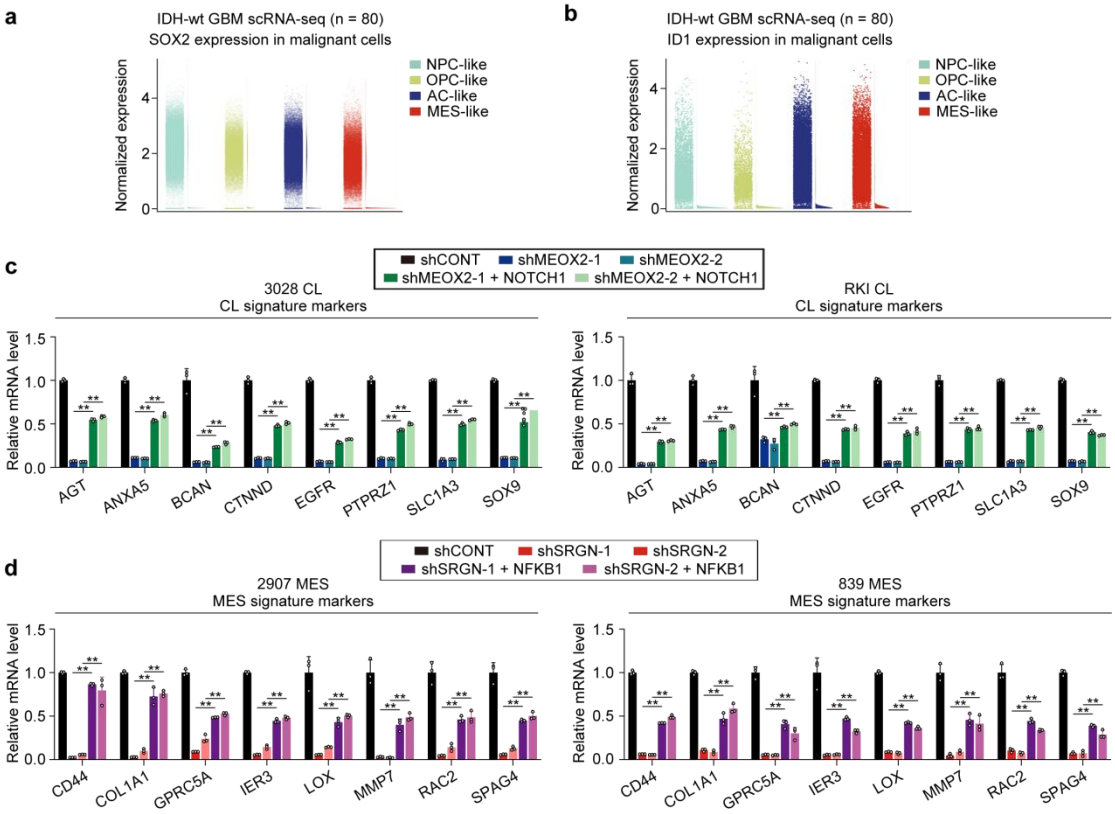

Response Fig R5. Expression of SOX2 and ID1 in different cellular states malignant cells in GBM scRNA-seq datasets.

a, Scatter plot showing normalized expression levels of SOX2 in different cellular state malignant cells from scRNA-seq dataset (in-house, GSE103224, GSE117891,

GSE131928, GSE141383, GSE173278, and GSE182109). **b,** Scatter plot showing normalized expression levels of ID1 in different cellular state malignant cells from scRNA-seq dataset (in-house, GSE103224, GSE117891, GSE131928, GSE141383, GSE173278, and GSE182109). **c,** Classical signature markers expressions assessed by quantitative RT-PCR after CL GSCs transduced with shCONT, shMEOX2-1, shMEOX2-2, shMEOX2-1 + NOTCH1, or shMEOX2-2 + NOTCH1. Data are presented as mean ± SD from three independent experiments. **p < 0.01. **d,** Mesenchymal signature markers expressions assessed by quantitative RT-PCR after MES GSCs transduced with shCONT, shSRGN-1, shSRGN-2, shSRGN + NFKB1, or shSRGN + NFKB1. Data are presented as mean ± SD from three independent experiments. **p < 0.01.

Reviewer 1, Comment 3: Related to comment 8, the authors need to provide an overview of the quality of the ATAC-seq data, including TSS enrichment scores for these samples, the total number of peaks, and the number of differential peaks across all conditions, rather than just detailing the experimental procedures.

Response:

We thank the reviewer for this valuable suggestion. We have now included a comprehensive quality assessment of our ATAC-seq data.

TSS enrichment scores were calculated by ATACseqQC R package. In our experiment, the control group exhibited a TSS enrichment score greater than 6, which meets the quality standard for high-quality ATAC-seq data. The experimental group showed a TSS enrichment score for approximately 3. We also calculated the FRiP (Fraction of reads in peaks) values for all samples. Except for sgMEOX2-1-2 (FRiP = 0.189), all samples achieved FRiP values ≥ 0.2, which is consistent with the general quality standard for ATAC-seq datasets. We propose that the reduced TSS enrichment scores in the MEOX2 knockout group may be attributed to the following factors: First, the MEOX2 knockout may have caused global chromatin closure, particularly in open chromatin regions near TSSs. Second, cell viability in the MEOX2 knockout groups were low. Dead or dying cells released fragmented DNA, which could dilute the specific signal from open chromatin regions and increased background noise. Peak calling was performed using MACS2. The TSS enrichments scores, FRiP values, and the total number of peaks for all samples are shown in the following table (Response Table. R6).

Sample ID	TSS enrichment score	FRiP value	Total number of peaks
sgCONT-1	11.19771	0.3739	381851
sgCONT-2	10.88038	0.3704	374990
sgMEOX2-1-1	2.921627	0.2494	583847
sgMEOX2-1-2	2.623493	0.1899	576664
sgMEOX2-2-1	2.720635	0.2669	641877
sgMEOX2-2-2	2.91143	0.2355	588612

Response Table R6. The TSS enrichments scores, FRiP values, and the total number of peaks for all samples.

Differential accessibility analysis was conducted using DESeq2. The number of differential peaks across all conditions are shown in the following table (Response Table. R7).

Comparison	Total differential peaks (FDR<0.05)
sgCONT vs. sgMEOX2-1	38841
sgCONT vs. sgMEOX2-2	36921
sgCONT vs. all sgMEOX2	48778

Response Table R7. Differential peaks across all conditions.

To further validate the reliability of our previous screening results, we performed additional ChIP-qPCR experiments. ChIP-qPCR analysis using the MEOX2 antibody revealed decreased enrichment at the promoter regions of JAG1, NOTCH1, MAML2, and PSEN1 following MEOX2 knockdown (Response Fig. R7). However, the quality of ATAC-seq data from the MEOX2 knockdown group was not high due to low cell viability after knockdown. These results further validate the reliability of our previous downstream signaling screening by integrating RNA-seq, ChIP-seq, and ATAC-seq data.

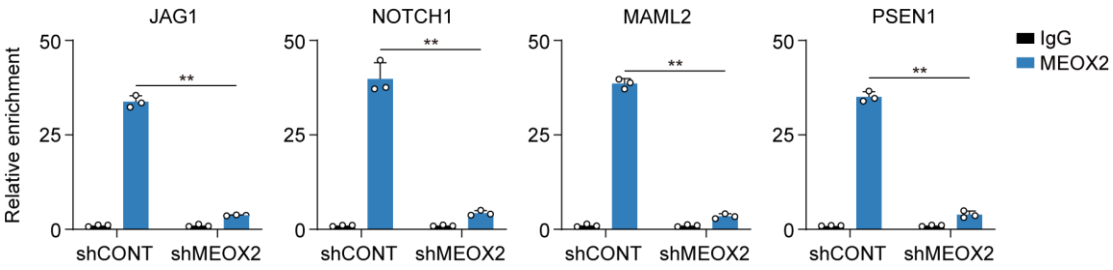

Response Fig R7. The relative enrichment of MEOX2 at JAG1, NOTCH1, MAML2, and PSEN1 promoters was assessed by ChIP-qPCR in shCONT and shMEOX2 3028 GSCs. Data are presented as mean ± SD from three independent experiments. **p < 0.01.

Reviewer #4:

Reviewer 4, Comment 1: Although many of my concerns have been addressed, I share similar concerns with Reviewer 1 that low expression of SRGN in GBM cells in general raises doubt about its functional significance, after I examined its expression in the Neftel dataset myself(see attachment 1). The authors' data also suggest it is expressed only in a small fraction (around 10%) of MES GSCs in scRNA-seq.

Response:

We thank the reviewer for raising this important point regarding the expression of SRGN. The apparent low detection rate in scRNA-seq data can be attributed to technical limitations. Single-cell RNA sequencing typically captures only 10-20% of the total transcriptome due to limited sequencing depth (*PMID*: 30089861). This technical constraint often leads to underestimation of gene expression, particularly for genes with moderate expression levels. Our analysis of deeper sequencing scRNA-seq data (GSE117891) showed substantially higher SRGN detection rates. Higher sequencing depth revealed more comprehensive expression patterns (80% in MES-like tumor cells). Additional validation was provided by high-depth bulk RNA-seq data of GSCs (GSE119834), which revealed SRGN expression in 100% of MES GSCs (Response Fig. R1). These findings collectively suggest that SRGN's functional significance should not be underestimated based solely on dropout effects in standard-depth scRNA-seq data. Moreover, our *in vitro* and *in vivo* experimental results have conclusively demonstrated the functional significance of SRGN in MES GSCs

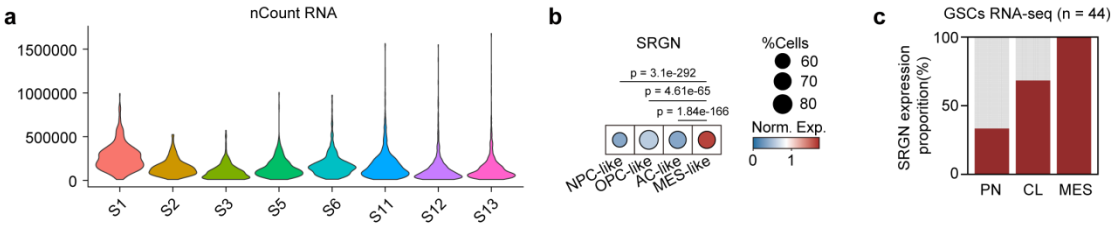

Response Fig R1. Expression distribution of SRGN across different cellular states in GSE117891 scRNA-seq dataset and GSE119834 bulk RNA-seq dataset. **a,** Violin plot showing nCount of each tumor sample in GSE117891. **b,** Bubble plot showing proportions and normalized expression levels of MEOX2 and SRGN in different cellular state tumor cells from GSE117891 scRNA-seq data. **c,** Proportion of SRGN expression in three subtype GSCs from RNA-seq dataset (GSE119834).

Reviewer 4, Comment 2: Since we happen to have the Ravi et al. spatial dataset, we

analyzed the expression of MEOX2 and SRGN, but couldn't replicate the authors' results in quite a few samples(see attachment 2, the obvious ones are highlighted by red boxes). Again, SRGN is barely expressed in some samples unlike what the authors are trying to show.

Response:

We appreciate the reviewer's careful examination. We believe the observed differences may be attributed to differences in the parameter settings and preprocessing steps used during the analysis. For example, for the visualization of MEOX2 expression in the UKF304T sample, we used SPATA2 R package and configured the parameters as shown in the figure (Response Fig. R2). We propose that the following factors account for the visual differences among specific samples: First, for data preprocessing, we used SPATA2's built-in denoising procedure. Second, the smoothing parameter was 0.02. Third, the color scale range used for visualization differed from that in the reviewer's analysis, which may have contributed to the discrepancies in the observed results.

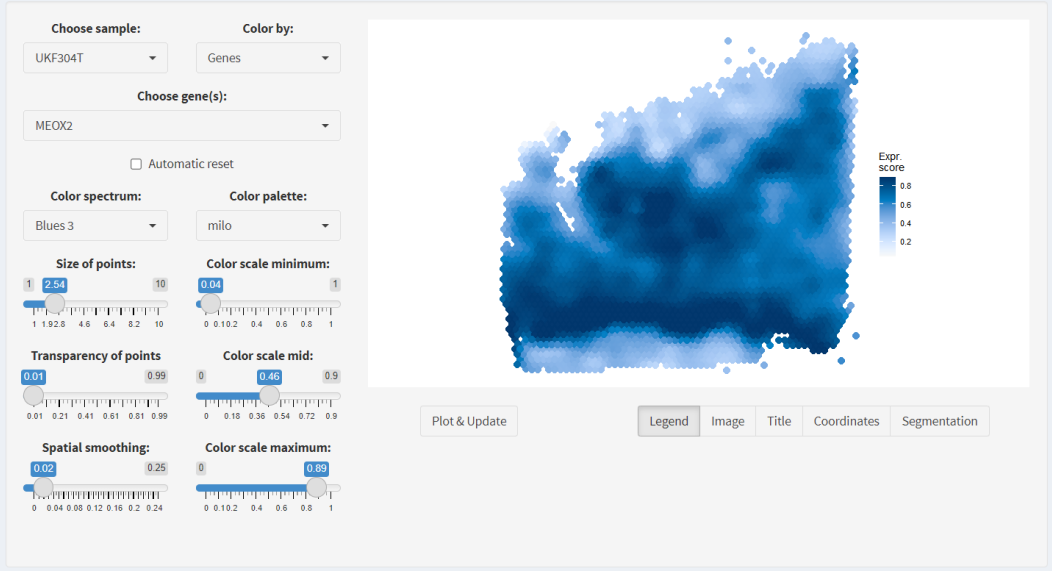

Response Fig R2. The parameters for the visualization of MEOX2 expression in the UKF304T sample using SPATA2.

However, during our review process, we found that the smooth parameter values were inconsistent across all samples in our previous presentation, particularly between the newly added samples and those presented earlier. We appreciate the detailed feedback from the reviewer, which allowed us to identify and address this issue. We sincerely apologize for the oversight in our initial analysis. Thank you for bringing this to our attention and for your thorough analysis. We have re-plotted the

images for all samples (smooth_span = 0.02) and updated the figure in Supplementary Fig. 3h (Response Fig. R3). The updated figures more effectively illustrate the distribution of SRGN expression and reveal that samples with low SRGN expression have relatively fewer MES-like cells.

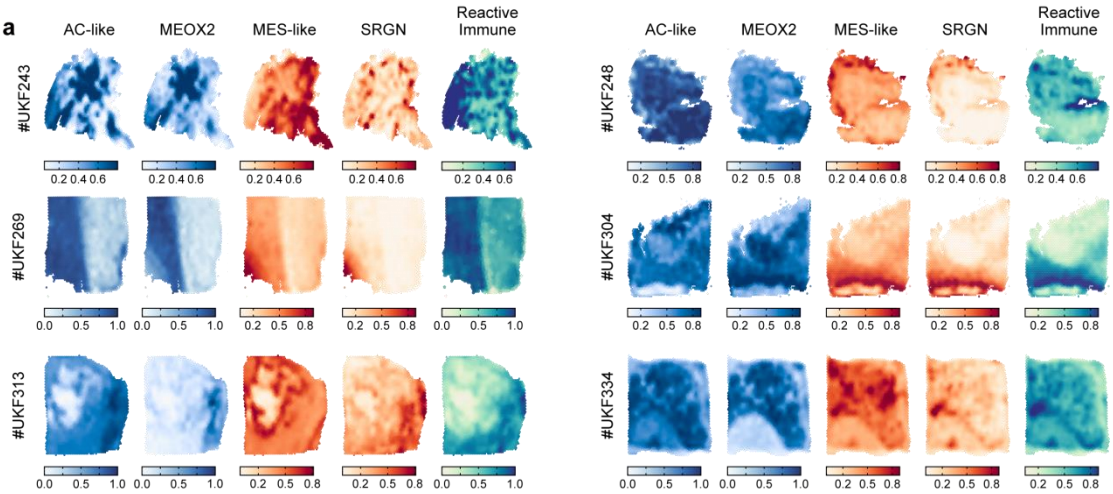

Response Fig R3. Scatter plot of the 2D representation of AC-like/MES-like cellular state, MEOX2/SRGN expression and reactive immune signature in GBM spatial transcriptomics.

Reviewer 4, Comment 3: Moreover,the authors did not properly address my previous concern whether MEOX2 and SRGN are specific for CL and MES GSCs from the same patient.

Response:

We appreciate the constructive comments. Our scRNA-seq analyses confirmed that MEOX2 and SRGN were enriched in AC-like and MES-like GSCs from the same patient (Response Fig. R3). Furthermore, we experimentally validated whether MEOX2 and SRGN are specific to CL and MES GSCs from the same patient. To isolate the four distinct cellular states of GSCs from WL1 GSCs, we used CD24 to identify NPC-like states, PDGFRA to identify OPC-like states, EGFR to identify AC-like states, and CD44 to identify MES-like states. This method was based on the approach reported by Neftel et al (*PMID*: 31327527). Both qPCR and Western blot results showed that MEOX2 was enriched in EGFR+ WL1 GSCs (representing AC-like cellular states), while SRGN displayed high expression in CD44+ WL1 GSCs (representing MES-like cellular states) (Response Fig. R4). These results demonstrated that MEOX2 and SRGN are reliable targets for AC-like and MES-like states at the individual patient level.

Response Fig R3. MEOX2 and SRGN are specific for CL and MES GSCs from the same patient.

a, Bubble plot showing proportions and normalized expression levels of MEOX2 and SRGN in different cellular state tumor cells from 3028 GSCs scRNA-seq data. **b,** Bubble plot showing proportions and normalized expression levels of MEOX2 and SRGN in different cellular state tumor cells from 2907 GSCs scRNA-seq data.

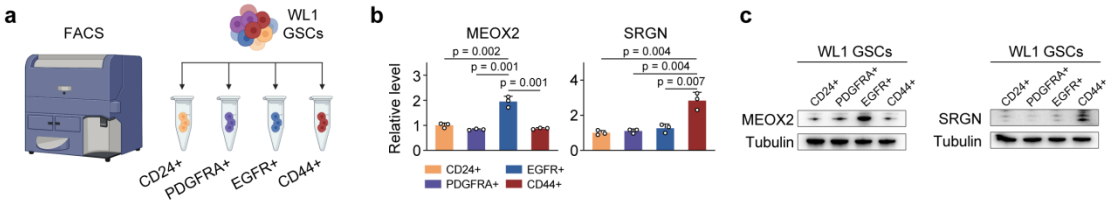

Response Fig R4. MEOX2 and SRGN are specific for CL and MES GSCs from the same patient.

a, Experimental workflow. Different cellular states of GSCs were sorted from WL1 GSCs. **b,** Relative mRNA expression of MEOX2 or SRGN normalized to 18S mRNA level in different cellular states WL1 GSCs. **c,** MEOX2 and SRGN protein levels were measured by western blotting in different cellular states WL1 GSCs. Tubulin was used as the loading control.

Reviewer #6:

Reviewer 6, Comment 1: "medicate" in abstract is likely meant to be "mediate"

Response:

We appreciate the reviewer's identification of the typographical error in the abstract. The term "medicate" has been corrected to "mediate" to accurately reflect the intended meaning.

Reviewer 6, Comment 2: Methods: It's unclear if cells are always grown as spheres or if they are in monolayers in some experiments?

Response:

We appreciate the reviewer raising this point. In our study, GSCs were maintained and cultured as spheres for all experiments, with only one exception: for immunofluorescence analyses (Fig. 4f). GSCs were cultured as monolayers to facilitate imaging and visualization. We have now clarified this detail in the Methods section. The revised descriptions are as follows:

*"**Culture of glioblastoma stem cells and other cell models***

GSCs were cultured as neurospheres in the neurobasal medium (Invitrogen) supplemented with 2% B27 supplement (Life Technologies), 1% L-glutamine, 1% sodium pyruvate, 20 ng/mL bFGF, and EGF (R&D Systems). GSCs were maintained and cultured as spheres for all experiments except immunofluorescence analyses, where cells were cultured as monolayers to facilitate imaging.

NSCs were cultured in neurobasal media supplemented with 2% B27, 20 ng/mL EGF, and bFGF. 293T cells were cultured in DMEM with 10% fetal bovine serum (FBS). U937 cells were maintained in RPMI1640 medium containing 10% FBS."

Reviewer 6, Comment 3: "Specificity" is often not really specific in terms of expression (e.g. Response Fig R4 and much single cell data in the paper.) Perhaps this should be softened to "enriched".

Response:

We appreciate the reviewer raising this important point. We agree with the reviewer

that “enriched” is a more precise term to describe the expression patterns observed in our data, particularly in the single-cell data. We have carefully reviewed the manuscript and modified the terminology from “specificity” to “enriched” where appropriate to describe our findings more accurately.

Reviewer 6, Comment 4: Reviewer 1, Comment 6: "The validation of the predictive results in this paper is conducted using four cell lines (CL: 3028 and RKI, MES: 2907 and 839)." This is critical point and sends the reader/reviewer down a "rabbit hole" looking for information. A comprehensive table of descriptive features should be included in the form of a supplementary table with many more pertinenet details than are presented.

Response:

We thank the reviewer for this constructive suggestion. We have now created a comprehensive supplementary table (Supplementary Table 5) with detailed information for GSCs. This detailed documentation will provide readers with clear and accessible information about our GSCs.

Supplementary Table 5. Glioblastoma stem cells information

	3028	RKI	2907	839
Patient age	65 years	Unknown	Unknown	Unknown
Patient sex	Female	Unknown	Unknown	Unknown
Tumor grade	Grade IV	Grade IV	Grade IV	Grade IV
Transcriptional subtype	Classical	Classical	Mesenchymal	Mesenchymal
IDH1 status	WT	WT	WT	WT
PTEN status	Mut	WT	WT	WT
TP53 status	Mut	Mut	WT	Mut
EGFR status	Amp	WT	WT	WT
PDGFRA status	WT	WT	Amp	WT
MYC status	WT	Amp	WT	Amp
CDKN2A status	WT	WT	WT	WT
ATRX status	WT	Mut	WT	WT
MET status	WT	WT	WT	WT
MDM2 status	WT	WT	Amp	WT
NF1 status	WT	WT	WT	Mut

WT: Wild Type; Mut: Mutant; Del: Deletion; Amp: Amplification

Reviewer 6, Comment 5: Reviewer 3, Comment 1: (defining GSC) - I'm not convinced the authors address the point. Featureplots of CD133, SOX2, OCT4, and CD15 would be more informative than the somewhat misleading plots in Supp. Fig. 1b--where the scales change wildly. If I'm reading this correctly, OCT4 is expressed in

only 3% of cells. However, adding a definition of GSC just adds another layer of abstraction that doesn't seem meaningful in the context of these experiments. Already the manuscript mixes TCGA and Neftel states. Futher, it is becoming increasingly apparent that most tumors express all states and signatures across a spectrum--with plasticity in response to standard-of-care and tumor progression.

Response:

We appreciate the reviewer's insightful comments. We have updated Supplementary Fig. 1b with new featureplots showing the expression of CD133, SOX2, OCT4, and CD15 to provide a more accurate representation of their expression patterns (Response Fig. R1).

The definition of GSCs has always been a subject of controversy. Our method for isolating GSC-like tumor cells was based on a protocol described in an article in ***Cell Stem Cell*** (2020, PMID: 31901251). The following method was employed in this study: *"In order to identify the potential GSC cell types for each tumor, we defined GSCs within our scRNA-seq dataset as any cell (independent of the previous clustering) expressing PROM1, FUT4, or L1CAM, in conjunction with SOX2, and not expressing TLR4 (which has been shown to be downregulated by GSCs in order to avoid immune surveillance)."* GSCs are driven by several core transcriptional regulators and cell surface markers. Therefore, we each selected two of the most reviewed transcription factors (SOX2 and OCT4) and surface markers (CD133 and CD15) to isolate GSC-like tumor cells from malignant cells in GBM scRNA-seq datasets (*PMID*: 26109046). GSC-like tumor cells isolated by this approach comprised 7.80% of the total malignant cell population. These analyses aimed to identify therapeutic targets with clinical utility in CL and MES GSCs. The inclusion of these analyses did not affect our target selection results. Analysis of all malignant cells in Supplementary Fig. 2 also demonstrated that MEOX2 and SRGN were enriched in AC-like and MES-like malignant cells, respectively.

We appreciate the reviewers' point that glioblastomas encompass a spectrum of cellular states with plasticity in response to progression and therapy. This phenomenon led us to explore therapeutic strategies targeting multiple cellular states simultaneously. Here, we further show the composition of the four cellular states among the malignant cells in each GBM sample (Response Fig. R2).

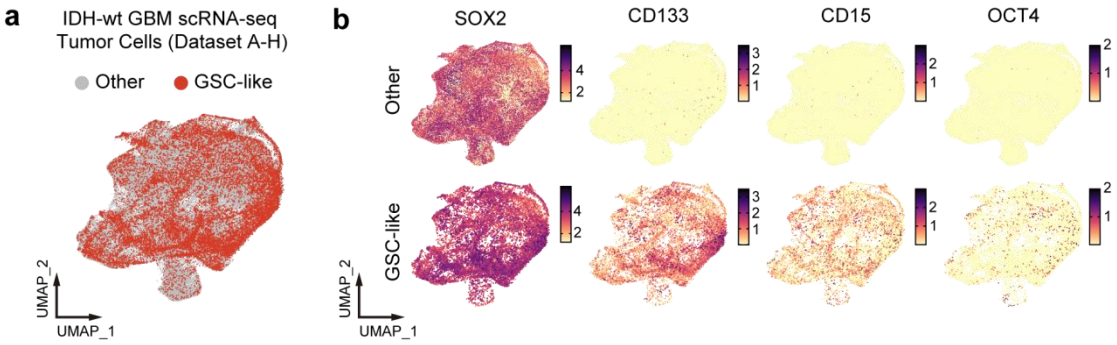

Response Fig R1. The distribution among the four cellular states in GBM scRNA-seq datasets.

a, GSC-like tumor cells mapped in UMAP coordinates of all tumor cells from dataset A-H (left). **b,** Featureplots showing normalized expression levels of SOX2, CD133, CD15, and OCT4 in GSC-like tumor cells and other tumor cells from dataset A-H.

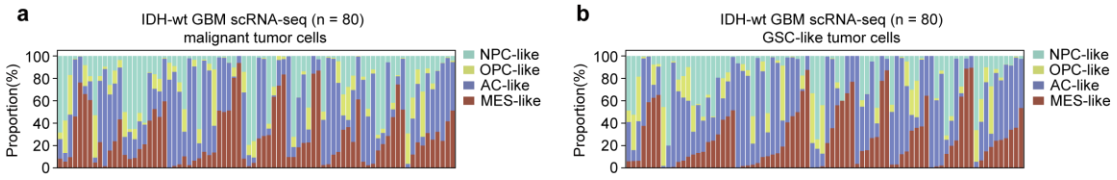

Response Fig R2. The distribution among the four cellular states in GBM scRNA-seq datasets.

a, Composition of four cellular states malignant cells in each GBM sample from scRNA-seq dataset (in-house, GSE103224, GSE117891, GSE131928, GSE141383, GSE173278, and GSE182109). **b,** Composition of four cellular states GSC-like tumor cells in each GBM sample from scRNA-seq dataset (in-house, GSE103224, GSE117891, GSE131928, GSE141383, GSE173278, and GSE182109).

Reviewer 6, Comment 6: Reviewer 3, Comment 2: (referencing meaningful literature on MES-CL immune microenvironment) - This was and continues to be an oversight of key references regarding the immune microenvironment in MES-CI states. Further, it is notable that MEOX2 and SRGN have been identified in glioma progression by a number of publications that are largely not referenced:

https://pmc.ncbi.nlm.nih.gov/articles/PMC5421891/

https://pubmed.ncbi.nlm.nih.gov/38672477/

https://pubmed.ncbi.nlm.nih.gov/28445977/

https://www.mdpi.com/2218-273X/14/4/461

https://pmc.ncbi.nlm.nih.gov/articles/PMC8672280/

https://www.nature.com/articles/s41419-022-04845-2

Response:

We thank the reviewer for bringing these important references to our attention. We have thoroughly revised our manuscript to include these key references and better contextualize our findings. The revised discussion sections are as follows:

"MEOX2 belongs to the homeobox genes family of transcription factors[30, 31]. These transcription factors can promote cell growth, migration, angiogenesis, and maintain cell quiescence[49]. Recent studies have revealed that MEOX2 acts as a critical transcriptional regulator in GBM progression. MEOX2 promotes GBM progression by driving the epithelial-mesenchymal transition, cytoskeletal dynamics, and focal adhesion formation, thereby enhancing tumor cell invasion and proliferation. Both are critical for tumor cells survival and growth[50, 51]. Our data extends these findings by showing that MEOX2 is enriched in CL GSCs. MEOX2-NOTCH axis plays an important role in CL GSCs' self-renewal and stemness maintenance. SRGN is a low molecular weight glycoprotein distributed in the cytoplasm. SRGN plays an essential role in the storage and secretion of cytokines, chemokines, and proteases and has been reported to participate in many physiological and pathological processes52. Recent studies highlighted SRGN's importane in GBM biology. SRGN facilitates glioblastoma invasion, metastasis, and immune evasion by enhancing inflammatory and proteolytic signaling cascades[53, 54]. Our results demonstrated that SRGN was a representative target of MES GSCs. SRGN characteristically regulated the proliferation and stemness of MES GSCs. SRGN regulated the NF-κB signaling pathway by maintaining NFKB1 protein stability."

Reviewer 6, Comment 7: Reviewer 3, Comment 5: "Single cell transcriptome differential analysis cannot guarantee that the isolated GSC like tumor cells function as true GSCs." This is a highly questionable statement. One can argue that scRNA-seq from a primary tumor is much more reflective of that natural state of glioma tumor propagating cells than cells cultured ex vivo--which are subject to cell culture artifacts, lack of stroma, drift, etc.

Response:

We thank the reviewer for this insightful comment. We acknowledge that our description was not accurately phrased. We agree that scRNA-seq captures tumor cells that better represent the natural tumor microenvironment than ex vivo cell culture models. We designed this screening strategy based on insights from a ***Cancer Cell***

review (2020, *PMID*: 32396858) that discussed the limitations of previous GSCs research. While both approaches (scRNA-seq and cultured GSCs) have their merits, they should be considered complementary. Integrating scRNA-seq and bulk RNA-seq screening approaches allows us to utilize data from multiple models. This strategy better reflects the biological state in GBM environments, leading to more accurate identification of CL and MES GSCs targets.

Reviewer 6, Comment 8: Reviewer 3, Comment 7: "These results suggest that MEOX2 and SRGN are characteristically up regulated in GBM and could serve as unique therapeutic targets for GBM." I think this again ignores a number of papers that I could find showing that MEOX2 and SRGN are upregulated in a number of cancers.
e.g. https://bmccancer.biomedcentral.com/articles/10.1186/s12885-020-06849-7 & https://journals.plos.org/plosone/article?id=10.1371/journal.pone.0114104

Response:

We appreciate the reviewer's comment regarding MEOX2 and SRGN expression in other cancers. We agree that our original statement needed clarification. Our results did not aim to underestimate the broader roles of MEOX2 and SRGN in other cancers but instead sought to emphasize their unique expression characteristics in GBM. Specifically, we found that MEOX2 and SRGN exhibit the highest fold-change differences in expression between tumor and normal tissues across all tumor types. When comparing expression levels across tumor tissues, MEOX2 ranked second, and SRGN ranked fifth in terms of expression among all cancer types (Response Fig. R3).These findings suggest their potential as promising therapeutic targets in GBM. In response, we revised the manuscript to:

"*To evaluate the potential of MEOX2 and SRGN as therapeutic targets, pan-cancer analysis was performed to examine their expression patterns across all tumor types. Interestingly, when comparing tumor vs. normal tissue expression across all cancer types, MEOX2 and SRGN exhibit the highest fold-change differences. When comparing expression levels across all tumor tissues, MEOX2 ranked second, and SRGN ranked fifth in terms of expression among all cancer types (Fig. 1k). Previous studies have demonstrated important roles for MEOX2 and SRGN in other cancers, with MEOX2 functioning in lung cancer and SRGN in melanoma[30, 31]. However, their remarkably high differential expression in GBM, together with our*

findings of subtype-specific expression, suggests their particular promise as therapeutic targets in GBM."

a

Pan-cancer analysis of MEOX2 expression

	Normal	Tumor	Fold change
GBM	3.21	0.25	12.98
LIHC	0.49	0.14	3.48
PCPG	0.57	0.23	2.45
KIRC	0.84	0.51	1.63
SARC	2.4	1.48	1.63
CHOL	0.28	0.29	0.99
ESCA	0.43	0.44	0.97
STAD	0.89	0.93	0.95
PAAD	1.35	1.47	0.92
SKCM	1.19	1.3	0.91
PRAD	0.43	0.58	0.73
LUAD	1.41	2.28	0.62
KICH	0.35	0.61	0.56
HNSC	0.53	0.98	0.54
THCA	1	1.87	0.53
COAD	0.43	0.94	0.46
LUSC	0.93	2.38	0.39
THYM	1.04	2.73	0.38
BRCA	1.21	3.49	0.35
READ	0.44	1.31	0.33
BLCA	0.43	1.42	0.3
KIRP	0.1	0.42	0.25
UCEC	0.2	1.43	0.14
CESC	0.12	1.77	0.07

b

Pan-cancer analysis of SRGN expression

	Normal	Tumor	Fold change
GBM	4.51	6.7	1.48
CHOL	4.48	4.99	1.11
KIRC	6.06	6.71	1.11
HNSC	4.72	5.21	1.1
ESCA	4.83	5.25	1.09
SARC	5.87	5.99	1.02
STAD	6.05	6.14	1.02
THCA	5.41	5.21	0.96
KIRP	5.55	5.26	0.95
PRAD	5.24	4.8	0.92
BRCA	5.93	5.4	0.91
PCPG	5.53	4.84	0.88
LIHC	4.95	4.31	0.87
THYM	6.58	5.72	0.87
COAD	5.79	4.97	0.86
UCEC	5.43	4.6	0.85
LUAD	7.86	6.63	0.84
PAAD	7.32	6.15	0.84
BLCA	6.37	5.15	0.81
CESC	6.43	5.15	0.8
READ	6.06	4.7	0.78
LUSC	7.95	6.01	0.76
SKCM	8.11	5.44	0.67
KICH	6.5	4.18	0.64

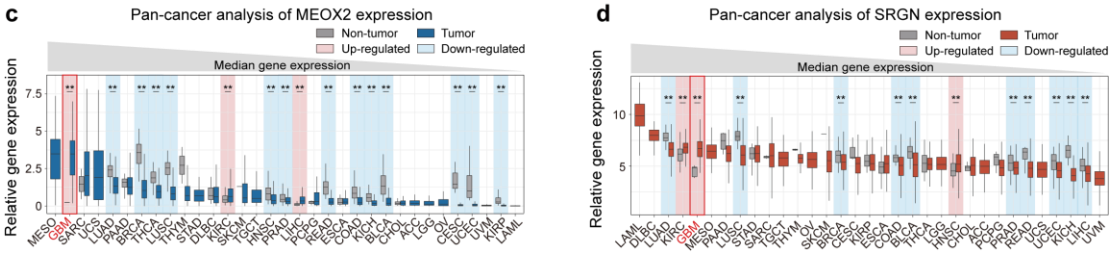

Response Fig R3. Pan-cancer analysis of MEOX2 and SRGN expression patterns.

a and b, Analysis of MEOX2 (left) and SRGN (right) expression across multiple cancer types compared to corresponding normal tissues.

c and d, Pan-cancer analysis of MEOX2 (left) and SRGN (right) expression levels in different tumors from the TCGA dataset.

Reviewer 6, Comment 9: Reviewer 3, Comment 8: More detail is needed on how these cells compare to the parental tumors. The authors should present an integration of their "GSCs" with primary glioma datasets and compared DEGs.

Response:

We appreciate the reviewer's comment. Unfortunately, we do not have sequencing data from the parental tumors corresponding to our GSCs. Furthermore, such a comparison may have limited interpretability, as the samples typically originate from different patients, and differences in sequencing platforms or methods may introduce technical biases. These factors make it challenging to draw definitive conclusions

about the DEGs between GSCs and primary GBM in this context. We analyzed differential expression analysis between GSCs and their corresponding DGCs (Response Fig. R4). This strategy has been widely used in glioblastoma research to identify GSC-specific markers and pathways (*PMIDs*: 38563585, 34615656, 36265493, and 39454581). To validate our screening results, we also compared MEOX2 and SRGN expression in GBM datasets and GSCs/NSCs ChIP-seq dataset. These results are presented in Fig. 1, Supplementary Fig. 2, and Supplementary Fig. 3.

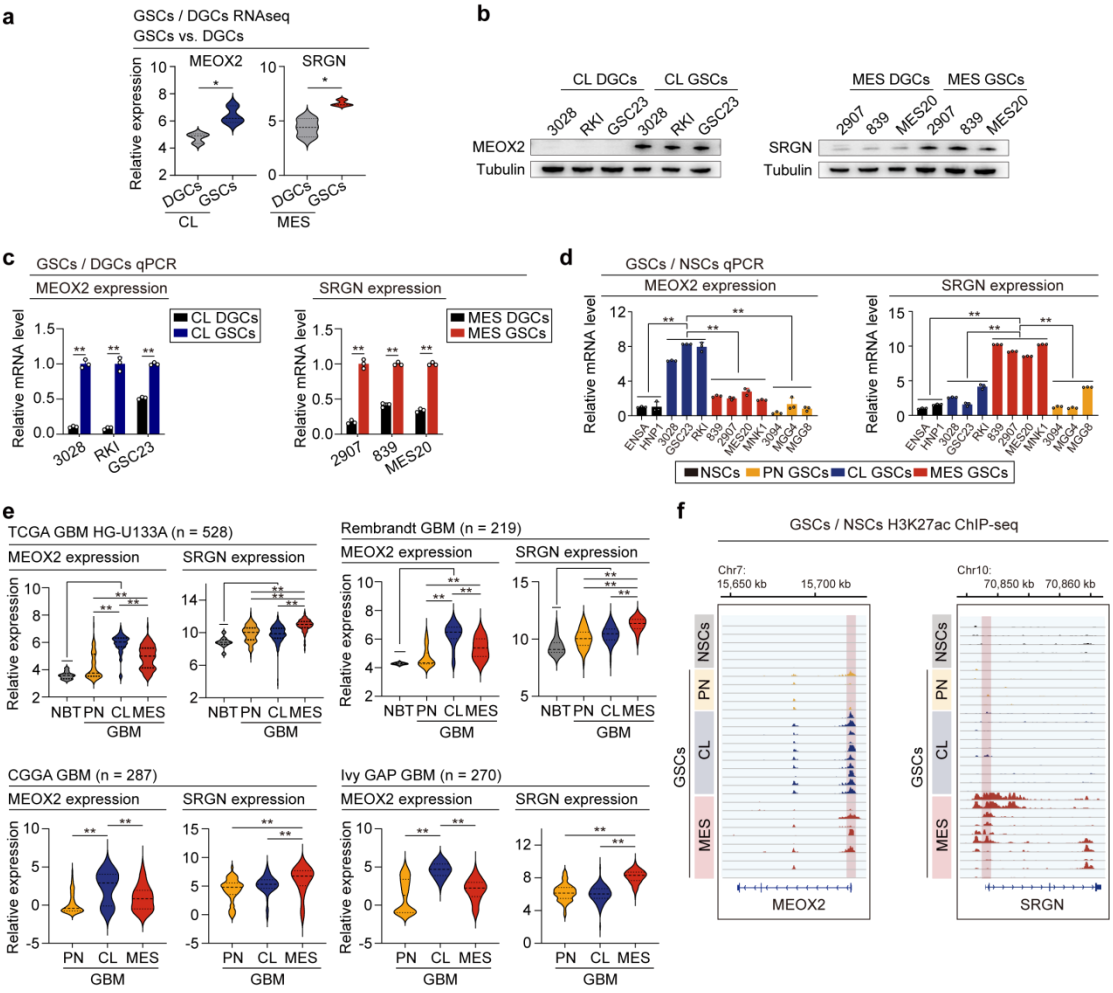

Response Fig R4. MEOX2 and SRGN are enriched in CL and MES GSCs, respectively

a, MEOX2 (left) and SRGN (right) gene expression in the GSCs (n = 3)/DGCs (n = 3) RNA-seq dataset (in-house generated). **b,** MEOX2 and SRGN protein levels were measured by western blotting in CL/MES DGCs (n = 3) and CL/MES GSCs (n = 3). Tubulin was used as the loading control. **c,** Relative mRNA expression of MEOX2 or SRGN normalized to 18S mRNA level in CL/MES DGCs (n = 3) and CL/MES GSCs (n = 3). **d,** Relative mRNA expression of MEOX2 or SRGN normalized to 18S mRNA level in NSCs (n = 2) and different subtype GSCs (n = 10). **e,** MEOX2 (left) and SRGN (right) gene expression in the TCGA GBM (HG-U133A), Rembrandt, CGGA, and Ivy

GAP GBM datasets. **f,** Promoter peaks in MEOX2 and SRGN gene regions derived from H3K27ac ChIP-seq data (GSE119776).

Reviewer 6, Comment 10: Reviewer 3, Comment 10: This doesn't directly address the point. There should be a direct comparison in low dimensional UMAP space to show if these cells align completely or if there are cellular states (likely in vitro due to culture artifacts) that don't appear in vivo. Scoring by modules by artificially normalized scales (e.g. Response Fig. R5) does not give the full picture as one gets aligning all of the data in a low dimensional space with batch correction/integration.

Response:

We appreciate the reviewer's suggestion to compare the cellular states in low-dimensional UMAP space directly. We then reanalyzed the data in low-dimensional UMAP space to visualize the alignment of cells from both conditions (Response Fig. R5). The integrated analysis revealed that all cellular populations corresponded to states present in patient tumors.

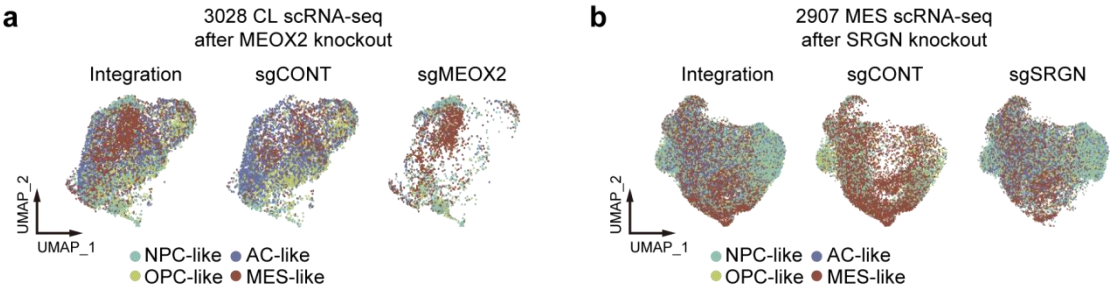

Response Fig R5. Knocking down MEOX2 mainly affected AC-like GSCs and knocking down SRGN primarily affected MES-like GSCs.

a, The UMAP plot of 3028 CL GSCs annotated by four cellular states. **b,** The UMAP plot of 2907 MES GSCs annotated by four cellular states.

Reviewer 6, Comment 11: Reviewer 3, Comment 13: addressed appropriately. However, I can't find the details on how this was accomplished in the methods. Adding an 8KB receptor to a lentivirus is near the limits of a virus--especially with a promoter and other elements.

Response:

We appreciate the reviewer's constructive comments. The method for overexpressing

NOTCH1 in GSCs was adapted from the protocol described in this article published in ***Nature Neuroscience*** (2019, *PMID*: 30559479). Full-length human NOTCH1 in the pCMV6 vector was purchased from Origene and cloned into the BamHI and XhoI restriction sites of the pcDNA 3.1 vector (Invitrogen) for the overexpression assay. 293T cells (ATCC, Cat# CRL-3216) were used to generate lentiviral particles by co-transfecting the packaging vectors psPAX2 and pMD2.G using a standard calcium phosphate transfection method in neurobasal complete medium. We have corrected the corresponding description in the Method section. The revised descriptions are as follows:

*"**Plasmids and lentiviral transduction***

Lentiviral constructs expressing non-overlapping shRNAs directed against human MEOX2 (TRCN0000427218 and TRCN0000433531), human SRGN (TRCN0000007985 and TRCN0000007987), human NOTCH1 (TRCN0000003359 and TRCN0000350330), human NFKB1 (TRCN0000006517 and TRCN0000006520) or a non-targeting control shRNA (SHC002) with no targets in the human genome were obtained from Sigma-Aldrich. For CRISPR/Cas9 experiments, sgRNAs were cloned into the lentiCRISPR v2 plasmid (Addgene, Cat# 52961). All shRNAs and sgRNAs sequences are listed in Supplementary Table 8. Full-length human MEOX2, SRGN, NOTCH1, and NFKB1 in the pCMV6 vector were purchased from Origene and cloned into the BamHI and XhoI restriction sites of the pcDNA 3.1 vector (Invitrogen) for the overexpression assay. 293T cells (ATCC, Cat# CRL-3216) were used to generate lentiviral particles by co-transfecting the packaging vectors psPAX2 and pMD2.G using a standard calcium phosphate transfection method in neurobasal complete medium."

The validation of overexpression efficiency is presented below (Response Fig. R6).

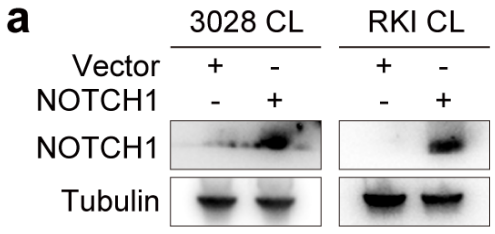

Response Fig R6. NOTCH1 overexpression in CL GSCs confirmed by western blot.

a, Protein level of NOTCH1 after overexpressing NOTCH1 in CL GSCs, as detected by western blotting.

Reviewer 6, Comment 12: Reviewer 3, Comment 16: Again, the authors show

expression in a normalized scale so it's not clear if there is any physiological relevance in terms of CD47-SIRPa.

Response:

We thank the reviewer for pointing out this critical concern. For the expression data shown in Fig. 5d-g, we have presented their unscaled expression levels in 4 tables below. These results demonstrate that the majority of anti-phagocytic signals were upregulated in CL and MES GSCs. MEOX2 knockout led to reduced expression of anti-phagocytic genes in CL GSCs, while SRGN depletion significantly downregulated anti-phagocytic gene expression in MES GSCs.

Fig. 5d, Anti-phagocytosis genes expression between four cellular states (NPC-like, OPC-like, AC-like, and MES-like) GSC-like tumor cells in scRNA-seq datasets.

gene_symbol	NPC-like	OPC-like	AC-like	MES-like
HLA-A	4.807793467	8.500044232	9.881484089	9.753637638
HLA-B	2.636897116	5.285086561	7.797246527	8.751662138
HLA-C	2.573725763	4.871712156	6.36552336	5.994909168
B2M	13.01810393	24.47990205	29.61057219	28.32725629
NLRC5	0.029676702	0.041328353	0.054466342	0.040139791
PSMB8	0.487642553	0.730930473	1.033624691	0.793801257
PSMB9	0.38286471	0.618206151	0.88429412	0.731995009
TAP1	0.223645309	0.329376819	0.488750688	0.403819391
TAP2	0.128608828	0.155016386	0.16274127	0.123604312
CD24	2.070460945	0.601745948	0.190102278	0.331803448
CD274	0.003151075	0.002981604	0.019391575	0.039218119
CD47	0.81634578	1.336920755	1.147174557	1.256043839
STC1	0.146674842	0.11337681	0.039461889	0.252336169

Fig. 5e, Anti-phagocytosis genes expression between three subtypes (PN, CL, and MES) GSCs in GSCs RNA-seq dataset (GSE119834).

gene_symbol	NSCs	PN GSCs	CL GSCs	MES GSCs
HLA-A	1427.277179	4512.921818	6410.623742	8342.405073
HLA-B	343.2312731	637.4433115	1518.403713	4527.905333
HLA-C	689.8377828	757.6065875	1627.237425	2135.34082
B2M	2631.118025	5123.900908	12021.76047	15630.34357
NLRC5	32.75429179	221.8345507	410.3834478	485.3900053
PSMB8	28.94330121	315.736973	476.0469346	1313.285211
PSMB9	32.19884693	152.0938677	324.9638768	638.7903184
TAP1	150.4464031	546.8709988	1537.018783	2265.106816
TAP2	217.8333237	794.4720707	808.7143528	1556.260019
CD24	4446.528508	199.1785469	193.2065907	142.2531826
PD-L1	8.303874634	10.44930539	16.42745698	63.76204802
CD47	2776.034553	2339.845619	1906.93608	3219.441076
STC1	43.77127599	174.9397722	189.100171	1705.436342

Fig. 5f, Anti-phagocytosis genes expression in MEOX2 knockout RNA-seq data.

gene_symbol	sgCONT	sgCONT	sgMEOX2_1	sgMEOX2_1	sgMEOX2_2	sgMEOX2_2
HLA-A	1096.14	1084.09	422.23	439.01	428.4	433.86
HLA-B	470.68	470.87	20.33	21.99	22.69	24.95
HLA-C	272.9	278.82	104.07	106.63	111.63	112.31
B2M	831.23	826.12	594.22	602.12	687.12	684.41
PSMB8	40.28	36.23	0.1	0	0	0
STC1	112.24	119.46	14.64	14.3	16.72	16.84
CD24	3.97	3.88	1.26	0.86	1.01	0.98
CD47	19.31	18.32	15.58	14.77	14.64	14.78

Fig. 5g, Anti-phagocytosis genes expression in SRGN knockout RNA-seq data.

gene symbol	sgCONT	sgCONT	sgSRGN_1	sgSRGN_1	sgSRGN_2	sgSRGN_2
HLA-A	1409.51	1346.46	511.32	508.34	521.45	517.3
HLA-B	1181.76	1183.66	497.68	495.36	509.07	498.92
HLA-C	724.78	720.23	292.55	284.58	287.6	287.66
B2M	719.9	753.92	497.81	525.71	460.07	450.77
PSMB8	106.27	108.28	75.72	72.25	72.29	69.37
PSMB9	106.78	103.64	51.48	54.78	49.84	50.9
TAP1	91.15	90.49	54.07	52.52	55.89	57.39
STC1	0.99	1.16	0.26	0.41	0.19	0.26
CD24	1.68	1.75	0.68	0.41	0.66	0.68

Reviewer #1:

Reviewer 1, Comment 1: The authors addressed my concern about GSC. Comment 2 is not addressed but it is OK to leave the inconsistency in the paper as it is not the major population. Comment 3 proved our concern about the quality of ATAC-seq data. I suggested removing those analyses and interpretations in the paper.

Response:

We appreciate the reviewer's valuable comments. Regarding your concern about the ATAC-seq quality, we fully agree with your assessment. Following your suggestion, we have removed all ATAC-seq data and related interpretations from the manuscript. We believe these changes have strengthened the manuscript by focusing on our most robust and reliable data.

The revised Figure 3 and Supplementary Fig. 6 are shown as follows:

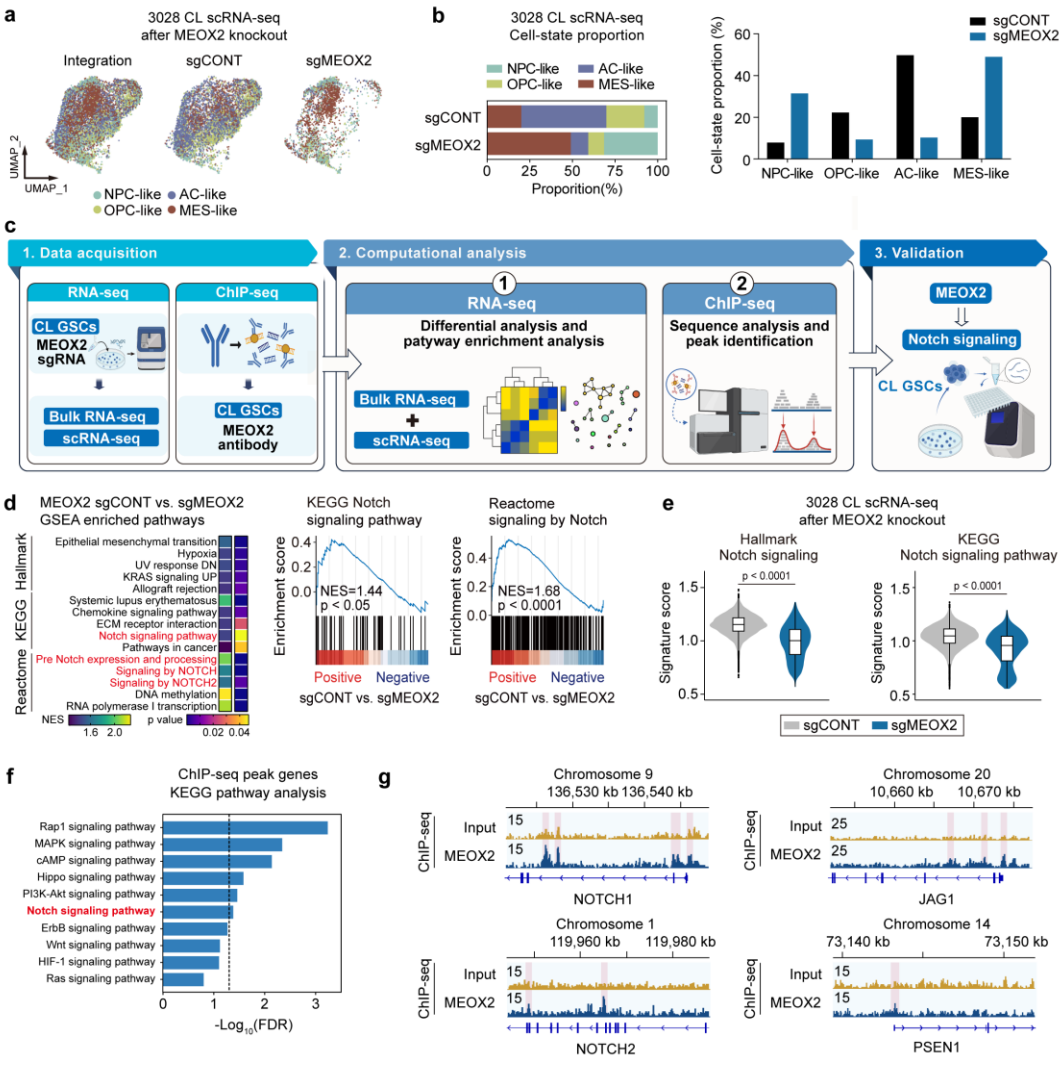

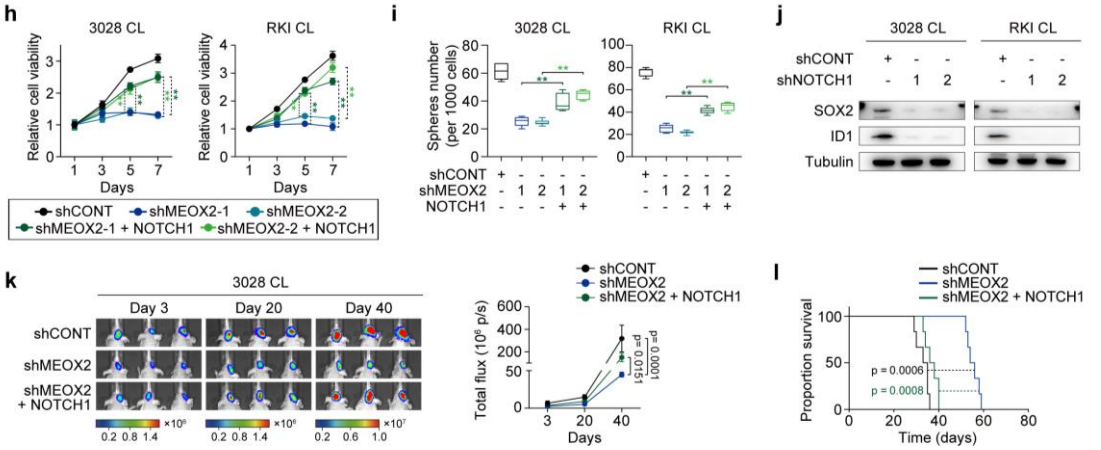

Response Fig R1 (Figure 3). MEOX2 functions through transcriptional activation of the Notch signaling pathway in CL GSCs.

a, The UMAP plot of 3028 CL GSCs annotated by four cellular states. **b,** Proportion changes of four cellular states cells in 3028 CL GSCs transduced with MEOX2 sgRNA or control sgRNA. **c,** Diagram depicting the screening workflow to identify the MEOX2 downstream mechanism. **d,** Gene set enrichment analysis (GSEA) of Hallmark, KEGG, and Reactome gene sets after MEOX2 knockout in 3028 (CL) GSCs. Normalized enrichment score (NES) and p values are shown by heatmap. **e,** Violin-box plots showing the notch signaling score (Hallmark and KEGG) of the GSCs scRNA-seq data (sgCONT vs. sgMEOX2). Two-tailed unpaired Wilcoxon rank-sum test. **f,** KEGG pathway enrichment analysis of MEOX2 ChIP-seq peak genes. **g,** Input or MEOX2 binding signals of NOTCH1, NOTCH2, JAG1, and PSEN1 from Chip-seq on 3028 (CL) GSCs. **h,** Overexpression of NOTCH1 rescued the decreased cell viability caused by MEOX2 knockdown in CL GSCs (n = 6 per group and time point). Data are presented as mean ± SD. **p < 0.01, one-way ANOVA with Dunnett's multiple-comparison test. **i,** Quantification of direct sphere number count of 3028 (CL) or RKI (CL) GSCs transduced with shCONT, shMEOX2 alone, or shMEOX2 with NOTCH1 overexpression (n = 6 per group). Data are presented as mean ± SD. **p < 0.01, one-way ANOVA with Dunnett's multiple-comparison test. **j,** IB analysis of SOX2 and ID1 levels in 3028 (CL) and RKI (CL) GSCs transduced with NOTCH1 shRNA or control shRNA. **k,** Bioluminescence images of mice bearing orthotopic xenografts derived from luciferase-expressing 3028 (CL) cells, show the effect of shMEOX2 or shMEOX2 + NOTCH1 on tumor growth (left). Intensities of luciferase signal in mice are shown (right). **l,** Kaplan-Meier survival curves of mice bearing intracranial tumors derived from 3028 CL GSCs (n = 6) from the three groups in (k).

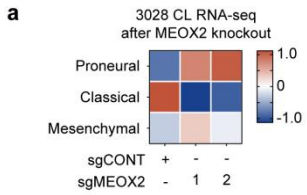

b

Group	gsva score			p value		
	PN	CL	MES	PN	CL	MES
sgCONT	-0.0202	0.4154	0.0965	0.9041	0.0009	0.8761
sgMEOX2-1	0.0363	-0.4899	-0.0882	0.3556	0.9910	0.4985
sgMEOX2-2	0.3746	-0.2124	0.0337	0.3187	0.9800	0.9800

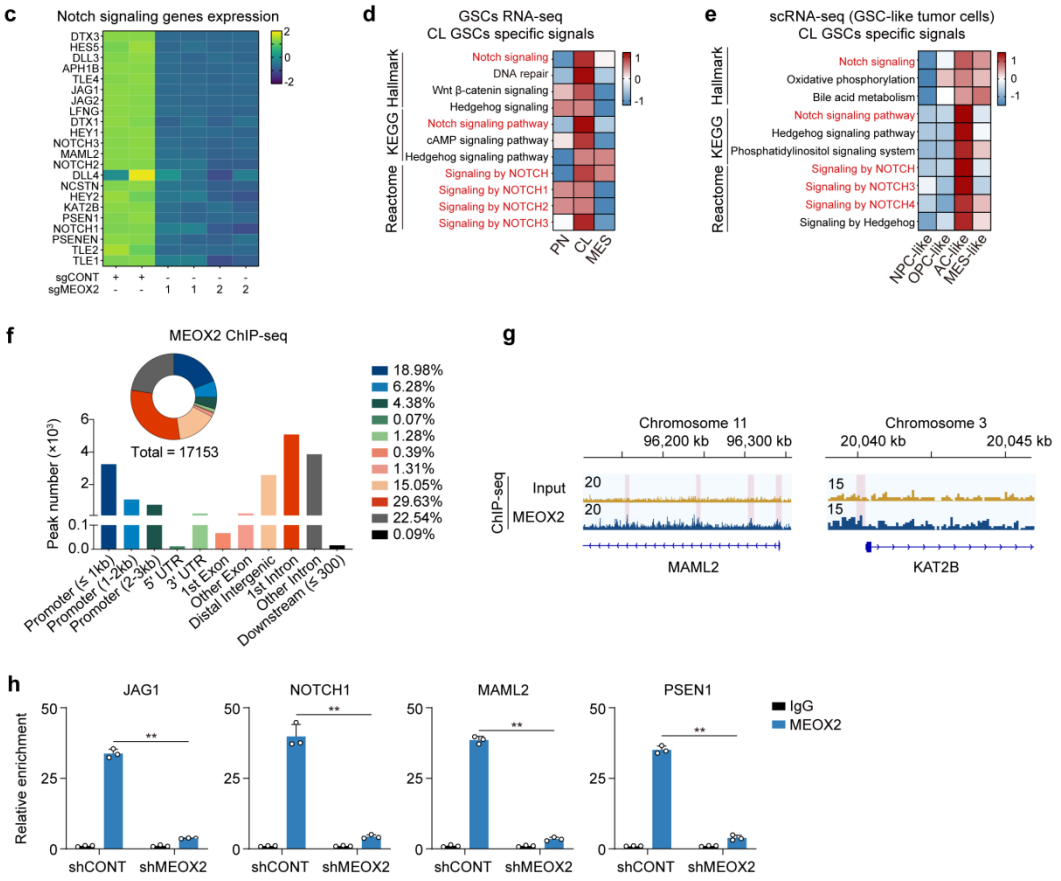

Response Fig R2 (Supplementary Fig. 6). MEOX2 transcriptionally regulates Notch signaling in classical GSCs, related to Figure 3.

a, Heatmap depicting the changes in subtype signature after MEOX2 knockout in 3028 CL GSCs. **b,** Summary of gsva score and p value of 3028 CL GSCs transduced with sgCONT, sgMEOX2-1, and sgMEOX2-2. **c,** Heatmap of Notch signaling pathway genes expression in MEOX2 knockout RNA-seq data. **d,** Heatmap of the pathway activities scored per cell by gsva between three subtypes (PN, CL, and MES) GSCs in GSCs RNA-seq datasets (GSE119834), using Hallmark, KEGG, and Reactome genesets. **e,** Heatmap of the pathway activities scored per cell by gsva between four cellular states (NPC-like, OPC-like, AC-like, and MES-like) GSC-like tumor cells in scRNA-seq datasets (in-house, GSE103224, GSE117891, GSE131928, GSE141383, GSE173278, and GSE182109), using Hallmark, KEGG, and Reactome genesets. **f,** The proportion (pie chart) and enrichment (bar chart) of the MEOX2 ChIP-seq peaks in different gene regions in 3028 (CL) GSCs. **g,** Input or MEOX2 binding signals of MAML2 and KAT2B from ChIP-seq on 3028 (CL) GSC. **h,** The relative enrichment of MEOX2 at JAG1, NOTCH1, MAML2, and PSEN1 promoters was assessed by ChIP-qPCR in shCONT and shMEOX2 3028 GSCs. Data are presented as mean ± SD from three independent experiments. **p < 0.01.

Reviewer #6:

Reviewer 6, Comment 1: Reviewer 6, Comment 5: Reviewer 3, Comment 1: (defining GSC) – I appreciate the authors providing featureplots which greatly clarify the expression.

However, the reasoning behind the definition of GSCs seems arbitrary and tautological. In the response they state:

“Our method for isolating GSC-like tumor cells was based on a protocol described in an article in Cell Stem Cell (2020, PMID: 31901251). The following method was employed in this study: “In order to identify the potential GSC cell types for each tumor, we defined GSCs within our scRNA-seq dataset as any cell (independent of the previous clustering) expressing PROM1, FUT4, or L1CAM, in conjunction with SOX2, and not expressing TLR4 (which has been shown to be downregulated by GSCs in order to avoid immune surveillance).”

But then they switch to saying:

“After isolating tumor cells in scRNA-seq datasets, we defined GSC-like tumor cells as any cell expressing CD133, CD15 or OCT4, in conjunction with SOX2 (Supplementary Fig.1b).”

And in the response:

“Therefore, we each selected two of the most reviewed transcription factors (SOX2 and OCT4) and surface markers (CD133 and CD15) to isolate GSC-like tumor cells from malignant cells in GBM scRNA-seq datasets (PMID: 26109046).” This reference is from 2015 and largely pre-dates what we’ve learned from scRNA-seq.

This "or" in "...any cell expressing CD133, CD15, or.." is quite arbitrary. Why not require a union of the markers or 2 of 3? Sox2 is basically expressed by a majority of cells in a tumor. But Sox2 is expressed by most proliferating neural progenitors--even more differentiated types. So requiring just one other marker seems capricious. I do not agree with the logic in the previous Cell Stem Cell paper (where they split so-called GSCs into 7 types), nor the current paper without functional justification.

Response:

We thank the reviewer for the thoughtful comments regarding the definition of GSC-like tumor cells in our study. The markers SOX2, CD133, CD15, and OCT4 were selected based on their well-established roles in GSCs and their association with stemness properties. These markers have been functional validated in multiple studies. Even in the recent high-impact reviews (***Nature Reviews Cancer 2022****, PMID:* 35710946 and ***Cancer Cell 2020***, PMID: 32396858), which synthesize the latest advances in GBM single-cell transcriptomics, maintain that these markers remain valuable for identifying functional GSCs. Currently, there is no effective method to accurately identify GSCs in scRNA-seq analysis. We adopted a method similar to that reported in the article from ***Cell Stem Cell 2020*** (PMID: 31901251), considering it to have a certain degree of rationality. As discussed in the ***Cancer Cell 2020*** (PMID: 32396858) review regarding current controversies in GSCs definitions: *"Fourth, the plethora of surface markers used to isolate GSCs might identify subsets of cells in different cellular states (and with different underlying genotypes). Thus, different groups and studies may use the term GSC to refer to completely different populations of cells. Moreover, GSCs are often contrasted with all other 'non-GSCs' with diminished tumor-propagating potential, although these likely contain a variety of distinct cellular states."* This is an inclusive strategy to capture GSCs heterogeneity. The use of "or" was based on the known heterogeneity of GSCs, where different subpopulations may express distinct marker combinations. Requiring the co-expression of all markers or a strict subset could exclude biologically relevant GSCs populations.

Upon further analysis, we found that this analytical approach did not affect the final results. In fact, conducting differential analysis without using this screening method, and instead performing differential analysis solely on malignant tumor cells in GBM scRNA-seq datasets (8 datasets, 80 samples), would not affect the final results (Response Fig. R1). After the above screening steps, we still identified MEOX2 and SRGN as typical targets of CL and MES GSCs, respectively.

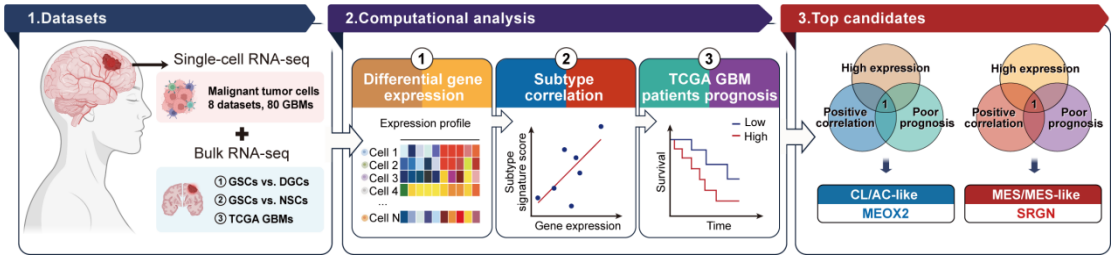

Response Fig R1. Diagram depicting the screening workflow to identify targets

for CL/AC-like and MES/MES-like subtype GSCs.

Reviewer 6, Comment 2:

Bottom two responses can be addressed by the same general approach:

Reviewer 6, Comment 9: Reviewer 3, Comment 8: More detail is needed on how these cells compare to the parental tumors. The authors should present an integration of their "GSCs" with primary glioma datasets and compared DEGs.
“We appreciate the reviewer’s comment. Unfortunately, we do not have sequencing data from the parental tumors corresponding to our GSCs.”

Reviewer 6, Comment 10: Reviewer 3, Comment 10: This doesn't directly address the point. There should be a direct comparison in low dimensional UMAP space to show if these cells align completely or if there are cellular states (likely in vitro due to culture artifacts) that don't appear in vivo. Scoring by modules by artificially normalized scales (e.g. Response Fig. R5) does not give the full picture as one gets aligning all of the data in a low dimensional space with batch correction/integration.
“The integrated analysis revealed that all cellular populations corresponded to states present in patient tumors.”

Specifically, scRNA-seq allows for facile integration across patients and datasets (e.g. Harmony, SCVI, or other atlas scale approaches). Large datasets of primary glioma are available (e.g. https://www.nature.com/articles/s41467-022-28372-y #data-availability) to easily integrate with the cell culture data. (The same parental data is not necessary as the tumors will generally fall into the same low dimensional space if enough samples are included. The authors should show whether their GSCs can be integrated with the primary datasets and fall within a similar low dimensional space. Simply scoring by the MES, CL, PN, etc. is too superficial to demonstrate the fidelity of these findings.

Response:

We thank the reviewer for this constructive comment. The dataset you provided (GSE182109) was previously incorporated in the analyses presented in our manuscript. We integrated the GSCs datasets with a total of 40 GBM samples, comprising 24 in-house generated samples and 16 samples from the GSE182109

dataset. The results demonstrated that GSCs could be integrated with the GBM datasets and occupied comparable positions in low-dimensional space (Response Fig. R2). Indeed, inter-patient tumor cell heterogeneity still persists after integration, which also suggests that homologous comparisons hold greater practical significance. Both qPCR and Western blot results showed that MEOX2 was enriched in EGFR+ WL1 GSCs (representing AC-like cellular states), while SRGN displayed high expression in CD44+ WL1 GSCs (representing MES-like cellular states) (Response Fig. R3). These results demonstrated that MEOX2 and SRGN are reliable targets for AC-like and MES-like states at the individual patient level. These findings strongly validates the reliability of our results.

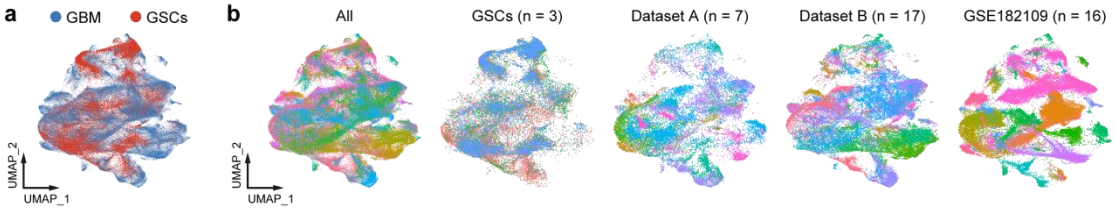

Response Fig R2. GSCs can be integrated with the GBM datasets and occupy a comparable position within the low-dimensional space.

a, The UMAP plot of GBM and GSCs. **b,** The UMAP plot of GBM and GSCs. Each color represents cells from individual samples.

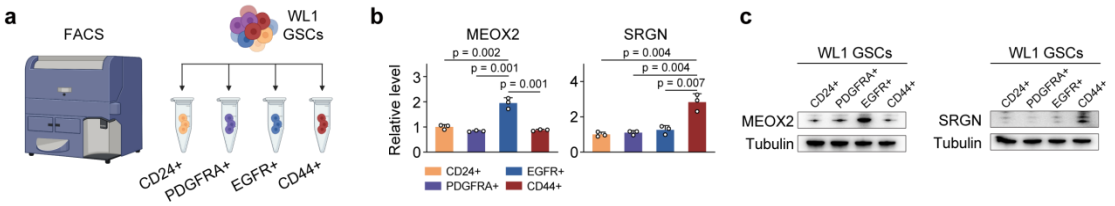

Response Fig R3. MEOX2 and SRGN are specific for CL and MES GSCs from the same patient.

a, Experimental workflow. Different cellular states of GSCs were sorted from WL1 GSCs. **b,** Relative mRNA expression of MEOX2 or SRGN normalized to 18S mRNA level in different cellular states WL1 GSCs. **c,** MEOX2 and SRGN protein levels were measured by western blotting in different cellular states WL1 GSCs. Tubulin was used as the loading control.

Reviewer #6:

Reviewer 6, Comment 1: I will "agree to disagree" about the import and ability to define putative glioma stem cells using "OR" logic with 4 markers. And agree that the discovered targets would precipitate through DEG analysis.

I would just suggest that very strong language be tempered in the discussion. Examples:
1) "GSCs are a driving force of intertumoral and intratumoral heterogeneity." In the next sentence, they cite two papers: "Single-cell sequencing and lineage tracking methods confirmed the existence of stem-like cancer cells in GBM, supported their importance in maintaining cell hierarchy, and further strengthened the concept of cell plasticity49, 50." In fact, one of these papers (Nat. Gen.) demonstrates that WT glioma shows a preponderance of dedifferentiation and lineage plasticity that doesn't fit with a hierarchical stem cell model like IDH1-mut tumors. I would submit that we should not take the existence and function of GSCs as such an element of faith but much remains to be determine empirically.
2) "Using genetic and pharmacologic techniques, we found that combination therapy with FDA approved agents against both CL and MES GSCs achieved the most effective tumor control." -I don't see any evidence of "control."

Response:

We thank the reviewer for the insightful comments and suggestions. We agree that some of the language in the discussion could be tempered to better reflect the current state of evidence and avoid overstatement. We have revised the manuscript accordingly to address these concerns.

1. Regarding the statement: “GSCs are a driving force of intertumoral and intratumoral heterogeneity.” The revised text reads:

“GSCs are thought to contribute to intertumoral and intratumoral heterogeneity, although the extent of their role and the mechanisms involved remain areas of investigation.”

2. Regarding the statement: “Using genetic and pharmacologic techniques, we found that combination therapy with FDA approved agents against both CL and MES GSCs achieved the most effective tumor control.” This has been revised to:

“Using genetic and pharmacologic techniques, we found that combination therapy with FDA-approved agents targeting both CL and MES GSCs resulted in a significant reduction in tumor growth in our experimental models.”

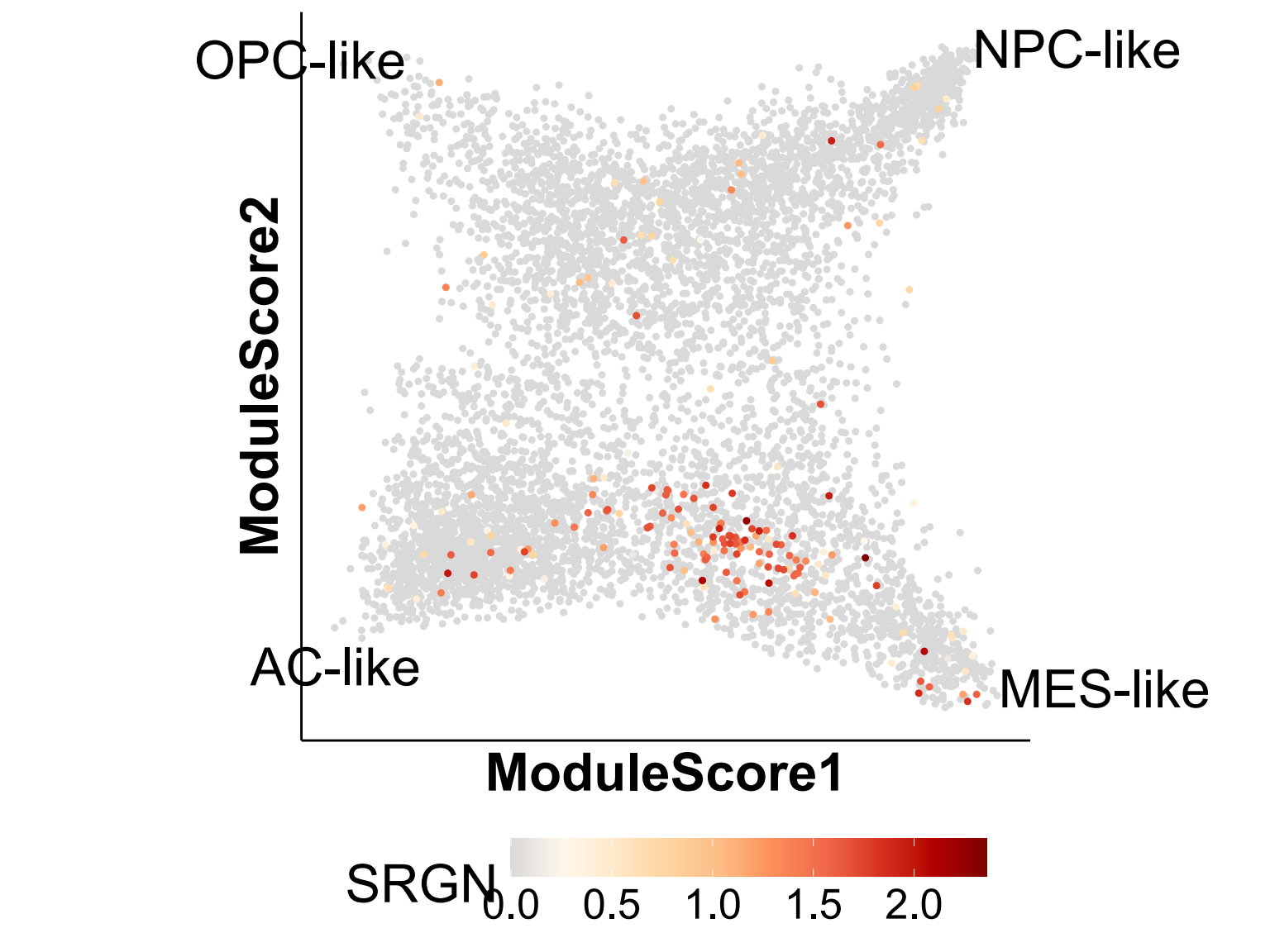
OPC-like
NPC-like
AC-like
MES-like
ModuleScore2
ModuleScore1
SRGN
0.0
0.5
1.0
1.5
2.0

MEOX2

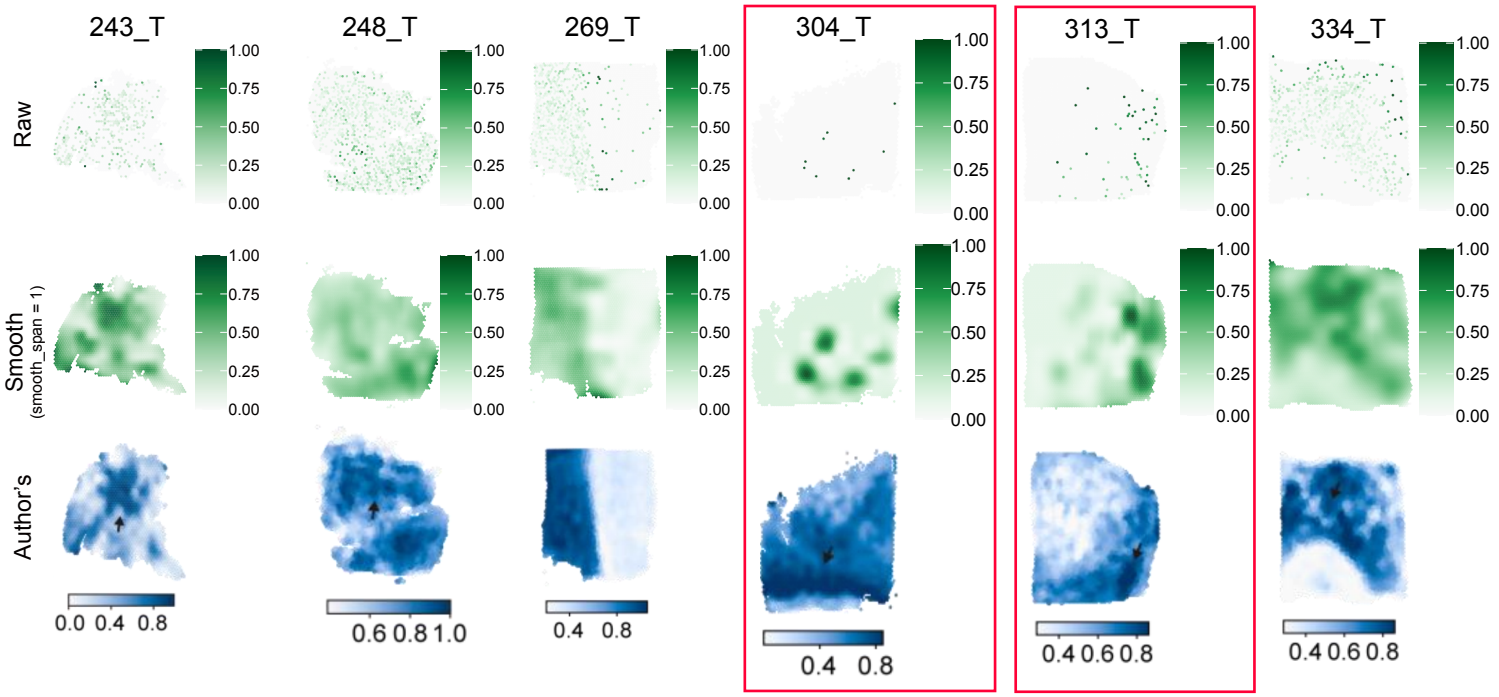
243_T
248_T
269_T
304_T
313_T
334_T
Raw
Smooth
(smooth_span = 1)
Author's
1.00
0.75
0.50
0.25
0.00
0.0 0.4 0.8
0.6 0.8 1.0
0.4 0.8
0.4 0.6 0.8

SRGN

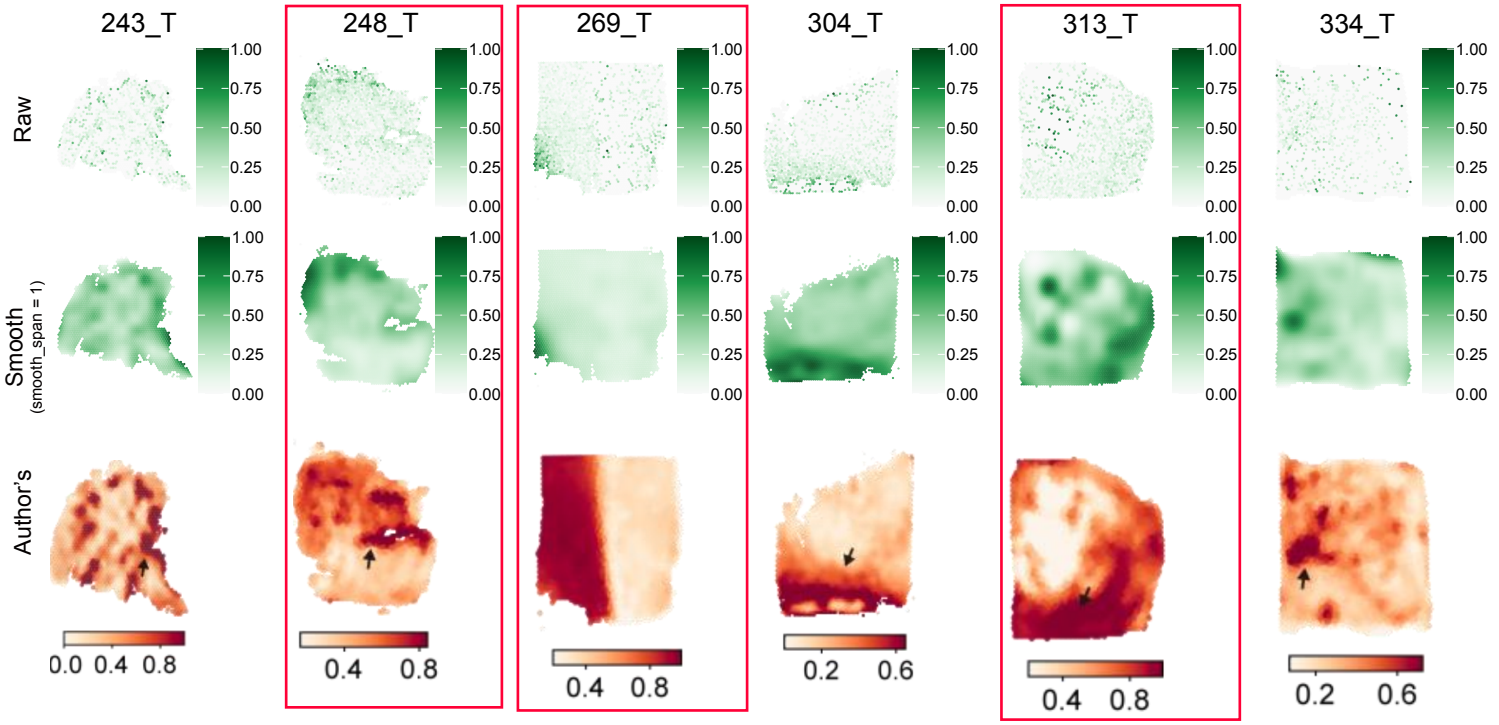
243_T
248_T
269_T
304_T
313_T
334_T
Raw
Smooth
(smooth_span = 1)
Author's
1.00
0.75
0.50
0.25
0.00
0.0 0.4 0.8
0.4 0.8
0.2 0.6